Fall 12-16-2016

Chemosensitization Effect of SP1017 on Multiple Myeloma

Hangting Hu
University of Nebraska Medical Center

The CHEMOSENSITIZATION EFFECT OF SP1017 ON MULTIPLE MYELOMA (MM)

By

Hangting Hu

A DISSERTATION

Presented to the Faculty of

The Graduate College in the University of Nebraska

In partial Fulfillment of the Requirements

For the Degree of Doctor of Philosophy

Department of Pharmaceutical Sciences

Under the Supervision of Professor Tatiana K. Bronich

Medical Center

Omaha, Nebraska

September, 2016

ACKNOWLEDGEMENTS

First and foremost, I would like to extend my sincere appreciation to my supervisor, Dr. Tatiana K. Bronich. During the past 5 years, she has been always there willing to listen and help me understand the complicated scientific problems. I have been constantly inspired and encouraged by her hard work, broad knowledge, critical thinking, and perpetual energy in scientific research. I appreciate all her contributions of time, ideas, and funding to support my doctoral study. With her as a mentor, I have learned many things not only professionally but also personally. Being as a great scientist, she still stays humble and keeps on learning and exploring new scientific knowledge. Her positive attitude and great passion in science really motivate and inspire me and I think I will keep learning in my future professional life. It is my great pleasure to work under her supervision and I am heartily thankful for her excellent mentoring.

I also would like to thank our collaborators, Dr. Edward A. Faber, Dr. Armen Petrosyan, Dr. Alexander V. Kabanov and Dr. Daria Y. Alakhova for their discussions and advices in the project. Dr. Edward A. Faber had the bi-weekly or monthly meeting with us to follow the progress of my project and also gave valuable ideas and comments. Dr. Armen Petrosyan was involved in the study of translocation of Cy5-L61 to ER and Golgi apparatus and Golgi fragmentation. I really appreciate their contributions to my project.

I would extend my gratitude to the members of my advisory committee which include Dr. Natalia A. Osna, Dr. Vimla Band and Dr. Jered C. Garrison for their constant support, advice and guidance throughout my study. They reviewed my work and gave me their insightful comments in every committee meeting, which are valuable for my project. Dr. Natalia A. Osna also advised and helped me in the study of proteasome inhibition and caspases activations.

I would like to thank all past and present members of the laboratory. In particular, I would like to thank Dr Swapnil S. Desale for teaching and helping with the tumor implantation of the mice model, Dr. Fan Lei for helping with the purification of Cy5-L61, Dr. Shaheen Ahmed for helping with the animal study of biodistribution of Cy5-L61, Kurti Soni for helping me with English editing and presentation and for all her encouragements in my bad situations, Xinyuan Xi, Dr. Svetlana Romanova, Tong Liu, Dr. Chantey Morris, Dr. Anya Brynskikh Boyum, Dr. Hardeep Singh Oberoi, Dr Jinjin Zhang and many others for their help in the lab and support. Many thanks to the administrative staff (Christine Allmon, Jamie Arbaugh, Keith Sutton, and Katina Winters) for their administration support. I would like to acknowledge the technical assistance from UNMC core facilities in my research and financial support from NIH, China Scholarship Council and UNMC Graduate Assistantship.

Lastly, I would like to thank my parents and all my friends in Omaha for their love, encouragement and support in the past five years.

THE CHEMOSENSITIZATION EFFECT OF SP1017 ON MULTIPLE MYELOMA (MM)

Hangting Hu, Ph.D.

University of Nebraska Medical Center, 2016

Advisor: Tatiana K. Bronich, Ph.D.

Multiple myeloma (MM) is a hematological malignancy of plasma cells that are predominantly located in bone marrow (BM). Despite recent improvements in MM treatment by introduction of several novel agents including immunomodulatory drugs, proteasome inhibitors and the use of the drug combinations, MM remains incurable and almost all patients eventually relapse or become refractory to the current treatment regimens. So the current challenge of MM treatments is to maintain treatment response, prevent relapse and eventually prolong survival.

Here we demonstrated that Pluronic block copolymers ((Pluronic L61: Pluronic F127 = 1:8 w/w, SP1017) significantly increase cytotoxicity of proteasome inhibitors (Bortezomib, BTZ or Carfilzomib, CFZ) in a panel of MM cells. Specifically, SP1017 (0.005%) co-treatment triggered 2-fold increase in drug cytotoxicity to MM cells. Lower concentrations of SP1017 (0.002%) showed lower, but still significant cytotoxicity when combined with proteasome inhibitors. The mechanistic basis for sensitization effect of SP1017 was multifactorial and included: 1) augmented inhibition of chymotrypsin-like proteolytic activity, concomitant with increased accumulation of poly-ubiquitinated proteins and proteotoxic stress; 2) translocation of Pluronic L61 into the endoplasmic reticulum (ER) and increase of ER stress response; 3) translocation of Pluronic L61 into the Golgi apparatus and increase of rate of Golgi fragmentation, concomitant with reduction of secretion of paraprotein; 4) enhanced depletion of reduced glutathione, that is essential for mitigation of drug-induced oxidative stress; 5) enhanced pro-apoptotic

activity of the proteasome inhibitors and; 6) decreased anti-apoptotic defense in MM cells. Importantly, SP1017 co-treatments restore drug sensitivity in BTZ/CFZ-resistant MM cells. Further studies have revealed that SP1017 co-treatment could also sensitize MM cells in co-culture models of the BM microenvironment, which triggers cytokine- and adhesion-mediated MM drug resistance. These results provide support for the design of therapeutic strategies aimed to counteract the drug resistance mechanisms in MM. We also demonstrated that combination of BTZ and SP1017 exerted enhanced antitumor efficacy in human MM/SCID mice model compared to BTZ alone, delaying the disease progression without causing systemic toxicity or hematological toxicity. Moreover, we observed the accumulation of the Cy5-L61 in the BM, which was proved by both fluorescence imaging and flow cytometry, indicating that Pluronic L61 could target and accumulate within the BM, thus playing an important role in sensitizing MM cells in the bone microenvironment to proteasome inhibitors.

LIST OF FIGURES

LIST OF TABLES

LIST OF ABBREVIATIONS

ABC transporters	ATP binding cassette transporters
ADH	adipic dihydrazide
AIF	apoptosis-inducing factor
APAR-1	apoptosis protease activating factor-1
ASOs	antisense oligonucleotides
ATF6	activating transcription factor 6
ATP	adenosine triphosphate
BBB	blood brain barrier
BBMECs	microviscosity in bovine brain microvessel endothelial cells
Bcl-2	B-cell CLL/lymphoma 2
Bcl-XL	BCL2-like 1
BCRP	breast cancer resistance protein
BID	domain death agoinst
BLI	bioluminescence imaging
BM	bone marrow
BMSCs	bone marrow stromal cells
BTZ	Bortezomib
CCK-8	Cell counting kit-8
CFZ	Carfilzomib
CHOP	CCAAT/enhancer-binding homologous protein
ChT-L	chymotrypsin-like
CM	Conditioned medium
CMC	critical micelle concentration
CMT	critical micelle temperature
CNS	central nervous system

c(RGDyK)	cyclic RGD [arginine-glycine-aspartic acid] peptide
CSCs	cancer stem cells
CyA	cyclosporine A
Cy5-L61	Cyanine 5-labeled Pluronic®L61
DEX	Dexamethasone
DISC	death-inducing signaling complex
DMF	Dimethylformamide
DOX	doxorubicin
DSF	disulfiram
dsRNA	double strandard RNA
ECL	enhanced chemiluminescence
ECM	extracellular matrix
EDTA	ethylenediaminetetraacetic acid
ELISA	Enzyme-linked Immunosorbent Assay
EPL	ε-polylysine
EPR	enhanced permeability and retention
ER	endoplasmic reticulum
FACS	Fluorescence-activated Cell Sorting
FADD	FAS-associated death domain
FDA	Food and Drug Administration
GADD153	growth arrest- and damage-inducible gene 153
GR	glucocorticoid receptor
GSH	glutathione
GSSG	glutathione disulfide or oxidized glutathione
GST	glutathione-S-transferases
HBSS	Hank's Balanced Salt Solution

HIF1	hypoxia inducible factor 1
HLB	hydrophilic–lipophilic balance
HSPs	heat-shock proteins
IL-6	interleukin-6
IMIDs	immunomodulatory drugs
IRE1α	inositol-requiring protein 1α
LRP/MVP	lung resistance-related protein /major vault protein
Luc	Luciferase
MAPK	mitogen-activated protein kinase
MDR	mutlidrug resistant
$\Delta\psi_m$	mitochondrial membrane potential
MM	multiple myeloma
MPA	metaphosphoric acid
mRNA	messenger RNA
MRP1	multidrug resistance-associated protein 1
MTT	3-(4,5-Dimethylthiazol-2-yl)-2,5-diphenyltetrazolium bromide
NAC	N-acetyl-L-cysteine
NBDs	nucleotide-binding domains
NFκB	nuclear factor kappa B
PBMC	Peripheral Blood Mononuclear Cells
PBS	phosphate buffered saline
PEO-*b*-PMA	poly (ethylene oxide)-*b*-poly(methacrylic acid)
PEG	poly (ethylene glycol)
PEG-PLL-PLLeu	poly (ethylene glycol)-b-poly(L-lysine)-b-poly(L-leucine)
PERK	protein kinase RNA-like ER kinase
PEI	polyethyleneimine

PFA	paraformaldehyde
P-gp	P-glycoprotein
PHis-PLA	poly(L-histidine)-poly (D,L-lactide)
PI	propidium iodide
PLGA	poly(lactide-co-glycolide)
PPO	poly (propylene oxide)
PSMB5	β5-subunit of proteasome
RES/ MPS	reticuloendothelial system/ mononuclear phagocyte system
RISC	RNA-induced silencing complexes
RNAi	RNA interference
ROS	reactive oxygen species
SDS-PAGE	sulfate-polyacrylamide gel electrophoresis
shRNAs	short-hairpin RNAs
siRNAs	small interfering RNA
TBS	Tris-buffered saline
tBID	truncated domain death agoinst
TMDs	transmembrane domains
Topo II	Type II topoisomerase
TPGS	D-α-tocopheryl polyethylene glycol 1000 succinate
UPP	ubiquitin-proteasome pathway
UPR	unfolded protein response
XIAP	X-linked inhibitor of apoptosis

LIST OF CONTRIBUTIONS

1. Chapter III— Dr. Armen Petrosyan made a major contribution into the studies of translocation of Cy5-L61 to ER and Golgi apparatus as presented in Fig 3.7 and Golgi fragmentation in Fig 3.8.
2. Chapter III and Chapter IV—Dr. Lei Fan assisted in purification of Cy5-L61, which was used to study intracellular colocalization of block copolymer.
3. Chapter IV—Dr. Shaheen Ahmed assisted in the animal study of biodistribution of Cy5-L61.
4. All experiments were mainly performed by Hangting Hu. The overall project was designed under the guidance of Dr. Tatiana K. Bronich. Dr. Edward A. Faber also provided valuable direction to this project. Dr. Tatiana K. Bronich and Dr. Armen Petrosyan provide important contributions in preparation of the manuscripts.
5. This work was supported by NIH grants to Dr Bronich (COBRE, Nebraska Center for Nanomedicine- 5P20GM103480).

CHAPTER I: INTRODUCTION

1.1 Mutlidrug resistant (MDR) tumors

Chemotherapy currently remains the main treatment option for cancers. However, patients suffer from its severe side effects, systemic toxicity and limited efficacy due to poor delivery of drug to cancer cells and/or intracellular targets. Multidrug resistance (MDR) to chemotherapy, as a result of intrinsic or acquired drug resistance of the tumor to chemotherapeutic agents, is a major obstacle in the treatment of cancer patients. Many primary tumors and metastatic lesions often relapse and develop drug resistance though they respond well to the chemotherapeutic treatment. The resistance of tumors occurs not only to a single cytotoxic drug used, but also occurs as a cross-resistance to a whole range of drugs with different mechanisms of action and cellular targets. The most investigated mechanisms with known clinical significance are: pump resistance and non-pump resistance **(Fig.1.1)**.

1.1.1 Pump resistance

Pump resistance depends on membrane-bound active drug efflux pumps that expel anticancer drugs out of the cells. The major efflux pumps belong to mammalian adenosine triphosphate (ATP)-binding cassette (ABC) transporters, a large member of functionally diverse transmembrane proteins that are associated with the plasma membrane of cells. There are 48 known human ABC transporters, classified into seven distinct subfamilies of proteins (ABC-A through ABC-G) on the basis of their sequence homology and domain organization [1]. The ABC transporters associated with MDR include (a) P-glycoprotein (P-gp, ABCB1), multidrug resistance-associated protein 1

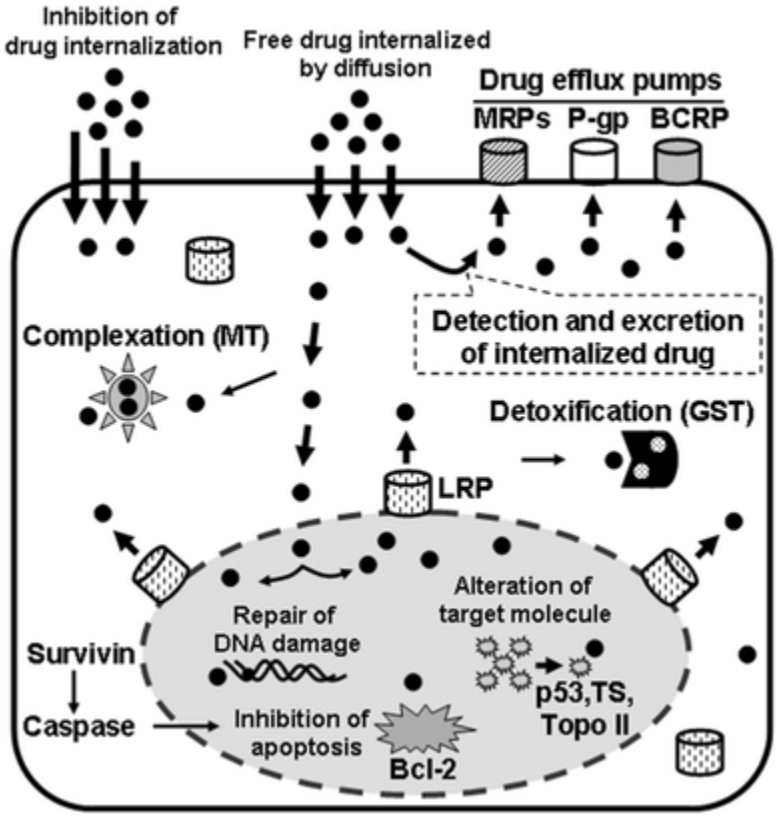

Fig.1.1 Mechanisms of multidrug resistance. (Adapted from [4])

(MRP1, ABCC1), and breast cancer resistance protein (BCRP, ABCG2). The most typical efflux pump in the cell membrane is P-gp, with a molecular weight of 170kDa due to the amplification of ABCB1 (MDR1) gene. P-gp has a typical structure for ABC transporter, glycosylated at the first extracellular loop and composed of 12 transmembrane domains (TMDs) and 2 intracellular nucleotide-binding domains (NBDs), which bind and hydrolyze ATP providing energy for transmembrane movement of the drugs [2]. The drug-binding pocket of P-gp is localized in the TM domain of the protein. The inward-open conformation of P-gp allows for substrate access both from cytoplasm and from the inner leaflet of the membrane but not from the upper leaflet or extracellular space. After the drug enters P-gp's binding site from the inner leaflet of the membrane, it stimulates the binding of the two molecules of ATP by NBDs followed by their dimerization, which causes the major conformational change in the protein and formation of the outward-facing structure, open to the extracellular space. The drug is released due to the change of the affinity of the protein to it or is facilitated by ATP hydrolysis, which brings the protein back to the initial state [3]. MRP1, a 190-kDa protein, belong to the C group of the ABC transporters. MRP1 is consist of 17 TMDs having P-gp like cores and acts as an ATP-dependent glutathione S-conjugate export pump, thus its MDR mechanism is entirely different from that of P-gp mediated resistance. However, many of the anticancer drugs are the substrates for both P-gp and MRP1 except taxanes which are poor substrates for MPR1 [2]. BCRP, also called the mitoxantrone resistance associated protein (MXR) or ABC transporter in placenta (ABC-P), belongs to a member of the G subfamily of ABC transporters. It is a half transporter consisting of six TMDs and an ATP-binding site and functions as either homodimers or homomultimers bridged by disulfide bonds [2, 4].

A 110 kDa protein originally named as lung resistance-related protein /major vault protein (LRP/MVP) is not an ABC transporter. It is a complex ribonucleoprotein located in the cytoplasm membrane, nuclear membrane and nuclear pore complex, not on the cell membrane like P-gp and MRP. It is involved in intracellular transport processes, the bidirectional distribution of compounds between the nucleus and the cytoplasm, which might confer MDR by transporting drugs away from their intracellular targets and by the sequestration of drugs [5]. It has been demonstrated that LRP is involved in resistance to DNA interacting drugs such as doxorubicin (DOX) by the redistribution of DOX from the nucleus to the cytoplasm [6].

1.1.2 Non-pump resistance

In addition to enhanced drug efflux by different drug transporters associated with tumor cells, several mechanisms of drug resistance exist that are independent from drug efflux transporters, and are classified as non-pump resistance mechanisms. Such mechanisms decrease the ability of anticancer drugs to induce cells death without interfering with the entry and accumulation of drugs in tumor cells. The mechanisms include but are not limited to the following classes: (1) altered drug targets such as decreased topoisomerase II levels and activity; (2) increased drug metabolism by detoxification systems, such as glutathione-medicated reduction; (3) alterations in cell cycle checkpoints as a result of mutated cell cycle proteins such as p53; (4) increased DNA repair capacity; (5) reduced ability to undergo apoptosis (6) chromosomal abnormalities in cancer cells lead to over-expression of anti-apoptotic genes; (7) altered signal transduction pathways in cancer cells governed via integrin receptors, growth factor receptors etc. leads to blockage of apoptosis and expression of MDR-linked genes

those involved in DNA repair and drug-efflux pumps; (8) hypoxia up-regulated expression of MDR-linked genes through activation of transcription factor hypoxia inducible factor 1 (HIF1) [7, 8, 9, 10].

Drug detoxification/inactivation is one of the contributing factors, where the toxic effect of cytotoxic drugs that gain entry inside the cells are successfully reduced with drug-metabolizing enzymes that are overexpressed in cancer cells such as isoforms of aldehyde dehydrogenase (ALDH1A1 and ALDH3A1) [11], glutathione-S-transferases (GST) [12], and cytochrome P4503A [13]. Enhanced DNA damage repair efficiency also pays a major role in MDR resistance. A widely used anticancer drug DOX exhibit topoisomerases (Topo II) inhibitory effect, which is a critical enzyme that is involved in DNA replication and repair. DOX stabilizes the Topo II complex preventing the release of DNA double helix and stopping the process of replication. However, resistant cancer cells can activate Topo II in response to DOX treatment to compensate for the damage and thereby increase the resistance against the treatment [14, 15]. Antiapoptotic defense, involving a huge complex of proteins, represents another important mechanism of MDR resistance to prevent transformation of a damage induced by anticancer drugs into apoptotic cell death. The anti-apoptotic members of this family, such as B-cell CLL/lymphoma 2 (Bcl-2) and BCL2-like 1 (Bcl-XL), prevent apoptosis either by sequestering proforms of death-driving cysteine proteases called caspases (a complex called the apoptosome) or by preventing the release of mitochondrial apoptogenic factors such as cytochrome c and apoptosis-inducing factor (AIF) into the cytoplasm. After entering the cytoplasm, cytochrome c and AIF directly activate caspases that cleave a set of cellular proteins to cause apoptotic changes [16]. It is evident that Bcl-2 overexpression results in the resistance of cells to different drugs, including DOX [17], paclitaxel [18], cisplatin [19], mitoxantrone [20], etc. Solid tumors are found within a

tumor microenvironment that is comprised of cancer cells and stromal cells (including fibroblasts, immune and inflammatory cells, etc.), embedded in an extracellular matrix [21].The tumor microenvironment is characterized not only by marked gradients in drug concentration but also by gradients in the rate of cell proliferation and by regions of hypoxia and acidity, all of which can influence tumor cell sensitivity to drug treatment [22]. The hypoxic situation which results from the reduced blood flow caused by abnormal angiogenesis or the compression/closing of blood vessels, can lead to the activation of genes such as ABC transporters, Bcl-2 family genes, glutathione, etc that contribute to a drug-resistant phenotype [23, 24, 25, 26].

1.2 Strageties to overcome MDR in cancer cells

Extensive studies have been conducted during the last several decades to enhance the efficacy of chemotherapy by suppressing or evading these MDR mechanisms including the use of new anticancer drugs that could escape from the efflux reaction, MDR modulators, chemosensitizers, multifunctional nanocarriers, and RNA interference (RNAi) therapy[27].

1.2.1 Anticancer drugs capable of overcoming MDR

Anticancer drugs that are not substrates of drug efflux transporters may offer improved therapeutic outcomes for patients by circumventing MDR. For instance, alkylating drugs (cyclophosphamide), antimetabolites (5-fluorouracil), and the anthracycline modified drugs (annamycin and doxorubicin-peptide) are among this category of anticancer drugs [28, 29, 30]. Novel camptothecin analogs with low polarity can circumvent ABCG2-associated drug resistance in ABCG2-overexpressing human

cell lines [31]. Taxanes, such as paclitaxel and docetaxel, are widely prescribed chemotherapeutic drugs to treat many forms of cancer including breast, ovarian and lung cancers [32]. Both paclitaxel and docetaxel are substrates for the ATP binding cassette multidrug transporters [33]. The novel taxane analog Tesetaxel (DJ-927) exhibited stronger cytotoxicity than paclitaxel and docetaxel in various tumor cells, especially against P-gp-expressing cells. The cytoxicity of DJ-927 was not affected by the P-gp expression level in tumor cells, or by the co-presence of a P-gp modulator [34]. Cabazitaxel (Jevtana), a novel tubulin-binding taxane with poor affinity for P-glycoprotein, was approved by US Food and Drug Administration (FDA) in June 2010 for second line use in advanced hormone refractory prostate cancer in docetaxel-pretreated men and is the first clinically approved taxane that can circumvent resistance caused by the overexpression of the P-gp drug efflux pump [35]. Other novel taxane analogs such as BMS-184476, RPR109881A, Ortataxel, Trabectedin-ET-743 are evaluated in clinical trials for their broad spectrum activity in sensitive and resistant tumor cell lines to overcome MDR [36].

1.2.2 MDR modulator

MDR modulators, also named as MDR inhibitors or chemosensitizor, are the compounds that have the ability to reverse the resistance against anticancer drugs by inhibiting ABC transporters but are not cytotoxic themselves [2]. Modulators targeting P-gp directed MDR belong to a number of chemical classes and have been classified as first, second and third generation MDR modulators based on their affinity for transporter proteins and their relative side effects [37]. First geneartion modulators includes drugs that were not specifically developed for inhibiting MDR but were used for other

pharmacological activities, such as calcium channel blockers (eg, verapamil), immunosuppressants (eg, cyclosporin A), antibiotics (eg,erythromycin), antimalarials (eg, quinine), psychotropic phenothiazines and indole alkaloids (eg, fluphenazine and reserpine), steroid hormones and anti-steroids (eg, progesterone and tamoxifen) and detergents (eg, cremophor EL) [38]. However, since their low affinity for ABC transporters required high doses to achieve the desired effect, first-geneartion modulators caused unacceptable high toxicity which limit their application. In addition, many of these chemosensitizers are substrates for other transporters and enzyme systems, resulting in unpredictable or adverse pharmacokinetic interactions in the presence of chemotherapy agents [39,40]. Clinical trials with first-generation MDR drugs failed for various reasons, often due to side effects [39, 41, 42]. The second-generation modulators include valspodar (PSC 833), dexverapamil, dexniguldipine, and biricodar (VX-710), which are more potent and less toxic than their predecessors [40]. A novel nonimmunosuppressive cyclosporin A, PSC-833, is shown to be a highly potent resistance modifier, being 7-10-fold more potent than the parent compound cyclosporin A, whilst approximately equal to cyclosporin A in the growth inhibitory effects of compound alone [43]. Valspodar has been studied in numerous clinical trials in combination with cytotoxic agents such as mitoxantrone, paclitaxel, dexamethasone, etoposide, cytarabine, in patients with various refractory carcinomas [44 , 45]. Dexverapamil is a stereoisomer of racemic verapamil and has approxiamately 25% of the cardiac activity of the racemic mixture, but appears to be equally potent in reversing MDR [46]. Second-generation P-gp modulators have a better pharmacologic profile than the first generation compounds, but they also retain some characteristics that limit their clinical usefulness. In particular, these compounds significantly inhibit the metabolism and excretion of cytotoxic agents due to the effect on cytochrome P450 isoenzyme 3A4-

mediated drug metabolism, thus leading to unacceptable toxicity in clinical trials [39]. For example, the combination of dexverapamil and etoposide, prednisone, vincristine, cyclophosphamide, and doxorubicin (EPOCH) produced more hematologic toxicity compared with EPOCH alone [47]. The third generation modulator is highly specific for MDR efflux pumps sparing any interaction with drug-metabolizing enzymes that do not alter pharmacokinetic interaction with other therapeutic agents. Tariquidar (XR9576), zosuquidar (LY335976), ONX-093 (OC144-093) and laniquidar (R101933) are among the third generation MDR modulators with increased specificity, potency, and fewer pharmacokinetic interactions [27]. LY335979 significantly enhanced the survival of mice implanted with P-gp-expressing murine leukemia (P388/ADR) when administered in combination with either daunorubicin or DOX or etoposide without any significant effect on the pharmacokinetics of these anticancer agents [48]. OC144-093 increased the life span of doxorubicin-treated mice engrafted with MDR P388 leukemia cells by >100% and significantly enhanced the in vivo antitumor activity of paclitaxel in MDR human breast and colon carcinoma xenograft models, without a significant increase in DOX or paclitaxel toxicity [49]. Clinical trials with these new third generation agents are ongoing, but none of them has found a general clinical use so far [27]. Recently, the fourth generation MDR modulator have been developed originating from natural resources such as plants, fungi and even marine organisms to lower the toxicity for better tolerance by the human body [50]. Curcumin is a common term used for a mixture of curcuminoids that are purified from the Indian spice turmeric powder, are known to have many biological activities, including anti-inflammatory, anti-cancer, and anti-viral properties [50]. In addition, both curcumin and its major metabolite tertrahydrocurcumin were found to restore drug sensitivity in cancer cells overexpressing the MDR-linked ABC transporters P-gp, MRP1 and ABCG2 by directly inhibiting their functions [51]. More

recently, curcumin was found to have the modulatory effect on ABCG2 efflux activity *in vivo* [52]. Flavonoids, the main group of polyphenolic compounds present in plants as well as marine bio source, has been studied and characterized extensively by numerous research groups to determine their ability to inhibit P-gp-, MRP1- and ABCG2-mediated efflux and restore drug sensitivity in MDR cancer cells [50]. Flavonoids was found to be bi-functional in reversing the MDR not only by competitively binding to the substrate-binding sites of transporters but also inhibiting the ATPases activity involved in drug efflux, thus enhancing the therapeutic index [53]. However, further studies are needed to elucidate the potential usage of natural products as chemosensitizers in MDR cancer chemotherapy.

1.2.3 Gene silencing by RNA interference (RNAi) or antisense oligonucleotides (ASOs) to overcome MDR

RNAi and ASOs are the two most widely used strategies for silencing gene expression. RNAi is a biological process that cells use to inhibit or silence specific gene expression through the destruction of specific mRNA molecules triggered by RNA molecules. Typically, RNAi can be achieved through two different pathways: 1) a RNA-based approach where effector small interfering RNA (siRNAs) are delivered to the target cells; 2) a DNA-based approach in which effector siRNAs are generated by the intracellular processing of RNA hairpin transcipts [27]. When a double strandard RNA (dsRNA) molecule is introduced into a cell, it is recognized and cleaved by the enzyme Dicer, a member of the RNaseIII family of dsRNA-specific endonucleases into short fragments of 21-23 nucleotides. These small fragments, referred to as siRNA, bind to proteins from a special family: the Argonaute proteins and form RNA-induced silencing complexes (RISC). Within the RISC, one strand of the dsRNA is removed, leaving the

remaining strand available to bind to messenger RNA (mRNA) target sequences according to the rules of base pairing: A binds U, G binds C, and vice versa. Once bound, the Argonaute protein can cleave and destroy the mRNA, thereby preventing it from being used as a translational template and silencing the expression of the gene from which the mRNA was transcribed [54]. The latter approach is primarily based on nuclear synthesis of short-hairpin RNAs (shRNAs) using gene expressing vectors, which are transcribed in the nucleus and transported to the cytoplasm via the miRNA export pathway and are processed into siRNAs by Dicer [55]. ASOs share the fundamental principle with RNAi: a single-stranded oligonucleotide binds a target RNA through Watson-Crick base pairing, then cleaves and destroys the target RNA [56].

RNAi has been extensively investigated in down-regulating the expression of MDR genes to restore drug sensitivity in cancer cells. Several effective sequences of siRNA and ASOs targeted to major drug efflux transporters (e.g. P-gp, MRP, BCRP, LRP proteins) were developed and successfully used in order to inhibit the expression of main drug efflux transporters. Nieth et al designed siRNA duplexes against two regions of the P-gp-encoding mRNA for disruption of P-gp-mediated drug extrusion and re-sensitization of gastrointestinal tumor cells to treatment with the antineoplastic agent daunorubicin [57]. Pichelr et al demonstrated two tested shRNAi constructs targeted against human MDR1 mRNA inhibited expression of P-gp by >90%, whereas control shRNAi had no effect [58]. Lv et al proved stable shRNA-medicated RNAi increased the sensitivity to mitoxantrone of anti-BCRP shRNA treated MCF-7/BCRP cells about 14.6-fold compared with the control [59]. Pan et al developed pSUPER-shRNA/mdr1 vector system to achieve knockdown of P-gp by RNAi in malignant cells and animals to restore their sensitivity to Adriamycin [60]. As unmodified, naked siRNA are relatively unstable in blood are rapidly degraded by endo-and exonucleases and they can hardly cross the cell

membrane due to their polyanionic and hydrophilic nature and relatively large molecular weight [61]. Typically, chemical modifications can be introduced into the RNA duplex structure so as to enhance biological stability without adversely affecting gene-silencing activity. Alternatively, they can be formulated with a delivery system that could enhance biological stability, facilitate intracellular uptake and specifically target to the tumor site of action [61]. Non-viral vectors are more promising because of their low toxicity, biodegradability, biocompatibility as well as availability as viral vectors (e.g. retrovirus, lentivirus, adenovirus, adeno-associated virus, and herpes simplex virus) due to their inflammatory and immunogenic effects [62]. Chemical non-viral vectors are broadly classified into inorganic particles, lipid based, polymer based and peptide based [63]. Nanocarriers designed for gene delivery can be synthesized from variety of materials including polymers, dendrimers, liposomes, carbon nanotubes, metal and metal-oxide nanoparticles [64]. For instance, novel biocompatible, lipid-modified dextran-based polymeric nanoparticles were used as the platform for MDR1 siRNA delivery, which efficiently suppresses P-gp expression in the drug resistant osteosarcoma cell lines [65]. The cationic polymers, namely lipid-substituted low molecular weight (2 kDa) polyethyleneimine (PEI) was used as a carrier for siRNA-mediated BCRP down-regulation, which sensitized the drug-resistant cells to cytotoxic effect of mitoxantrone by a ~14-fold decrease in the IC_{50} value [66].

RNAi and ASOs can be also used for suppression of proteins mainly responsible for nonpump resistance in order to sensitize MDR tumor cells. The siRNA-based therapeutics can induce apoptosis of cancer cells by targeting anti-apoptotic factors, such as survivin, Bcl-2, X-linked inhibitor of apoptosis (XIAP), and HIF1α [67]. siRNA-based silencing of the survivin splice variant 2B inhibits cell growth in vitro and reduces tumor growth in orthotopic models of taxane-resistant ovarian cancer [68]. Bcl-2 siRNA

and Bcl-xl siRNA in transfected HepG2 cells blocked the target gene, induced apoptosis in HepG2 cells and increased the sensitivity to chemotherapeutic drugs 5-fluorouracil and 10-hydroxycamptothecin [69].XIAP gene silencing enhanced chemosensitivity of P-gp expressing chondrosarcoma cells to DOX in comparison to nonsilencing control group [70]. Silencing the HIF-1α gene reversed MDR in colon cancer cells by increasing the sensitivities to Adriamycin, vincristine, 5-fluorouracil and inducing a marked increase in the apoptotic level of each corresponding drug [71].

1.2.4 Multifunctional nanoparticles for chemotherapy

Nanoparticles such as polymeric nanoparticles, solid lipid nanoparticles, magnetic nanoparticles, dendrimers, liposomes, micelles, quantum dots, etc. are extensively explored for cancer diagnosis, treatment, imaging, and as ideal vectors to overcome drug resistance by diverting ABC-transporter mediated drug efflux mechanisms [72]. Nanoparticles enhance the therapeutic efficacy of anticancer agents at the target site of action due to their passive and active tumor targeting abilities, which can reduce systemic toxicity and potentially circumvent the problem of drug resistance [27]. Passive targeting takes advantage of the unique pathophysiological characteristics of tumor vessels, enabling nanodrugs to accumulate in tumor tissues. Typically, tumor vessels are highly disorganized and dilated with a high number of pores, resulting in enlarged gap junctions between endothelial cells and compromised lymphatic drainage. The 'leaky' vascularization, which refers to the enhanced permeability and retention (EPR) effect, allows migration of macromolecules up to 400 nm in diameter into the surrounding tumor region [73]. Long circulation times will allow for effective transport of the nanoparticles to the tumor site through the EPR effect, which can be modulated by

the interactions of the nanoparticles with the environment and can be modified by changing the nanoparticles' size, particle shape, and surface characteristics [74]. Well-designed nanoparticles in the 10–100 nm size range and with a surface charge either slightly positive or slightly negative should have accessibility to and within disseminated tumors when dosed into the circulatory system [74]. The lower bound is on the basis of sieving coefficients for the glomerular capillary wall, as it is estimated that the diameter threshold for first-pass elimination by the kidneys is 10nm [75]. Moreover, researchers determined that the nanoparticle's capacity to navigate between the tumor interstitium after extravasation increased with decreasing size. By contrast, larger nanoparticles (diameter>100 nm) do not extravasate far beyond the blood vessel because they remain trapped in the extracellular matrix between cells [76]. When nanoparticles enter the bloodstream, the particle surface may experience nonspecific protein adsorption (opsonization), thereby making them more visible to phagocytic cells. After opsonization, nanoparticles, especially the large ones (diameter>200 nm [77]) could be rapidly cleared through phagocytosis by macrophages of the reticuloendothelial system (RES; also known as the mononuclear phagocyte system (MPS)) in the liver and spleen. The surface of nanoparticles can be modified by hydrophilic polymers that results in decreased clearance by the RES/ MPS system, thus increased circulation time. When attached to the surface of nanoparticles, the hydrophilic polymer poly (ethylene glycol) PEG improves the solubility and stability of the nanocarriers in an aqueous solution and imparts stealth characteristics by shielding the nanoparticles from opsonin adsorption and subsequent clearance by the RES/ MPS, leading to longer blood circulation times and improved pharmacokinetic properties [78]. However, targeting cancer cells using the EPR effect is not feasible in all tumors as the degree of tumor vascularization and porosity of tumor vessels can vary with the tumor type and status [79]. To overcome the

limitation of passive targeting, nanoparticles with active targeting were developed by conjugation of peripherally conjugated targeting moieties (folate, transferrin, aptamers, antibodies, peptides, or other small molecules that only bind to specific receptors on the cell surface) for increase endocytosis of the nanoparticles [80]. The folate receptor, a glycosylphosphatidylinositol anchored cell surface receptor with extremely high affinity binding to folate molecule, is overexpressed on a variety of tumors such as epithelial, ovarian, cervical, breast, lung, kidney, colorectal, and etc. , while its expression is limited in healthy tissues and organs [81]. Therefore, modification of nanocarrier with folate molecules has been extensively investigated for targeted drug delivery systems. Poly(lactide-co-glycolide) (PLGA)–PEG micelles with folate conjugated at the PEG terminal end of PEG–PLGA di-block copolymer, entrapping a high loading amount of DOX demonstrated superior cellular uptake over DOX and DOX micelles against a folate-receptor positive cell line. The enhanced cellular uptake was caused by a folate-receptor mediated endocytosis process, which also resulted in increased cytotoxicity. The decrease of cardiotoxicity indicates that the targeting moiety was able to differentiate between healthy and tumor tissue with greater specificity than untargeted DOX [82].Studies from our group also demonstrated a tumor-specific delivery and superior antitumor effect in vivo of an anti-cancer drug using diblock copolymer poly(ethylene oxide)-*b*-poly(methacrylic acid) (PEO-*b*-PMA) to form nanogels decorated with folate targeting groups for ovarian cancer treatment [83]. Folate-decorated polypeptide-based nanogels formed by biodegradable amphiphilic block copolymers, poly(ethylene glycol)-*b*-poly(L-glutamic acid)-*b*-poly(L-phenylalanine) significantly suppressed the growth of intraperitoneal ovarian tumor xenografts outperforming their nontargeted counterparts without extending their cytotoxicity to the normal tissues [84].

Moreover, nanoparticles can bypass drug efflux by ABC transporter as they are internalized via either non-specific or specific endocytosis which results in a higher intracellular accumulation of the drug. Endocytosis involves multiple steps. First, the cargo is engulfed in membrane invaginations that are pinched off to form membrane-bound vesicles, also known as endosomes (or phagosomes in case of phagocytosis). Second, the endosomes deliver the cargo to various specialized vesicular structures, which enables sorting of cargo towards different destinations. Finally, the cargo is delivered to various intracellular compartments, recycled to the extracellular milieu or delivered across cells [85]. There are four main mechanisms of endocytosis: clathrin-mediated endocytosis, caveolae-mediated endocytosis, micropinocytosis and other clathrin-and caveolea-independent endocytosis [86]. Clathrin- and caveolae-mediated endocytosis indicates receptor-mediated endocytosis. Many types of cells use the clathrin- and caveolae-mediated endocytosis pathways to internalize nanoscale materials, including viruses and nanoparticles [87]. Mechanistically, Clathrin-mediated endocytosis involves engulfment of receptors (such as transferrin receptor, low density lipoprotein receptor, epidermal growth factor receptors, human epidermal growth factor receptor 2 and etc.) associated with their ligands to a coated pit, which forms due to polymerization of a cytosolic protein called clathrin-1 and assembly proteins like AP180 and AP-2. The assembled vesicle (ca. 120 nm) is pinched off from the plasma membrane and the vesicles fuse with the early endosomes where they are sorted to late endosomes/lysosomes, to trans-Golgi network or to the recycling endosomes to be transported back to plasma membrane [85]. Clathrin-mediated endocytosis appears to be defined as the most prominent mechanism for the PEG-PLA nanoparticles, PLGA nanoparticles, silica-based nanomaterials, chitosan nanoparticles, Pluronic® micelles and surface modified nanoparticles with the

surface ligand such as transferrin [85, 88]. Caveole-mediated endocytosis is the most common type of clathrin-independent receptor-mediated endocytosis. After binding to the cell membrane, nanocarrier move along the membrane to the caveolar invagination and form caveolar endocytic vesicles. The released caveolar vesicle can fuse with early endosome or caveosome, an endosomal compartment with neutral pH. Several nanomaterials are reported to enter cells via caveolae, including polymeric micelles with cross-linked anionic core, DOXIL®, polysiolxane nanoparticles, quantum dots, Abraxane®, Pluronic® unimers and surface-modified nanoparticles with the surface ligands include folic acid, albumin, and cholesterol [85, 88].

The majority of anticancer agents including paclitaxel, etoposide and docetaxel are highly hydrophobic, which leads to poor aqueous solubility and low bioavailability at the target site and limits the use of intravenous (IV) administration. The use of nanocarriers such as lipid- or phospholipid-based nanocarriers, polymer-or dendrimer-based nanocarriers and albumin-based nanoformulation can enhance the solubility of hydrophobic drugs in aqueous solutions, prevent drugs from premature in vivo degradation and provide sustained and controlled drug release over a long period of time [89]. Acidic extracellular pH is a major feature of tumor tissue, extracellular acidification being primarily considered to be due to lactate secretion from anaerobic glycolysis [90]. Much research effort has been directed to the development of pH-sensitive polymeric nanoparticles for intracellular drug delivery in that there exist natural pH gradients in the tumor microenvironment (pH 6.5–7.2) and in the endosomal/lysosomal compartments of tumor cells (pH 4.0–6.5). Taking advantage of acidic extracellular pH (6.5–7.2) in the tumor compared with the normal tissues, pH-sensitive nanoparticles have been developed to achieve accelerated drug release at the tumor site. Moreover, polymeric nanoparticles are usually internalized by cancer cells via

endocytosis. Following endocytosis, rapid endosomal acidification occurs due to a vacuolar proton ATPase-mediated proton influx, which leads to a drop of pH levels in the endosomes to approximately 5.0–6.5 and 4.0–5.0 in the lysosomes [91]. In the past few years, acid-sensitive nanoparticles that are prone to swelling, dissolution or degradation at endosomal/lysosomal pH (4.0–6.5) have been devised to obtain fast intracellular drug release in tumor cells in order to enhance the therapeutic efficacy, reverse multidrug resistance in tumors and resolve the extracellular stability and intracellular drug release dilemma. One type of pH-sensitive nanoparticles has been designed based on polymers containing protonable amine groups, such as primary, secondary and tertiary amines [88]. For example, pH-sensitive nanoparticles of poly(ethylene glycol)-poly(L-histidine)-poly(L-lactide) (PEG_{45}-$PHis_{45}$-$PLLA_{82}$) triblock copolymers had higher release rate at pH 5.0 compared to pH 7.4 due to protonation of the imidazole groups in the PHis block, inducing a high antitumor effect in HepG2 cells [92]. DOX-loaded PEGylated nanogels containing a pH-sensitive polyamine core exhibited superior antitumor activity against drug-resistant human hepatoma HuH-7 cells compared with their free DOX and the DOX-loaded, pH-insensitive, PEGylated nanogel. Using fluorescence microscopy, pH-sensitive PEGylated nanogel in HuH-7 cells was found to be initially localized within the endosome and/or lysosome, with subsequent release of DOX from the nanogel in response to the endosomal pH, and ultimately, diffusion via the cytoplasm into the cell nucleus [93]. Our lab also has developed the DOX-loaded PEO-*b*-PMA polymer micelles that exhibited noticeable pH-sensitive behavior with accelerated release of DOX in acidic environment due to the protonation of carboxylic groups in the cores of the micelles, resulting in a potent cytotoxicity against human A2780 ovarian carcinoma cells [94]. Another type of pH-sensitive nanoparticles has also been developed by incorporating acid-cleavable bonds such as hydrazone, acetal, imine and oxime bonds onto polymer

main or side chains [91]. For example, DOX was conjugated via pH-sensitive hydrazone linkage along with PEG to a biodegradable, non-toxic and non-immunogenic nanoconjugate platform: poly (β-L-malic acid) (PMLA). DOX-nanoconjugates were found stable under physiological conditions. The majority of DOX (>80%) was released from the PMLA-platform under acidic pH prevalent in late endosome and lysosomes [95]. Benzoinc imine bond was used cholate grafted poly (L-lysine), (PLL-CA)/PEG-DOX vesicle, resulting in pH respnisive permeability and dissociation of the nanoparticles following an environmental pH dropping from 7.4 to 5.0 [96].

1.2.5 Combinatorial nanoparticles against MDR in cancer

Many combinatorial nanoparticle formulations have been developed by co-delivering combination of chemosensitizing agents and chemotherapy agents to reverse MDR in in vitro and in vivo cancer models, including combinations of MDR modulators with chemotherapeutics and combination of MDR-targeted siRNA with chemotherapeutics [97].

1.2.5.1 Combinations of MDR modulators with chemotherapeutics

The combination of a chemotherapeutic drug with a MDR modulator has emerged as a promising strategy to restore the sensitivity of tumor cells and enhance the therapeutic efficacy of cancer treatment both in vitro and in vivo. The first attempt to co-deliver a MDR modulator with chemotherapeutics was polyalkylcyanoacrylate nanoparticles loaded with P-gp inhibitor cyclosporine A (CyA) and DOX. The incorporation of DOX and CyA in the same nanoparticle formulation elicited the most effective growth rate inhibition to multidrug-resistant murine P388/ADR leukemia cell line compared to other alternative approaches such as

mixed solution of DOX + CyA, DOX-only nanoparticles or DOX-nanoparticles with free CyA, probably as a result of a synergistic effect due to the rapid release of a high amount of CyA at the surface of the cell membrane allowing a facilitated intracellular diffusion of DOX [98]. Paclitaxel and tariquidar (P-gp inhibitor) loaded PLGA nanoparticles showed significantly higher cytotoxicity in vitro than nanoparticles loaded with paclitaxel alone, which could be correlated with increased accumulation of paclitaxel in drug-resistant adenocarcinoma cells. Paclitaxel and tariquidar (P-gp inhibitor) biotin-functionalized loaded PLGA nanoparticles showed significantly greater anti-tumor efficacy and higher overall survival rate in a mouse model of drug-resistant tumor at a paclitaxel dose that was ineffective in the absence of tariquidar [99]. To ensure two drugs could be simultaneously delivered to tumor region at the optimum ratio, and the MDR modulator could be released earlier and faster than the chemotherapeutic drug to inactivate P-gp and subsequently inhibit the pumping out of the chemotherapeutic drug, a smart pH-sensitive polymeric micelles system loaded with DOX and disulfiram (DSF) (P-gp inhibitor) was developed. DOX was conjugated to poly (styrene-co-maleic anhydride) (SMA) derivative with adipic dihydrazide (ADH) through an acid-cleavable hydrazone bond, and then DSF was encapsulated into the micelles formed by the self-assembly of SMA-ADH-DOX conjugate. The co-delivery system enabled a temporal release of two drugs: encapsulated DSF was released fast to inhibit the activity of P-gp and restore cell apoptotic signaling pathways, while the conjugated DOX was released in a sustained and pH-dependent manner and highly accumulated in cancer cells to exert therapeutic effect. It was proved that the co-delivery system exhibited superior anti-tumor activity high tumor accumulation and excellent antitumor effect in MDR tumor with low systemic toxicity in MCF-7/ADR tumor-bearing mice [100]. Except for being as inhibitors of drug efflux transporters, some compounds also sensitize the MDR tumor by

repairing the dysfunctional apoptotic associated with MDR. Curcumin, an inhibitor of nuclear factor kappa B (NFκB) as well as a potent down-regulator of ABC transporters, was encapsulated in flaxseed oil containing nanoemulsion formulations with paclitaxel. The coadministration system increased accumulation of paclitaxel and enhanced apoptosis within MDR-1 positive SKOV3TR ovarian adenocarcinoma cells [101]. Curcumin was observed to not only inhibit the nuclear efflux of DOX but also downregulate the gradual expression of MDR1 and BCL-2 at the mRNA level, leading higher cytotoxicity of K562 human leukemia cells treated with DOX /curcumin loaded PLGA nanoparticles. Both the drugs induced a number of apoptotic pathways, leading to a higher expression of a number of apoptotic proteins [102]. Curcumin was also demonstrated to reverse cis-platin resistance and trigger apoptotic death of human lung adenocarcinoma A549/DDP cells by promoting HIF-1α degradation and activating caspase-3, respectively [103].

1.2.5.2 Combinations of MDR-targeted siRNA with chemotherapeutics

Coadministration of anticancer drugs and siRNAs offer another very promising strategy to enhance the therapeutic efficacy in various MDR tumor models. As discussed above, siRNAs can down-regulate the expression of MDR proteins to overcome both pump resistance and nonpump resistance. For example, PEI-coated mesoporous silica nanoparticles loaded with P-gp siRNA and DOX restore the DOX sensitivity in drug-resistant KB-V1 squamous carcinoma cell line where the delivered siRNA silenced the expression of P-gp which consequently increased the intracellular concentration of DOX [104]. In vivo studies demonstrated significantly greater inhibition of tumor growth in a drug-resistant tumor bearing mouse model following treatment with biotin-functionalized

PLGA-PEI nanoparticles encapsulating both paclitaxel and P-gp targeted siRNA at a paclitaxel dose that was ineffective in the absence of gene silencing [105]. siRNAs that overcome nonpump resistance of MDR have been encapsulated in nanocarriers combined with anti-cancer therapeutics. Zheng et al. reported the co-delivery of Bcl-2 siRNA and docetaxel using polymer micelles formed by poly (ethylene glycol)-b-poly(L-lysine)-b-poly(L-leucine) (PEG-PLL-PLLeu) triblock copolymers. The hydrophobic PLLeu core entrapped with anticancer drugs, while the PLL polypeptide cationic backbone allowed for electrostatic interaction with the negatively charged siRNA. The co-delivery system downregulated the anti-apoptotic Bcl-2 gene and enhanced antitumor activity with a smaller dose of DTX, resulting in the significantly inhibited tumor growth of MCF-7 xenograft murine model as compared to the individual siRNA and only DTX treatments [106]. Wang *et al.* developed a new nanocarrier platform E-NP, composed of amphiphilic block copolymer of methoxy poly(ethylene glycol)–poly(lactide-co-glycolide) (mPEG–PLGA) and ε-polylysine (EPL), simultaneously delivering both hydrophilic and hydrophobic chemotherapeutics along with siRNA. Dox was packaged into the hydrophilic core of the nanoemulsion, while paclitaxel was encapsulated into the hydrophobic layer. Survivin siRNA was complexed onto the surface of the nanoemulsion through electrostatic interactions with EPL. Survivin siRNA, which was adsorbed on the outmost layer of the NPs and released first before both DOX and TAX could reach the tumor cells, sensitized and expanded the current chemotherapeutic regimen of DOX and paclitaxel [107].

1.3 Pluronic® block copolymers for overcoming MDR in cancer

Polymer-based nanotechnology became one of the fastest growing areas of pharmaceutical research and attracted tremendous attention during the last two decades. As discussed above, the roles polymer nanoformulation play included: 1) increase of drug solubility and stability by drug encapsulation, which alone exhibit poor solubility, undesired pharmacokinetics and low stability in a physiological environment.; 2) passive or active targeting of drug into tumor sites by the EPR) effect or molecular targeting moieties modified on the surface of the nanoformulation; 3) increased cellular uptake by either “passive” endocytosis or receptor-mediated endocytosis, thus bypassing drug efflux transporters on the plasma member; 4) controlled and sustained release of the drug at the tumor site in response to specific tumor conditions, such as pH or presence of particular enzymes, thus reducing systemic toxicity; 5) simultaneous delivery of several cytotoxic drugs or cytotoxic drugs with MDR modulator/siRNA to achieve synergetic anti-tumor effect. Additionally, polymeric carriers can exhibit biological activity of their own, acting as a biological response modifier that potentiates the drug cytotoxic effect in tumor cells [108]. One of the promising examples of amphiphilic block copolymers which benefit the above properties is Pluronic® block copolymers, which are listed in the U.S. and British Pharmacopoeia under the name “poloxamers” as excipients and are widely used in a variety of clinical applications [109, 110]. Previous studies demonstrated that Pluronic® block copolymers sensitize MDR cancer cells resulting in increased cytotoxic activity of Dox, paclitaxel, and other drugs by 2-3 orders of magnitude [111, 112]. A lot of efforts have been spent on overcoming drug resistance of Pluronic® block copolymers working as drug nanocarriers as well as chemosensitizer for MDR cells.

1.3.1 Pluronic® block copolymers as micellar nanocarriers for drug delivery

Pluronic® block copolymers consist of hydrophilic poly (ethylene oxide) (PEO) and hydrophobic poly (propylene oxide) (PPO) blocks arranged in A-B-A triblock structure: PEO-PPO-PEO, which is non-ionic in nature. Due to the amphiphilic nature of these block copolymers, Pluronic® block copolymers are an important class of surfactants and widely used in pharmaceutical systems as suspending, adjuvants, adhesives, emulsifying agents and coating material for controlled and site specific drug delivery systems [113]. Because of large solubility differences between hydrophobic and hydrophilic moieties, in aqueous medium they are able to self-assemble into polymeric micelles consist of water-insoluble cores and water-soluble shells. Depending on blocks length, core can assemble into various supramolecular structures characterized by different morphologies above a certain concentration or temperature [113]. Due to this characteristic, the core–shell (core of PPO and shell of PEO) micelles of Pluronic® can be used to solubilize poorly water soluble drugs and can function as effective drug carriers [114, 115].

1.3.1.1 Pluronic® block copolymers structure

Pluronic® block copolymers, PEO_x-PPO_y-PEO_x, is an amphiphilic copolymer, in which the number of hydrophilic PEO and hydrophobic PPO units can be altered. The physical and chemical properties of Pluronic® block copolymers can be finely tuned by modifying the molar mass ration between the PEO and PPO blocks (from 1:9 to 8:2). The structure formula of Pluronic® block copolymers is shown in **Fig. 1. 2**. **Table 1.1** presents a list of selected Pluronic® copolymers which are commercial available from

BASF Corp. Copolymers with various *x* and *y* values result in variable hydrophilicity/hydrophobicity, which are characterized by distinct hydrophilic–lipophilic balance (HLB) [115]. The trade names of the Pluronic® block copolymers are also known such as L61, P85 and F127. The First letter L, P or F refers to the liquid, paste or solid form of the block copolymers. The Last digit multiplied by the gives the mass percent of the PEO block while the first one or two digits refer to the Pluronic® grid and provide 1/300 of the molar mass of the PPO block. For example, L61 is liquid with 10% of molar mass percentage of PEO per individual block copolymer molecule (unimer) and PPO molecular mass of 1800 g/mol. F127 is paste with 70% of molar mass percentage of PEO per unimer and PPO molecular mass of 3600 g/mol [116].

1.3.1.2 Micellization and solubilization

The solubility of Pluronic® block copolymers in water depends on their structure as well as the temperature. Below room temperature, both types of blocks within a Pluronic® molecule are hydrated and are relatively soluble in water. Increase of the temperature promotes dehydration of firstly, PPO block and secondly, PEO blocks, thus decreasing the solubility of the block copolymers. At physiological temperature, 37°C, PPO chains are water-insoluble while PEO chains are well-hydrated and water-soluble. Below critical micelle concentration (CMC), the amphiphilic molecules have a strong tendency to be absorbed at the air/water interface. With the increase of the concentration of block copolymers, a point, defined as CMC, is reached when both the interface and the bulk of the solvent (water) become saturated with monomeric copolymers. The unimer molecules aggregate to form micelles through the process called “micellization” at the concentrations of block copolymer above CMC in water by

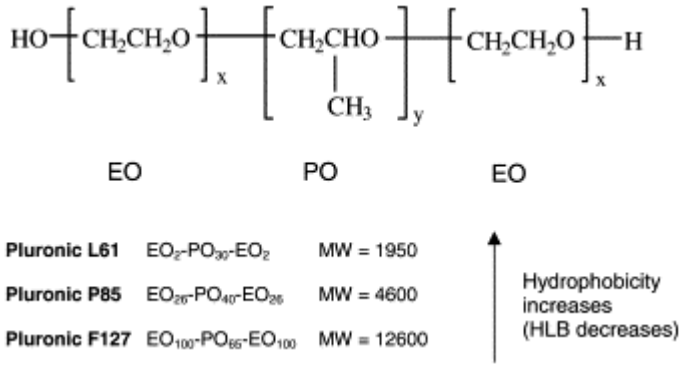

Fig. 1.2 Pluronic® block copolymers available from BASF (Wyandotte, MI), contain two hydrophilic EO blocks and a hydrophobic PO block. (Adapted from [184])

Table 1.1 Physicochemical characteristics of Pluronic® block copolymers

Copolymer	MW[a]	Average no. of EO units (x)[b]	Average no. of PO units (y)[b]	HLB[c]	Cloud point in 1% aqueous solution (°C)[c]	CMC (M)[d]
L35	1900	21.59	16.38	19	73	5.3×10^{-3}
L43	1850	12.61	22.33	12	42	2.2×10^{-3}
L44	2200	20.00	22.76	16	65	3.6×10^{-3}
L61	2000	4.55	31.03	3	24	1.1×10^{-4}
L62	2500	11.36	34.48	7	32	4.0×10^{-4}
L64	2900	26.36	30.00	15	58	4.8×10^{-4}
F68	8400	152.73	28.97	29	>100	4.8×10^{-4}
L81	2750	6.25	42.67	2	20	2.3×10^{-5}
P84	4200	38.18	43.45	14	74	7.1×10^{-5}
P85	4600	52.27	39.66	16	85	6.5×10^{-5}
F87	7700	122.50	39.83	24	>100	9.1×10^{-5}
F88	11 400	207.27	39.31	28	>100	2.5×10^{-4}
L92	3650	16.59	50.34	6	26	8.8×10^{-5}
F98	13 000	236.36	44.83	28	>100	7.7×10^{-5}
L101	3800	8.64	58.97	1	15	2.1×10^{-6}
P103	4950	33.75	59.74	9	86	6.1×10^{-6}
P104	5900	53.64	61.03	13	81	3.4×10^{-6}
P105	6500	73.86	56.03	15	91	6.2×10^{-6}
F108	14 600	265.45	50.34	27	>100	2.2×10^{-5}
L121	4400	10.00	68.28	1	14	1.0×10^{-6}
P123	5750	39.20	69.40	8	90	4.4×10^{-6}
F127	12 600	200.45	65.17	22	>100	2.8×10^{-6}

[a] The average molecular weights provided by the manufacturer (BASF, Wyandotte, MI).

[b] The average numbers of EO and PO units were calculated using the average molecular weights.

[c] HLB values of the copolymers; the cloud points were determined by the manufacturer.

[d] CMC values were determined previously using pyrene probe [117].

(Adapted from [139])

the driving force of the hydrophobic interactions of the PPO blocks [118].The CMC of the block copolymers is strongly dependent on the lengths of the blocks. An increase in the length of the hydrophobic PPO block elevates the net hydrophobicity of the Pluronic® molecule and favors the segregation of the PPO chains into the micelle core, resulting in a CMC decrease. In contrary, an increase in the lengths of the PEO blocks elevates the probability of contacts of the PPO units with the PEO units within the core of the micelles, which decreases the hydrophobicity of the core and results in destabilization of the micelle. Therefore, the CMC increases as the hydrophilic PEO block length is increased [118].

Pluronic® micelles are commonly pictured as spheres with a PPO inner core and a hydrophilic PEO corona. The micelle size, aggregation number and morphology of the Pluronic® block copolymers aggregates strongly depend on the block copolymer composition, specifically, the lengths of PEO and PPO units, the block copolymer concentration and environmental parameters such as temperature and the quality of the solvent [119, 120]. Spherical micelles commonly have an average hydrodynamic diameter ranging from about 20 to 80nm, within the preferred nanoparticles size range 10–100 nm discussed above and aggregation numbers ranging from 10 to several dozen [120]. Except for the spherical structure, additional micelle morphologies include lamella and rods (cylinders). Nagarajan predicted the formation of cylindrical and lamellar structures by modeling the framework of a simple molecular theory of solubilization. It was found that solubilization is shown to induce a transition in aggregate shapes from spheres to cylinders and then to lamellae [120]. For example, the lamellar aggregates are favored when the ratio of PEO: PPO is small while spherical aggregates are favored when the PEO: PPO ratio is large. Typically, for block copolymers containing 40 or more weight percent PEO, only spherical aggregates form at 25°C. For block

copolymers containing 30 wt% PEO, cylindrical aggregates are possible. Block copolymers containing 20 or less weight percent PEO generate lamellae [120]. It has been demonstrated that increase of the temperature, which induced the decrease of solubility, led to the transition into cylindrical or lamellar geometries [121].

The hydrophobic core can serve as a microenvironment that can enhance the loading efficiency of hydrophobic drugs which alone exhibit poor solubility, undesired pharmacokinetics and low stability in a physiological environment. This process is referred to as "solubilization". The outer hydrophilic shell severs as a stabilizing interface between the hydrophobic core and the aqueous medium to ensure the micelles remain in a dispersed state and decrease undesirable drug interactions with cells and proteins [115]. The extent of drug incorporation in Pluronic® micelles is dependent on factors including the molecular volume of the solubilizate, the interfacial tension of the solubilizate against waster, length of the core and shell-forming blocks in the copolymer and the polymer and solubilizate concentrations [122]. It seems reasonable that longer PPO blocks would produce larger hydrophobic inner core, suggesting hydrophobic core of micelles as locus of solubilization [123]. Moreover, Nagarajan demonstrated that the amount of the incorporated solubilizate increases as the molecular volume of the solubilizate decreases [120]. Furthermore, the solubilization capacity is increased when high compatibility exsists between the micellar core and the solubilizate and the solubilizate-water interfacial tension is lower [122].

1.3.1.3 Stability and drug release of Pluronic® micelles

The CMC and the partition coefficient are the major thermodynamic constants determining the stability of the micellar carrier and the drug release in equilibrium

condition. The dilution of the micelles, for example, in the body fluids, leads to the release of the encapsulated drug. If the system is diluted below the CMC, the micelles are completely disintegrated and the drug is prematurely release the drug into blood following intravenous injection [118]. The low stability of Pluronic® micelles results in failure of increase in drug circulation time and delivery of the drug to the tumor site by the EPR effect, which limits the practical use of systemic delivery of drugs. In order to overcome the poor stability and low drug entrapment efficiency of Pluronic® micelles, several methods have been developed.

Mixed micelles composed different Pluronic® block copolymers were explored to encapsulate hydrophobic drug with high drug loading capacity as well as improving the stability of the micellar systems. Mixed micelles composed of relatively hydrophobic Pluronics® L61/P123/P105 and relatively hydrophilic Pluronics® F127 incorporating insoluble anticancer therapeutics have been evaluated in vitro and in vivo [124, 125, 126, 127]. The relatively hydrophobic block copolymers with a greater portion of PPO, was able to load satisfactory hydrophobic drug content. However, due to the rather short PEO length, the stability of micelles is not desirable. Owing to the high PEO-PPO ratio, F127 possessed a lower CMC value, creating a stable and effective delivery system. Mixed micelles of ionic and nonionic surfactants show advantageous solubilization behavior and an expanded stability when compared with the pure nonionic system. The phospholipids mixed micelles had lower CMC than that of polymeric micelles and overcame the thermodynamic instability present in polymeric micelles [128]. Vitamin E succinate modified pluronic® micelles showed enhanced encapsulation efficiency and better stability as compared to the non-modified controls [129].

Another method to increase the stability of Pluronic® micelles is the formation of crosslinks within their outer shells. To form crosslinks, the two terminal alcohols on L121

were first chemically converted into aldehydes (L121-CHO) using the Dess–Martin periodinane. Diamine compounds were then used to bridge the converted aldehyde termini on L121-CHO via conjugated Schiff bases. After crosslinking, the morphology of the L121 micelles remained spherical in shape, the sizes were comparable before and after crosslinking and the micelle stability was greatly enhanced [130]. The stabilization of Pluronic® micelles composed of Pluronic® P94 and F127 was obtained through incorporation of a hydrophobic cross-linking agent and subsequent photo-polymerization, which prevented micelle disruption below CMC or the critical micelle temperature (CMT), the temperature below which only single chains are present, while maintaining the integrity of the PEO corona and the hydrophobic properties of the PPO core [131].

Another attractive strategy to eliminate the burst and premature release of the drug could be forming polymeric micelles by conjugating drugs to the polymer backbone via covalent bonds, which can hold the drug firmly in the micelles during circulation in the blood. To form the DOX- Pluronic® F68 conjugate, the end group of pluronic® F68 was modified to a carboxyl group and then then chemically conjugated with DOX via an amide. Drug release profile showed that the DOX- Pluronic® F68 micelles maintained a sustained DOX release at pH 7.4. The release of DOX from the micelles was accelerated when the PH was reduced to 6.0 comparing with PH 7.4, due to the protonation of carboxylic groups at the acidic PH [132]. Another novel polymer-drug conjugate was prepared by the chemical reaction between the copolymer Pluronic® P123 and the docetaxel via a pH sensitive hydrazone bond. With a low CMC, these pH sensitive P123- docetaxel conjugates could self-assemble into nano-size polymeric micelles in aqueous solution. With the introduction of the covalent hydrazone bonds, these pH sensitive polymeric conjugate micelles were proved to exhibit their stability

against the rat plasma and show a pH dependent drug release, showing the potential to antitumor drug delivery [133].

1.3.1.4 Pluronic®-based drug delivery systems

Pluronic® micelles containing water insoluble or poorly water-soluble drugs [134], polypeptides [135], plasmid DNA [136], oligonucleotides [137] as well as diagnostic imaging agents [138] have been investigated as potential drug delivery systems in multiple applications. For example, Pluronic® micelles were utilized for delivery of central nervous system (CNS) drugs across the blood brain barrier (BBB) [139, 140, 141], oral delivery of drugs to improve oral bioavailability [142, 143], pulmonary delivery of drugs by inhalation [144] and especially tumor-specific delivery of antineoplastic agents [145, 146]. Following are the examples of Pluronic®-based drug delivery systems targeted to the MDR tumors.

SP1049C, which contained DOX in the mixed micelles of Pluronics L61 and F127, was the first in class polymeric micelle drug to advance to clinical stage [124] and has successfully completed phase II clinical trial which showed high objective response rates (47%) in the evaluable population and increased median survival (10 months) and progression free survival (6.6 months) in patients with inoperable metastatic adenocarcinoma of the esophagus and gastro esophageal junction with toxicity profile similar to that of Dox at equivalent dose and administration schedule [147].SP1049C also have been shown recently to decrease the tumorigenicity and aggressiveness of cancer cells in vivo, suppress BCRP overexpression and the Wnt-β-catenin signaling activation observed with Dox alone, significantly alter the DNA methylation profiles, as well as depletes CD 133+ cells populations, which displayed cancer stem cells (CSCs)-

like properties and were much more tumorigenic compared to CD133- cells in murine leukemia model [148]. Other systems paclitaxel, methotrexate, or docetaxel loaded polymeric micelles mixed with Pluronic® P105 and F127 has been evaluated in vitro and in vivo [125,127,127]. All the systems indicated that drug loaded Pluronic® micelles displayed higher anti-tumor efficacy than free drug in both MDR cancerous cell lines and MDR tumor xenografts with higher blood circulation time and less systemic toxicity in comparison with drug alone injection. Moreover, docetaxel-loaded P105/F127 mixed micelles displayed a higher cytotoxicity towards human lung adenocarcinoma A549-Taxol resistant cells than Taxotere®, the commercial preparation that approved by the FDA in 2004 . Longer mean residence time in circulation, larger area under the plasma concentration-time curve and higher tumor inhibition rate were observed with docetaxel-loaded P105/F127 mixed micelles compared to Taxotere®, indicating the potential of P105/F127 mixed micelle as a drug drug delivery system to overcome multidrug resistance in lung cancer [127].

Targeting moieties- conjugated Pluronic® block copolymers have been developed to form micelles for active targeting. cyclic RGD [arginine-glycine-aspartic acid] peptide (c(RGDyK)) that can bind to the integrin protein richly expressed at the site of tumor vascular endothelial cells and tumor cells with high affinity and specificity, was conjugated to the *N*-hydroxysuccinimide-activated PEO terminus of the Pluronic F127 block copolymer. c(RGDyK)-decorated Pluronic F127 and P105 mixed micelles are developed in this study to form a dual-functional drug delivery system for the antiangiogenesis and modulation of drug resistance [149]. Folic acid and its conjugate were widely used for selective delivery of anti-cancer agents to cells with folate receptors. Folic acid functionalized Pluronic P123/F127 mixed micelles was efficiently internalized into the cells through by folate receptor-mediated endocytosis, leading to

faster and larger extent of drug delivery by folic acid-conjugated micelles compared with that by non-targeted micelles [125].

Pluronic®-based drug delivery systems were also explored for gene delivery. A I Belenkov et al evaluated PEI grafted with nonionic amphiphilic block copolymer, Pluronic® P85 (P85-g-PEI) as a carrier for Ku86 ASO delivery [150]. Compared with PEI/DNA complex, P85-g-PEI/DNA formulations significantly reduced aggregation due to the effect of nonionic chains that are soluble in aqueous dispersions and prolonged the circulation time after systemic administration while the high transfection activity was remained. Jianan She and other authors developed and investigated a new co-delivery system, P85-PEI/ D-α-tocopheryl polyethylene glycol 1000 succinate (TPGS) complex nanoparticle, conveying chemotherapeutic agent and RNA for reversing drug resistance [151]. TPGS was used to improve micelle stability and drug loading; P85 was used for preparing micelles and inhibit GST activity, which may contributed to the direct decrease of the metabolism of drug and potentiate the drug-induced cell apoptosis and PEI was used to bind shRNA. The IC_{50} of formulation against PTX resistant human lung adenocarcinoma epithelial (A549/T cells) was 360-fold lower than that of free drug and better antitumor efficacy of formulation was observed in vivo.

1.3.2 Pluronic® block copolymers acting as chemosensitizer for MDR cells

Besides the ability to self-assemble into micelles, Relatively hydrophobic Pluronic® block copolymers at concentrations below the Critical Micelle Concentration (CMC) with intermediate length of PEO units from 30 to 60 and HLB <20 [152, 153] can sensitize MDR cancer cells mainly by ABC transporters inhibition and selective ATP depletion, which is accompanied with generation of reactive oxygen species (ROS) and

simultaneously inhibition of glutathione/glutathione S-transferase (GSH/GST) detoxification system [154 , 155 , 156]. On the other hand, the Pluronic-caused impairment of respiration in mitochondria decreased the mitochondrial membrane potential, promoted release of cytochrome c and overall enhanced pro-apoptotic signaling (Bax, p53, APAF1, caspase 9 and caspase 3) and mitigated anti-apoptotic cellular defense (Bcl-2 and Bcl-xl) of MDR cells **(Fig.1.3)** [157].

1.3.2.1 Structure-functional relationship of Pluronic® block copolymers

The relationship between composition of Pluronic® block copolymers and their biological response-modifying effects has been investigated. Batrakova et al demonstrated that the MDR sensitizing effects were achieved by Pluronic® block copolymers at the concentration below the CMC. When the concentration below the CMC, the resistance reversion indexes (i.e., ratio of the IC_{50} of the drug in the assay buffer and Pluronic solution ($IC_{50.0}/IC_{50}$)) rapidly increased with increasing copolymer concentration and reached 400-fold (KBv) and 3400-fold (MCF-7/ADR) as copolymer concentration approached the CMC values. At concentration above the CMC, the leveling off of cytotoxicity was observed and the drug cytotoxicity decreased as concentration continued to rise **(Fig.1.4A)** [152]. Thus, the sensitizing effect on MDR cells is mediated by the copolymer signal chain unimers, rather than the micelles.

The specific effects on transporter activity profiles and the critical factors that influence transporter activity (i.e., membrane fluidization, energy depletion) in both sensitive and drug resistant cells has been conducted with a series of Pluronic® block copolymers with a wide range of HLB [152, 153]. Results of R123 (the fluorescent dye,

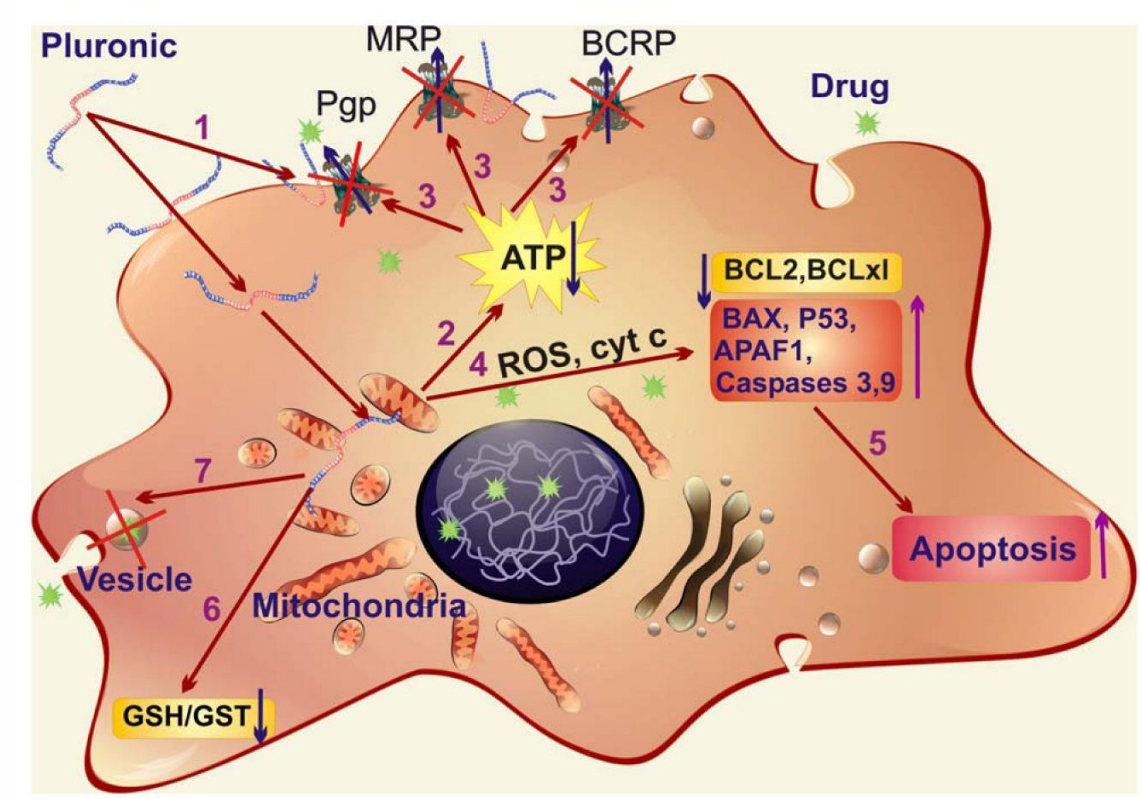

Fig.1.3 Multiple effects of Pluronic® block copolymers in MDR cells: 1) incorporation of Pluronic molecules into membranes and decrease of the membrane microviscosity; 2) induction of ATP depletion; 3) inhibition of drug efflux transporters; 4) release of cytochrome c from mitochondria and increase in ROS levels in cytoplasm; 5) increase of pro-apoptotic signaling and decrease of anti-apoptotic defense in MDR cells; 6) inhibition of the glutathione/glutathione S-transferase detoxification system; and 7) abolishment of drug sequestration within cytoplasmic vesicles. (Adapted from [119])

P-gp substrate) accumulation studies suggested that the sensitizing effects of Pluronic® block copolymers in MDR cells depend on the copolymer hydrophobicity. The entire set of the hydrophilic Pluronic® block copolymers with HLB varying from 20-29, presented in **Table.1.1**, at concentrations below the CMC, had no or little effect on R123 accumulation. Except for the HLB values, the length of PPO block also plays an important role in the inhibiting the P-gp transporters. It was found a bell-shaped dependency of the length of hydrophobic PPO segment in inducing R123 uptake. The maximal effects on the drug uptake were characteristic of Pluronic® block copolymers with intermediate length of PPO block ranging from 30 to 60 **(Fig.1.4B)** [153]. The same bell-shaped curves were observed of the total microviscosity factor values (value of total cellular membrane microviscosity in the control group in the absence of the Pluronic® block copolymers versus those observed in the presence of the Pluronic® block copolymers) or ATP depletion factor (ATP intracellular levels in the absence of the Pluronic® block copolymers versus those observed in the presence of the Pluronic® block copolymers) corresponding to the length of PPO blocks. Lipophilic copolymers with intermediate PPO block decreased the microviscosity in bovine brain microvessel endothelial cells (BBMECs), indicating their incorporation into the lipid bilayer and subsequent increase in membrane fluidization and reduced the intracellular ATP level at significantly high extent. Very lipophilic block copolymers with long PPO blocks, the most membranotropic block copolymers, anchor in the plasma membranes and remain there for an extended period of time. As a result, although they are potent inhibitors of P-gp ATPase, they are less efficiently transported into the cell and cause less ATP depletion and, consequently, have less effect on P-gp efflux system compared with the intermediate block copolymers. In contrast, the block copolymers displaying intermediate lipophilicity transport across the membranes, and spread throughout

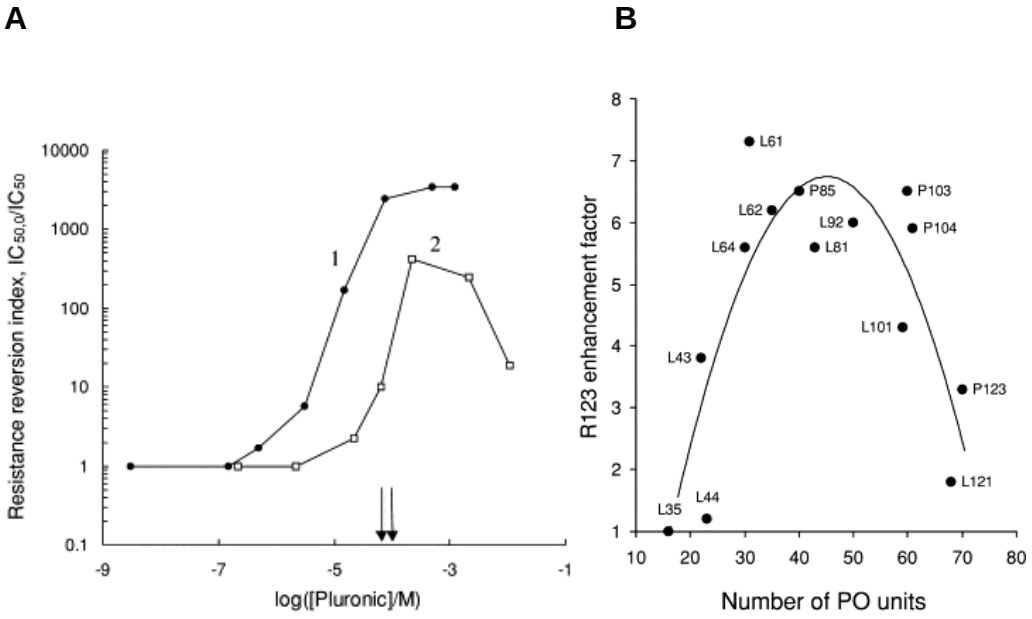

Fig.1.4 (A) Effects of Pluronic® block copolymers on cytotoxicity of DOX with respect to MDR cells: curve 1, MCF7/ADR cells were treated with doxorubicin–L61 compositions; curve 2, KBv cells were treated with doxorubicin–P85 compositions containing varying concentrations of the block copolymer. Resistance reversion indexes (ratio of IC_{50} of DOX in the assay buffer and Pluronic® solution) are plotted as functions of the concentration of the block copolymers. (B) Efficacy of Pluronic® block copolymer composition in MDR KBv cells. R123 enhancement factors are defined here as the ratios of R123 accumulation in the cells in the presence of the block copolymer to R123 accumulation in the assay buffer. (Adapted from [152])

the cytoplasm and reach cellular organelles and to some extent the nuclei. Another factor of low sensitization effect of very lipophilic block copolymers is due to their low CMC. They tend to form micelles at low concentrations of the copolymers in aqueous solutions and decrease the inhibition effect of Pluronic® molecules on ABC transporters of MDR cells. Overall, the most efficacious block copolymers are those with intermediate lengths of PPO block and relatively hydrophobic structure (HLB <20), such as Pluronic® P85 or Pluronic® L61.

1.3.2.2 Inhibition of ABC transporter activity by Pluronic® block copolymers: role of Pluronic-membrane interaction

ABC transporters are one of the distinctive characteristics of MDR tumors as discussed before. The Pluronic® copolymer-cell interaction starts from the cell membrane, where the ABC transporters are located. Pluronic® block copolymers binding to cell membrane is associated with two steps: 1) hydrophilic interactions of PEO chain blocks with the polar groups of the lipids at the membrane surface (absorption at the membrane) and the hydrophobic interactions of PPO chain blocks with the fatty acid residues in the lipid bilayer (insertion in the membrane) [9]. Relatively hydrophilic Pluronic® block copolymers could only absorb on the membrane without penetrating into the lipid bilayer while relatively hydrophobic copolymers could insert into the membrane below the polar head groups, loosen the lipid packaging and translocate through the membrane. The immersed Pluronic® block copolymers disrupt the plasma membrane integrity, which results in decreased membrane microviscosity, accompanied with conformational changes in the transport proteins and inhibition of P-gp or MRP ATPase activity in the cells overexpressing these transporters [158, 159]. Moreover, ATPase

activity inhibition by Pluronic® block copolymer may be attributed to sterically hindered protein-drug interaction in the appropriate binding sites, supported by the observation of the decreases in the maximal reaction rates and increases in apparent Michaelis constants for these transporters in the presence of Pluronic® P85 [159].

Pluronic® P85 was found to have more pronounced inhibition effects on P-gp ATPase activity compared with the effects on MRP1 and MRP2 [159]. One reason could be the structure of MRPs is more robust and less vulnerable to the conformational changes caused by P85 than the structure of P-gp. The other reason is due to the high affinity drug-binding sites of MRPs, making less accessible for the hindrance by the block copolymer than similar sites of P-gp since Pluronic unimers can selectively localize in particular domains of cellular membrane called caveolae /lipid rafts and employ caveolae-mediated endocytosis pathway for cellular entry [88], where P-gp is believed to localize and properties of rafts are essential for the transporter's proper function while MRP may have different localization [119].

Inhibition of drug efflux transporters and enhancement of the drug accumulation in MDR tumors in the presence of Pluronic® block copolymers was demonstrated in vitro and in vivo [110, 112]. Moreover, Pluronic® block copolymers attributed to overcome the BBB and achieved the brain delivery of a wide range of therapeutic agents in vitro and in vivo [160, 161, 162]. Pluronic® P85 block copolymer increases apical to basolateral transport of a broad spectrum of drugs in the polarized monolayers of BBMECs as in vitro models of the blood brain barrier. The coadministration of 1% P85 with radiolabeled digoxin, a P-gp substrate, in wild-type mice increased the brain penetration of digoxin 3-fold and the digoxin level in the P85-treated wild-type mice was similar to that observed in the P-glycoprotein-deficient animals, indicating Pluronic® P85 can enhance the delivery of digoxin to the brain through the inhibition of the P-gp-mediated efflux

mechanism. Modification of a BBB-impermeable polypeptide, horseradish peroxidase, with Pluronic® P85 moieties via biodegradable disulfide links enhance the transport of this polypeptide across the BBB and accumulation of the polypeptide in the brain in vitro and in vivo, providing the potential of the brain delivery of many therapeutic polypeptides that severely restricted by the BBB [163].

1.3.2.3 Effect of Pluronic® block copolymers on cancer cells' metabolism

One of the factors contributing to sensitization effects on MDR by Pluronic® block copolymers is the increased ATP depletion, which is crucial for the supporting of energy for ABC transporter activity and other life processes [158]. Pluronic® unimers translocate across the plasma membrane via a caveolae-mediated endocytosis pathway [88] and rapidly (15min after exposure to the cells) colocalizes with mitochondria [156]. It has been proved that Pluronic® P85 first inhibited the cytochrome c oxidase (complex IV) and then the NADH-ubiquinone oxidoreductase (complex I) of the mitochondria respiratory chain at relatively low doses (0.001% and 0.01% for complexes IV and I, respectively), decreased oxygen consumption and caused ATP depletion in MDR cells, while non-MDR cells require significantly higher doses of Pluronic® copolymers to achieve similar functions [156]. Moreover, i.v. injections of DOX formulated with 0.2% Pluronic P85 in tumor bearing mice caused significant reduction in ATP levels in P388/ADR tumors, while P388 tumors are not affected. Similar effects were observed with P85 alone although Dox/P85 is considerably more effective in ATP depletion. The selectivity of Pluronic® copolymers to MDR phenotype may attribute to innate metabolic and physiological differences between MDR and non-MDR cells. Notably, MDR cells are associated with a drastic change in cellular metabolism by using a different major fuel

source in energy production. Specifically, the MDR cells predominantly utilize fatty acid as a source of electrons entering the respiration chain while the non-MDR cells predominantly employ glucose metabolism for this purpose. Since the PPO blocks of Pluronic® molecules may interact with fatty acids even at low (unimers) concentrations and effectively immobilize fatty molecules inside micelle cores at higher concentrations, it may affect the respiration mechanism at higher extent in MDR cells. Furthermore, MDR cells also have lower mitochondria membrane potential and more uncoupled respiration due to the mitochondria membrane leakage and higher level of mitochondrial uncoupling protein 2, resulting in inefficient ATP synthesis and thus making the mitochondria of MDR cells even more vulnerable to the depolarization effects compared with that of the sensitive cells [164]. It was observed at about an orders of magnitude lower concentration of P85 necessary for 50% decrease of mitochondria membrane potential in the MCF7/ADR cells compared to MCF7 cells [156].

Interestingly, higher responsiveness of the respiratory chain to Pluronic copolymers appears to be at least partially associated with P-gp expression, since increased inhibition of oxygen consumption was observe not only in drug selected MDR cells, but also in MDCKII/MDR1 P-gp-transfected cells [155, 156]. P-gp plays multiple roles in cells, such as inducing alteration in the membrane lipid composition [165], increasing the synthesis of glycolipid, globotriaosylceramide [166] and pumping the substrates inside mitochondria [167], leading to drastic effect on membrane structure, cell signaling and mitochondrial activities and thus contributing to the increased responsiveness of molecular “targets” of Pluronic copolymers.

1.3.2.4 Effect of Pluronic® block copolymers on proapoptotic signaling

Oxidative stress is a condition of excessive ROS formation or a diminished ability of cells to scavenge ROS by antioxidant networks. The formed peroxides and free radicals will damage various cellular components including proteins, lipids and DNA that can culminate in cell death [168]. GSH, the ubiquitous tripeptide, is the major cellular antioxidant that protects the cells against ROS, toxins and drugs. GSH has a sulfhydryl (SH) group on the cysteinyl portion, which accounts for its strong electron-donating character. As electrons are lost, the molecule becomes oxidized, and two such molecules become linked (dimerized) by a disulfide bridge to form glutathione disulfide or oxidized glutathione (GSSG). In healthy cells, more than 90% of the total glutathione pool is in the reduced form (GSH). When cells are exposed to increased levels of oxidative stress, GSSG accumulates and the ratio of GSSG to GSH increases [169]. An increased ratio of GSSG-to-GSH is an indication of oxidative stress. Additionally, GST, the major cellular detoxifying enzyme performs a range of functional roles using GSH as a cosubstrate or coenzyme. Researches indicated that MDR is associated with elevated GSH level and GST catalytic activity [170, 171]. Batrakova EV et al demonstrated Pluronic® P85 inhibited GSH/GST detoxification system by depleting levels of GSH and inactivating GST in MDR cancer cells [154]. Moreover, as discussed above, Pluronic® block copolymers quickly reach mitochondrial and inhibit complex I and IV of mitochondria electron transfer chain in MDR cells, stimulating the production of ROS in the resistant, but not in the sensitive cells, where it remained at the basal level [156].

Pluronic® P85 was observed to localize in mitochondria after 15min of the cell exposure by incorporation of P85 into mitochondria membranes followed by alteration of the membrane structure, permeabilization of outer mitochondrial membrane, decrease of mitochondria membrane potential and release of cytochrome c, which are the early signs

of mitochondrial apoptotic pathway [156]. In cytoplasm, cytochrome c binds to apoptosis protease activating factor (APAR-1) and forms apoptosome, which cleaves and activates the procaspase-9 and forms caspase 9. The activated caspase 9 further activates the effector caspases, such as caspase 3, which all together contribute to the completion of apoptosis. Indeed, Formulation of DOX with P85 increased the expression levels of the proapoptotic genes (BAX, P53, APAF1, Caspase 9 and Caspase 3) while simultaneously downregulating the intracellular levels of antiapoptotic genes (BCL2 and BCLXL) compared to free DOX in MDR cells [**Error! Bookmark not defined.**]. Furthermore, the effect of DOX/P85 formulations on apoptosis was evaluated in vivo. Data indicated that i.v. injection of DOX/P85 into drug-resistant tumor (3LL-M27) -bearing mice formulations increased the level pro-apoptotic signals of caspase 8 and caspase 9, promoting tumor apoptosis compared to injection of DOX alone [110].

1.3.2.5 Pluronic® block copolymers prevent development of MDR

In addition to the chemosensitization effects listed above, Pluronic® block copolymers have been proved to prevent the development of MDR upon selection with cytotoxic drugs in vitro and in vivo [172, 173]. Specifically, the human breast carcinoma MCF7 cell line was cultured in increasing concentration of either DOX alone or DOX formulated with 0.001% P85 (below the CMC) in the medium. After 305 days of escalating the drug exposure, the cells cultured in the presence of Pluronic® P85 were unable to stably grow in concentrations of Dox that exceeded 10ng Dox/ml of culture media. However, MCF7 cells cultured in the absence of the block copolymer resulted in the selection and stable growth of cells that tolerated 1000 times higher concentration of the drug (10,000ng Dox/ml culture media) **(Fig.1.5A)**. Detailed characterization of the isolated sublines demonstrated that those cells selected in the DOX-P85 formulation did

not show amplification of the MDR1 gene while cells selected with Dox alone showed an elevated level in the expression of the MDR1 gene along with a corresponding increase in the expression level of the drug efflux transporter, P-gp, contributing to the high resistance of the cells to Dox **(Fig.1.5B)**. Moreover, it was demonstrated that selection of cells with DOX and DOX-P85 formulation resulted in very different changes in the gene expression pattern in the cells, which may potentially enhance therapeutic outcomes of DOX-P85 formulation [172]. Similar results were observed in murine lymphocytic leukemia cells (P388) when selected for DOX resistance with or without P85. Cells selected with DOX-P85 formulation in vitro and in vivo exhibited some increases in IC(50) values compared to parental cells, but these values were much less than IC_{50} in respective cells selected with DOX alone. In addition to MDR1, P85 abolished alterations of genes implicated in apoptosis, drug metabolism, stress response, molecular transport and tumorigenesis [173]. Overall, if resistance is intrinsic, Pluronic sensitizes the tumor, whereas if resistance is acquired, MDR cells no longer have a selective advantage as Pluronic prevents development of MDR.

1.3.2.6 Pluronic® block copolymers suppress cancer stem cells (CSCs)

Tumors are complex heterogeneous tissues comprising phenotypically and functionally different cancer cells. One theory suggests that the heterogeneity of tumor cells arises as a result of differentiation of small cell subpopulation within the tumor, called tumor-initiating cells or CSCs, with indefinite potential for self-renewal that drive tumorigenesis [174]. CSCs are intrinsically drug resistant to chemotherapeutics by overexpressing drug efflux transporters such as P-gp and BCRP, having extensive survival and anti-oxidant networks and having most of their time in the G_0 nondividing cell cycle state [175].

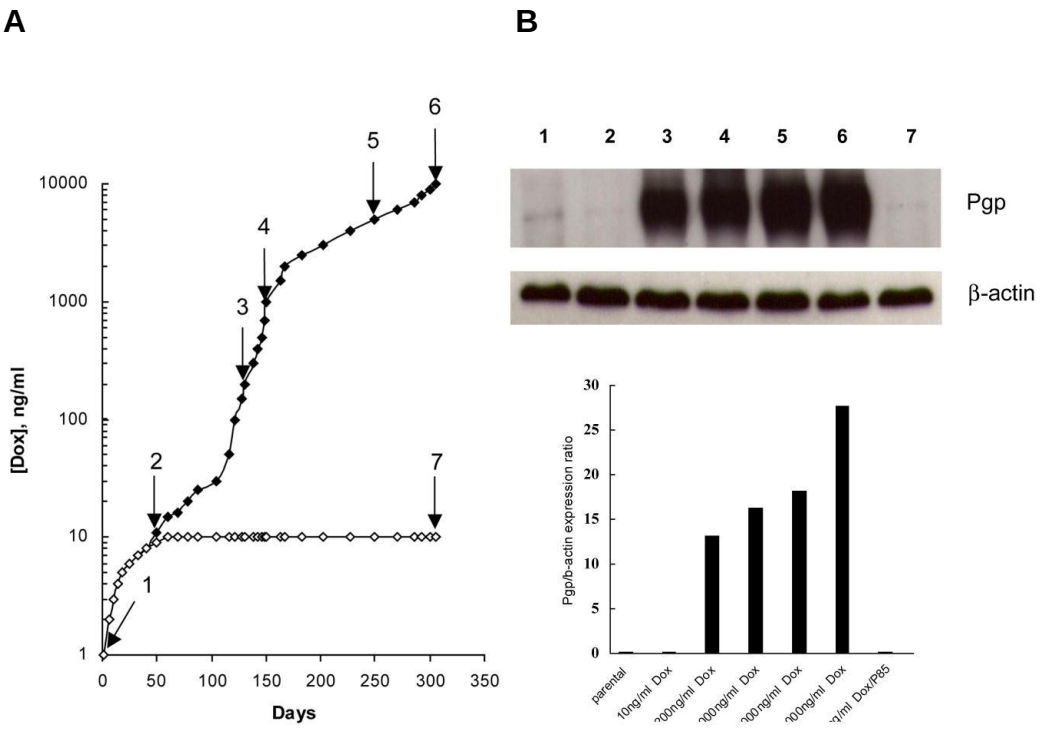

Fig.1.5 (A) Time course of the development of drug resistance in MCF7 cell lines cultured with Dox either alone (filled diamonds) or in combination with 0.001% P85 (open diamonds). [Dox] is the concentration of Dox in the growth medium. (B) Western blot data for expression of P-gp in MCF7 parental cells, and selected MCF7/ADR cells tolerating: 10ng/ml Dox; 200ng/ml Dox; 1000ng/ml Dox; 5000ng/ml Dox; 10,000ng/ml Dox; and 10ng/ml Dox with 0.001% P85. The cells were harvested at different points of selection as presented in (a) arrows 1-7. (Adapted from [172])

Since CSCs share certain characteristics of MDR cells such as overexpressing drug efflux transporters and altered metabolic pathways, Pluronics have been applied to sensitize CSCs to chemotherapeutic drugs. A recent study demonstrated that SP1049C treatment reduced tumor aggressiveness, in vivo tumor formation frequency in mice bearing the leukemia ascetic cells and in vitro clonogenic potential of the leukemia cells derived from the treated animals compared to drug, saline and polymer controls. SP1049C also prevented overexpression of BCRP and activation of Wnt-β-catenin signaling observed with DOX alone significantly altered the DNA methylation profiles of the cells and decreased $CD133^+$ P388 cells populations, which displayed CSC-like properties and were more tumorigenic compared to CD133− cells [148].

Overall, capacities of forming micelles and encapsulating water-insoluble anticancer drugs, MDR sensitization by multiple mechanisms, prevention of MDR development, depletion of tumorigenic cell subpopulations, and decrease of tumorigenicity and tumor aggressiveness offer significant advantages for the development of Pluronics formations of approved and/or experimental therapeutics.

1.4 Other applications of Pluronic® block copolymers in cancer treatment

Doxil®, the first nanoformulated drug approved by the US FDA, was designed to reduce cardiotoxicity of DOX by encapsulating it in PEGylated (stealth) liposome. However, the therapeutic effectiveness of Doxil® is limited by its penetration to the tumor and poor release of the active drug from the liposome at the tumor site. In clinical studies, Doxil® produced less cardiotoxicity but did not show significant improvement of progression-free survival compared with free DOX for breast cancer patients [176]. Thus, combination of Doxil® therapy with the regimens that enhance permeability of

tumor vasculature is necessary to improve the therapeutic effect. Pluronic® P85 was proved to increase the process of solute diffusion across planar lipid and liposomal membranes without affecting the overall integrity of the membranes [177]. Zhao Y et al demonstrated enhancement of drug release from the liposomes and increase of therapeutic efficacy of Doxil® by administering Pluronic® P85 once the liposomal drug accumulates in the tumor sites [178]. Specifically, DOX was observed to rapidly entered cells (15min) and then accumulated in the nucleus (60min) while little if any drug was seen in the intracellular vesicles and nucleus even after 24h exposures of the cells to the highest dose of Doxil® (200 μg/mL). Anti-tumor growth and distribution of drug were evaluated when Pluronic P85 was i.v. injected 1h, 48h, or 96h after the Doxil® administration in A2780 human ovarian cancer xenografts. The greatest anti-tumor effect of single injection of Doxil® was achieved when Pluronic P85 was administered 48h after Doxil®, when the liposomal drug was already distributed to the tumor sites .The Confocal tile scanning images of tumor section showed that copolymer treatment induced the release of the drug in the tumors from the vessels regions to the bulk of the tumor. Therefore, systemic application of the Pluronic® block copolymers may be a useful adjuvant to the Doxil® -based chemotherapy regimens.

Another application could be intraceullar delivery of the unimers of Pluronic® P85 to MDR cells by mixed micellar system based mainly on the pH-sensitive copolymer of poly(L-histidine)-poly (D,L-lactide)-polyethyleneglycol-poly (D,L-lactide)-poly (L-histidine) (PHis-PLA-PEG-PLA-PHis) and Pluronic® F127, which overcomes the poor micellar stability of plain puronics micelles [179]. The micelles with inserted Pluronic® P85 unimers demonstrated more efficient intracellular delivery of Pluronic® P85 unimers to the cytosol of the MDR cells than the triple-component mixed micelles and plain Pluronic® micelles, which was confirmed by the subcellular colocalization of Pluronic®

P85 unimers with mitochondria and led to enhanced MDR reversal effect. In addition, the potential of such system has been confirmed by the higher antitumor efficiency against MCF-7/ADR tumors and lower cellular ATP levels in the isolated tumors. The idea of incorporation of Pluronic®P85 unimers and drug together into the mixed micelles may contribute to more efficient MDR reversal by Pluronic® block copolymers.

Besides acting as chemosensitzer for MDR cells, Pluronic® block copolymers were also shown to improve the outcome of the radiofrequency ablation induced hyperthermia in solid and tumors and sensitize cancer cells to hyperthermia in vitro and in vivo [180]. Consistent with the structure-functional relationships as chemosensitzer for MDR cells, the thermosensitzing activity of Pluronic® block copolymers was associated with copolymer structure properties including molecular weight, HLB values and PO length. Pluronics with lower molecular weight between 1100 to 3200 Da and a HLB <8 demonstrated the highest thermossensitizing ability with Pluronics L31, L61, L62, L10 and L64 among the most effective copolymers for hyperthermia sensitization under tested conditions. Most encouraging, L61 in synergy with hyperthermia significantly reduced tumor growth progression in vivo compared to tumors treated with hyperthermia alone [181]. The thermosensitization ability of Pluronic® block copolymers may be directly linked to its ability to interact with plasma membrane and induce membrane fluidization as cells become more sensitive to treatment when hyperthermia induced increase of membrane fluidity [182]. Another factor contributing to the thermosensitization effect is that the combination of low-grade hyperthermia and Pluronic treatment induced depletion of ATP levels and decreased expression of heat shock protein 70 (HSP 70), the chaperone molecules that assist in protein folding in the active confirmation and are expressed rapidly as a result of cellular stresses such as hyperthermia to increase the thermoresistance of the tumors [183].

Pluronic® block copolymers also demonstrated exciting opportunities for development of novel gene therapies [184]. It was discovered SP1017 (0.25% Pluronic L61 and 2% Pluronic F127) significantly increases intramuscular expression of plasmid DNA by 5- to 20- fold compared to naked DNA [185]. Pluronic® P85 enhanced levels of expression of a reporter gene (luciferase) by 17 to 19-fold in immunocompetent C57Bl/6 and Balb/c mice by activating the p53 and NFκB signaling pathways. High levels of expression of a reporter gene (luciferase) were sustained for at least 40 days and the area under the gene expression curve increased by at least 10 times compared to the DNA alone in mice. In addition Pluronic increased the number of DNA copies and thus affected initial stages of gene transfer in a promoter selective manner [186]. Pluronic® P85 was also shown to enhance gene transfection in HepG2 cells under ultrasound irradiation in vitro. The transfection efficacy in ulstrasound+P85 group was three times higher than in single ultrasound group [187]. Thus, Pluronic® block copolymers could be a good candidate applicable in multiple gene therapy protocols involving intramuscular injection of plasmid DNA by 1) enhancing the gene transfer and 2) activating the transcription of the genes.

1.5 Statement of purpose

MM is the second most common hematologic malignancy characterized by infiltration in the bone marrow (BM) of malignant plasma cells with production of monoclonal proteins. In the last decade, the introduction of immunomodulatory drugs (IMIDs), and of new front-line agents such as the proteasome inhibitors (Bortezomib, BTZ or Carfilzomib, CFZ) have significantly improved overall survival [188]. In spite of current efficient therapeutic regimens for MM patients, like almost all anti-cancer

drugs, drug resistance becomes a major concern and almost all patients eventually relapse or become refractory to current treatment regimens [189, 190]. For instance, BTZ (PS-341, Velcade), the first proteasome inhibitor approved by U.S. FDA, used as a first-in-class drug in MM by reversibly inhibiting the chymotrypsin-like activity at the β5-subunit and to a lesser extent inhibit the trypsin-like activity at the β1-subunit. However, many patients may be intrinsically resistant to it or develop resistance in the course of treatment [191]. Although real mechanisms of resistance to BTZ in MM patients are not yet deciphered, mutation in β5-subunit of proteasome (PSMB5) which impair BTZ binding, alterations of gene and protein expression in stress response, cell survival and antiapoptotic pathways and MDR have been indicated to be involved [192]. The BM microenvironment supported by fibroblast-like BM stromal cells, osteoblasts, and osteoclasts which secrete soluble factors and extracellular matrix proteins can facilitate the survival, differentiation, and proliferation of MM cells and offer protection from chemotherapeutic agents, thereby increases the probability for the development of drug resistance [193, 194]. According to the chemosensitization effect on MDR cells by Pluronic® block copolymers discussed above, we propose to use the combination of proteasome inhibitors together with mixture of Pluronics (SP1017) for MM treatment to increase the drug sensitivity of cancer cells. Moreover, almost all of the previous studies on sensitizing effect indicated that Pluronic® block copolymers only sensitize MDR cells but have little effects on sensitive cells [155, 156]. Here our study mainly focuses on the effect of Pluronic® block copolymers on sensitive MM cells and the related targets of the sensitization effect.

Our hypothesis of this research is that SP1017 will sensitize multiple myeloma in vitro and in vivo by targeting multiple molecular mechanisms. To test this hypothesis, the following specific aims will be addressed.

Specific aim 1: To determine the chemosensitization effect of SP1017 on both sensitive and drug-resistant MM cell lines combined with proteasome inhibitors.

Specific aim 2: To investigate the related molecular mechanisms of the sensitization effect of SP1017 combined with proteasome inhibitors.

Specific aim 3: To evaluate the treatment efficacy of the combination of SP1017 with proteasome inhibitor BTZ in human MM/SCID mice model.

1.6 References

[1] Linton KJ. Structure and Function of ABC Transporters. Physiology (Bethesda). 2007 Apr;22:122-130.

[2] Ozben T. Mechanisms and strategies to overcome multiple drug resistance in cancer. FEBS Lett. 2006 May 22;580(12):2903-2909.

[3] Aller SG, Yu J, Ward A, Weng Y, Chittaboina S, Zhuo R, Harrell PM, Trinh YT, Zhang Q, Urbatsch IL, Chang G.. Structure of P-glycoprotein reveals a molecular basis for poly-specific drug binding. Science. 2009 Mar 27; 323(5922):1718-1722.

[4] Kibria G, Hatakeyama H, Harashima H. Cancer multidrug resistance: mechanisms involved and strategies for circumvention using a drug delivery system. Arch Pharm Res. 2014 Jan; 37(1):4-15.

[5] Dalton WS, Scheper RJ. Lung Resistance-Related Protein: Determining Its Role in Multidrug Resistance. J Natl Cancer Inst. 1999 Oct 6;91(19):1604-1605.

[6] Kitazono M, Sumizawa T, Takebayashi Y, Chen ZS, Furukawa T, Nagayama S, Tani A, Takao S, Aikou T, Akiyama S. Multidrug Resistance and the Lung Resistance-Related Protein in Human Colon Carcinoma SW-620 Cells. J Natl Cancer Inst. 1999 Oct 6;91(19):1647-1653.

[7] Stavrovskaya AA. Cellular mechanisms of multidrug resistance of tumor cells. Biochemistry (Mosc). 2000 Jan;65(1):95-106.

[8] Cerqueira BB, Lasham A, Shelling AN, Al-Kassas R. Nanoparticle therapeutics: Technologies and methods for overcoming cancer. Eur J Pharm Biopharm. 2015 Nov;97(Pt A):140-151.

[9] Broxterman HJ, Lankelma J, Hoekman K. Resistance to cytotoxic and anti-angiogenic anticancer agents: similarities and differences. Drug Resist Updat. 2003 Jun;6(3):111-127.

[10] Alakhova DY, Kabanov AV. Pluronics and MDR reversal: an update. Mol Pharm. 2014 Aug 4;11(8):2566-2578.

[11] Sládek NE, Kollander R, Sreerama L, Kiang DT. Cellular levels of aldehyde dehydrogenases (ALDH1A1 and ALDH3A1) as predictors of therapeutic responses to cyclophosphamide-based chemotherapy of breast cancer: a retrospective study. Rational individualization of oxazaphosphorine- based cancer chemotherapeutic regimens. Cancer Chemother Pharmacol. 2002;49:309–321.

[12] Wang K, Ramji S, Bhathena A, Lee C, Riddick DS. Glutathione S-transferases in wild-type and doxorubicin-resistant MCF-7 human breast cancer cell lines.Xenobiotica. 1999 Feb;29(2):155-170.

[13] Bedard PL, Di Leo A, Piccart-Gebhart M. Taxanes: optimizing adjuvant chemotherapy for early-stage breast cancer. Nat Rev Clin Oncol. 2010;7:22–36.

[14] Beck WT, Danks MK, Wolverton JS, Granzen B, Chen M, Schmidt CA, Bugg BY, Friche E, Suttle DP. Altered DNA topoisomerase II in multidrug resistance. Cytotechnology. 1993; 11(2): 115-119.

[15] Eijdems EW, de Haas M, Timmerman AJ, Van der Schans GP, Kamst E, de Nooij J, Astaldi Ricotti GC, Borst P, Baas F. Reduced topoisomerase II activity in multidrug-resistant human non-small cell lung cancer cell lines. Br J Cancer. 1995 Jan;71(1):40-7.

[16] Tsujimoto Y. Role of Bcl-2 family proteins in apoptosis: apoptosomes or mitochondria? Genes Cells. 1998 Nov;3(11):697-707.

[17] Davis JM, Navolanic PM, Weinstein-Oppenheimer CR, Steelman LS, Hu W, Konopleva M, Blagosklonny MV, McCubrey JA. Raf-1 and Bcl-2 induce distinct and common pathways that contribute to breast cancer drug resistance. Clin Cancer Res. 2003 Mar;9(3):1161-1170.

[18] Srivastava RK, Sasaki CY, Hardwick JM, Longo DL. Bcl-2-mediated drug resistance: inhibition of apoptosis by blocking nuclear factor of activatred T lymphocytes (NFAT)-induced Fas ligand transcription. J Exp Med. 1999 Jul 19;190(2):253-265.

[19] Yu L, Wang Z. Difference in expression of Bcl-2 and Bcl-xl genes in cisplatin-sensitive and cisplatin-resistant human in ovarian cancer cell lines. J Huazhong Univ Sci Technolog Med Sci. 2004;24(2):151-153.

[20] Hermanson DL, Das SG, Li Y, Xing C. Overexpression of Mcl-1 Confers Multidrug Resistance, Whereas Topoisomerase IIβ Downregulation Introduces Mitoxantrone-Specific Drug Resistance in Acute Myeloid Leukemia. Mol Pharmacol. 2013 Aug;84(2):236-243.

[21] Chen F, Zhuang X, Lin L, Yu P, Wang Y, Shi Y, Hu G, Sun Y. New horizons in tumor microenvironment biology: challenges and opportunities. BMC Med. 2015 Mar 5;13:45.

[22] Trédan O, Galmarini CM, Patel K, Tannock IF. Drug Resistance and the Solid Tumor Microenvironment. J Natl Cancer Inst. 2007 Oct 3;99(19):1441-1454.

[23] Comerford KM, Wallace TJ, Karhausen J, Louis NA, Montalto MC, Colgan SP. Hypoxia-inducible Factor-1-dependent Regulation of the Multidrug Resistance (MDR1) Gene. Cancer Res. 2002 Jun 15;62(12):3387-3394.

[24] Scotto KW. Transcriptional regulation of ABC drug transporters. Oncogene. 2003 Oct 20;22(47):7496-7511.

[25] Wang JH, Wu QD, Bouchier-Hayes D, Redmond HP. Hypoxia upregulates Bcl-2 expression and suppresses interferon-gamma induced antiangiogenic activity in human tumor derived endothelial cells. Cancer. 2002 May 15;94(10):2745-2755.

[26] Lu H, Samanta D, Xiang L, Zhang H, Hu H, Chen I, Bullen JW, Semenza GL. Chemotherapy triggers HIF-1–dependent glutathione synthesis and copper chelation that induces the breast cancer stem cell phenotype. Proc Natl Acad Sci U S A. 2015 Aug 18;112(33):E4600-4609.

[27] Saraswathy M[1], Gong S.. Different stragegies to overcome multidrug resistance in cancer. Biotechnol Adv. 2013 Dec;31(8):1397-1407.

[28] Consoli U, Priebe W, Ling YH, Mahadevia R, Griffin M, Zhao S, Perez-Soler R, Andreeff M. The novel anthracycline annamycin is not affected by P-glycoprotein-related multidrug resistance: comparison with idarubicin and doxorubicin in HL-60 leukemia cell lines. Blood. 1996 Jul 15;88(2):633-44.

[29] Perez-Soler R, Neamati N, Zou Y, Schneider E, Doyle LA, Andreeff M, Priebe W, Ling YH. Annamycin circumvents resistance mediated by the multidrug resistance-associated protein (MRP) in breast MCF-7 and small-cell lung UMCC-1 cancer cell lines selected for resistance to etoposide. Int J Cancer. 1997 Mar 28;71(1):35-41.

[30] Mazel M, Clair P, Rousselle C, Vidal P, Scherrmann JM, Mathieu D, Temsamani J. Doxorubicin-peptide conjugates overcome multidrug resistance. Anticancer Drugs. 2001 Feb;12(2):107-116.

[31] Yoshikawa M, Ikegami Y, Hayasaka S, Ishii K, Ito A, Sano K, Suzuki T, Togawa T, Yoshida H, Soda H, Oka M, Kohno S, Sawada S, Ishikawa T, Tanabe S. Novel camptothecin analogues that circumvent ABCG2-associated drug resistance in human tumor cells. Int J Cancer. 2004 Jul 20;110(6):921-927.

[32] Jordan MA, Wilson L. Microtubules as a target for anticancer drugs. Nat Rev Cancer. 2004 Apr;4(4):253-265.

[33] Oshiro C, Marsh S, McLeod H, Carrillo MW, Klein T, Altman R. Taxane Pathway. Pharmacogenet Genomics. 2009 Dec;19(12):979-983.

[34] Shionoya M, Jimbo T, Kitagawa M, Soga T, Tohgo A. DJ-927, a novel oral taxane, overcomes P-glycoprotein-mediated multidrug resistance in vitro and in vivo. Cancer Sci. 2003 May;94(5):459-466.

[35]Abidi A. Cabazitaxel: A novel taxane for metastatic castration-resistant prostate cancer-current implications and future prospects. J Pharmacol Pharmacother. 2013 Oct;4(4):230-237.

[36] Dong X, Mumper RJ. Nanomedicinal strategies to treat multidrug-resistant tumors: current progress. Nanomedicine (Lond). 2010 Jun;5(4):597-615.

[37] Ullah MF.Cancer Multidrug Resistance (MDR): A Major Impediment to Effective Chemotherapy. Asian Pac J Cancer Prev. 2008 Jan-Mar;9(1):1-6.

[38] Liscovitch M, Lavie Y. Cancer multidrug resistance: A review of recent drug discovery research. IDrugs. 2002 Apr;5(4):349-355.

[39] Thomas H, Coley HM. Overcoming Multidrug Resistance in Cancer: An Update on the Clinical Strategy of Inhibiting P-Glycoprotein. Cancer Control. 2003 Mar-Apr;10(2):159-165.

[40] Krishna R, Mayer LD. Multidrug resistance (MDR) in cancer: Mechanisms, reversal using modulators of MDR and the role of MDR modulators in influencing the pharmacokinetics of anticancer drugs. Eur J Pharm Sci. 2000 Oct;11(4):265-283.

[41] Ferry DR, Traunecker H, Kerr DJ. Clinical trials of p-glycoprotein reversal in solid tumor. Eur J Cancer. 1996 Jun;32A(6):1070-1081.

[42] Theis JG, Chan HS, Greenberg ML, Malkin D, Karaskov V, Moncica I, Koren G, Doyle J. Assessment of systemic toxicity in children receiving chemotherapy with cyclosporine for sarcoma. Med Pediatr Oncol. 2000 Apr;34(4):242-249.

[43] Twentyman PR, Bleehen NM. Resistance modification by PSC-833, a novel non-immunosuppressive cyclosporin [corrected]. Eur J Cancer. 1991;27(12):1639-1642.

[44] Visani G, Milligan D, Leoni F, Chang J, Kelsey S, Marcus R, Powles R, Schey S, Covelli A, Isidori A, Litchman M, Piccaluga PP, Mayer H, Malagola M,Pfister C. Combined action of PSC 833 (Valspodar), a novel MDR reversing agent, with mitoxantrone, etoposide and cytarabine in poor-prognosis acute myeloid leukemia. Leukemia. 2001 May;15(5):764-771.

[45] Fracasso PM, Brady MF, Moore DH, Walker JL, Rose PG, Letvak L, Grogan TM, McGuire WP. Phase II Study of Paclitaxel and Valspodar (PSC 833) in Refractory Ovarian Carcinoma: A Gynecologic Oncology Group Study. J Clin Oncol. 2001 Jun 15;19(12):2975-2982.

[46] Gruber A, Peterson C, Reizenstein P. D-verapamil and L-verapamil are equally effective in increasing vincristine accumulation in leukemic cells in vitro. Int J Cancer. 1988 Feb 15;41(2):224-226.

[47] Wilson WH, Bates SE, Fojo A, Bryant G, Zhan Z, Regis J, Wittes RE, Jaffe ES, Steinberg SM, Herdt J. Controlled trial of dexverapamil, a modulator of multidrug resistance, in lymphomas refractory to EPOCH chemotherapy. J Clin Oncol. 1995 Aug;13(8):1995-2004.

[48] Dantzig AH, Law KL, Cao J, Starling JJ. Reversal of multidrug resistance by the P-glycoprotein modulator, LY335979, from the bench to the clinic. Curr Med Chem. 2001 Jan;8(1):39-50.

[49] Newman MJ, Rodarte JC, Benbatoul KD, Romano SJ, Zhang C, Krane S, Moran EJ, Uyeda RT, Dixon R, Guns ES, Mayer LD. Discovery and characterization of OC144-093, a novel inhibitor of P-glycoprotein-mediated multidrug resistance. Cancer Res. 2000 Jun 1;60(11):2964-2972.

[50] Wu CP, Ohnuma S, Ambudkar SV. Discovering Natural Product Modulators to Overcome Multidrug Resistance in Cancer Chemotherapy. Curr Pharm Biotechnol. 2011 Apr;12(4):609-620.

[51] Limtrakul P, Chearwae W, Shukla S, Phisalphong C, Ambudkar SV. Modulation of function of three ABC drug transporters, P-glycoprotein (ABCB1), mitoxantrone resistance protein (ABCG2) and multidrug resistance protein 1 (ABCC1) by tetrahydrocurcumin, a major metabolite of curcumin. Mol Cell Biochem. 2007 Feb;296(1-2):85-95.

[52] Shukla S, Zaher H, Hartz A, Bauer B, Ware JA, Ambudkar SV. Curcumin inhibits the activity of ABCG2/BCRP1, a multidrug resistance-linked ABC drug transporter in mice. Pharm Res. 2009 Feb;26(2):480-487.

[53] Conseil G, Baubichon-Cortay H, Dayan G, Jault JM, Barron D, Di Pietro A. Flavonoids: a class of modulators with bifunctional interactions at vicinal ATPand steroid-binding sites on mouse P-glycoprotein. Proc Natl Acad Sci U S A. 1998 Aug 18;95(17):9831-9836.

[54] Agrawal N, Dasaradhi PV, Mohmmed A, Malhotra P, Bhatnagar RK, Mukherjee SK.RNA interference: biology, mechanism, and applications. Microbiol Mol Biol Rev. 2003 Dec;67(4):657-685.

[55] Kim D, Rossi J. RNAi mechanisms and applications. Biotechniques. 2008 Apr;44(5):613-616.

[56] Watts J and Corey D*Gene silencing by siRNAs and antisense oligonucleotides in the laboratory and the clinic. J Pathol. 2012 Jan; 226(2): 365–379.

[57] Nieth C, Priebsch A, Stege A, Lage H. Modulation of the classical multidrug resistance (MDR) phenotype by RNA interference (RNAi). FEBS Lett. 2003 Jun 19;545(2-3):144-150.

[58] Pichler A, Zelcer N, Prior JL, Kuil AJ, Piwnica-Worms D. In vivo RNA Interference–Mediated Ablation of MDR1 P-Glycoprotein. Clin Cancer Res. 2005 Jun 15;11(12):4487-4494.

[59] Lv H, He Z, Liu X, Yuan J, Yu Y, Chen Z. Reversal of BCRP-mediated multidrug resistance by stable expression of small interfering RNAs. J Cell Biochem. 2007 Sep 1;102(1):75-81.

[60] Pan GD, Yang JQ, Yan LN, Chu GP, Liu Q, Xiao Y, Yuan L. Reversal of multi-drug resistance by pSUPER-shRNA-mdr1 in vivo and in vitro. World J Gastroenterol. 2009 Jan 28;15(4):431-440.

[61] Xu CF, Wang J. Delivery systems for siRNA drug development in cancer therapy. Asian J. Pharm. Sci., 10 (2015), pp. 1–12

[62] Nayerossadat N, Maedeh T, Ali PA. Viral and nonviral delivery systems for gene delivery. Adv Biomed Res. 2012;1:27.

[63] Ramamoorth M, Narvekar A. Non Viral Vectors in Gene Therapy- An Overview. J Clin Diagn Res. 2015 Jan;9(1):GE01-6.

[64] Singh S.Nanomaterials as Non-viral siRNA Delivery Agents for Cancer Therapy. Bioimpacts. 2013;3(2):53-65.

[65] Susa M, Iyer AK, Ryu K, Choy E, Hornicek FJ, Mankin H, Milane L, Amiji MM, Duan Z. Inhibition of ABCB1 (MDR1) Expression by an siRNA Nanoparticulate Delivery System to Overcome Drug Resistance in Osteosarcoma. PLoS One. 2010 May 24;5(5):e10764.

[66] Aliabadi HM, Landry B, Mahdipoor P, Hsu CY, Uludağ H. Effective down-regulation of Breast Cancer Resistance Protein (BCRP) by siRNA delivery using lipid-substituted aliphatic polymers. Eur J Pharm Biopharm. 2012 May;81(1):33-42.

[67] Guo P, Coban O, Snead NM, Trebley J, Hoeprich S, Guo S, Shu Y. Engineering RNA for Targeted siRNA Delivery and Medical Application. Adv Drug Deliv Rev. 2010 Apr 30;62(6):650-666.

[68] Vivas-Mejia PE, Rodriguez-Aguayo C, Han HD, Shahzad MM, Valiyeva F, Shibayama M, Chavez-Reyes A, Sood AK, Lopez Berestein G. Silencing surviving splice variant 2B leads to antitumor activity in taxane-resistant ovarian cancer. Clin Cancer Res. 2011 Jun 1;17(11):3716-3726.

[69] Lei XY, Zhong M, Feng LF, Zhu BY, Tang SS, Liao DF. SiRNA-mediated Bcl-2 and Bclxl gene silencing sensitizes human hepatoblastoma cells to chemotherapeutic drugs. Clin Exp Pharmacol Physiol. 2007 May-Jun;34(5-6):450-456.

[70] Kim DW, Kim KO, Shin MJ, Ha JH, Seo SW, Yang J, Lee FY. siRNA-based targeting of antiapoptotic genes can reverse chemoresistance in P-glycoprotein expressing chondrosarcoma cells. Mol Cancer. 2009 May 15;8:28.

[71] Chen J, Ding Z, Peng Y, Pan F, Li J, Zou L, Zhang Y, Liang H. HIF-1α Inhibition Reverses Multidrug Resistance in Colon Cancer Cells via Downregulation of MDR1/P-Glycoprotein. PLoS One. 2014 Jun 5;9(6):e98882.

[72] Kapse-Mistry S, Govender T, Srivastava R, Yergeri M. Nanodrug delivery in reversing multidrug resistance in cancer cells. Front Pharmacol. 2014 Jul 10;5:159.

[73] Bamrungsap S, Zhao Z, Chen T, Wang L, Li C, Fu T, Tan W. Nanotechnology in Therapeutics A Focus on Nanoparticles as a Drug Delivery System. Nanomedicine (Lond). 2012 Aug;7(8):1253-1271.

[74] Davis ME, Chen ZG, Shin DM. Nanoparticle therapeutics: an emerging treatment modality for cancer. Nat Rev Drug Discov. 2008 Sep;7(9):771-782

[75] Chen ZG. Small-molecule delivery by nanoparticles for anticancer therapy. Trends Mol Med. 2010 Dec;16(12):594-602.

[76] Albanese A, Tang PS, Chan WC. The Effect of Nanoparticle Size, Shape, and Surface Chemistry on Biological Systems. Annu Rev Biomed Eng. 2012;14:1-16.

[77] Shubayev VI, Pisanic TR 2nd, Jin S. Magnetic nanoparticles for theragnostics. Adv Drug Deliv Rev. 2009 Jun 21;61(6):467-77.

[78] Ruoslahti E, Bhatia SN, and Sailor MJ. Targeting of drugs and nanoparticles to tumors. J Cell Biol. 2010 Mar 22; 188(6): 759–768.

[79] Yu MK, Park J, Jon S. Targeting Strategies for Multifunctional Nanoparticles in Cancer Imaging and Therapy. Theranostics. 2012;2(1):3-44.

[80] Steichen SD, Caldorera-Moore M[2], Peppas NA[3]. A review of current nanoparticle and targeting moieties for the delivery of cancer therapeutics. Eur J Pharm Sci. 2013 Feb 14;48(3):416-427.

[81] Yoo H, Park T. Folate-receptor-targeted delivery of doxorubicin nano-aggregates stabilized by doxorubicin–peg–folate conjugate. J Control Release. 2004 Nov 24;100(2):247-256.

[82] Yoo HS, Park TG. Folate receptor targeted biodegradable polymeric doxorubicin micelles. J Control Release. 2004 Apr 28;96(2):273-283.

[83] Nukolova NV, Oberoi HS, Cohen SM, Kabanov AV, Bronich TK. Folate-Decorated Nanogels for Targeted Therapy of Ovarian Cancer. Biomaterials. 2011 Aug;32(23):5417-5426.

[84] Desale SS, Soni KS, Romanova S, Cohen SM, Bronich TK.Targeted delivery of platinum-taxane combination therapy in ovarian cancer. J Control Release. 2015 Dec 28;220(Pt B):651-659.

[85] Sahay G, Alakhova DY, Kabanov AV. Endocytosis of Nanomedicines. J Control Release. 2010 Aug 3;145(3):182-195

[86] Hillaireau H, Couvreur P. Nanocarriers' entry into the cell: relevance to drug delivery. Cell Mol Life Sci. 2009 Sep;66(17):2873-2896.

[87] Oh N, Park JH. Endocytosis and exocytosis of nanoparticles in mammalian cells. Int J Nanomedicine. 2014 May 6;9 Suppl 1:51-63.

[88] Sahay G, Batrakova EV, Kabanov AV. Different internalization pathways of polymeric micelles and unimers and their effects on vesicular transport. Bioconjug Chem. 2008 Oct;19(10):2023-9.

[89] Narvekar M, Xue HY, Eoh JY, Wong HL. Nanocarrier for Poorly Water-Soluble Anticancer Drugs—Barriers of Translation and Solutions. AAPS PharmSciTech. 2014 Aug;15(4):822-833.

[90] Kato Y, Ozawa S, Miyamoto C, Maehata Y, Suzuki A, Maeda T, Baba Y. Acidic extracellular microenvironment and cancer. Cancer Cell Int. 2013 Sep 3;13(1):89.

[91] Meng F, Zhong Y, Cheng R, Deng C, Zhong Z. pH-Sensitive Polymeric Nanoparticles for Tumor-Targeting Doxorubicin Delivery: Concept and Recent Advances. Nanomedicine (Lond). 2014 Mar;9(3):487-499.

[92] Liu R, Li D, He B, Xu X, Sheng M, Lai Y, Wang G, Gu Z. Anti-tumor drug delivery of pH-sensitive poly(ethylene glycol)-poly(L-histidine-)-poly(L-lactide) nanoparticles. J Control Release. 2011 May 30;152(1):49-56.

[93] Oishi M, Hayashi H, Iijima M and Nagasaki Y. Endosomal release and intracellular delivery of anticancer drugs using pH-sensitive PEGylated nanogels. J. Mater. Chem. 2007,17, 3720-3725

[94]Kim JO, Kabanov AV, Bronich TK. Polymer micelles with cross-linked polyanion core for delivery of a cationic drug doxorubicin. J Control Release. 2009 Sep 15;138(3):197-204.

[95] Patil R, Portilla-Arias J, Ding H, Konda B, Rekechenetskiy A, Inoue S, Black KL, Holler E, Ljubimova JY. Cellular Delivery of Doxorubicin via pH-Controlled Hydrazone Linkage Using Multifunctional Nano Vehicle Based on Poly(β-L-Malic Acid). Int J Mol Sci. 2012;13(9):11681-11693.

[96] Zhu L, Zhao L, Qu X, Yang Z. pH-sensitive polymeric vesicles from coassembly of amphiphilic cholate grafted poly(L-lysine) and acid-cleavable polymer-drug conjugate. Langmuir. 2012 Aug 21;28(33):11988-96.

[97] Hu CM, Zhang L.Nanoparticle-based combination therapy toward overcoming dug resistance in cancer. Biochem Pharmacol. 2012 Apr 15;83(8):1104-1111.

[98] Soma CE, Dubernet C, Bentolila D, Benita S, Couvreur P. Reversion of multidrug resistance by co-encapsulation of doxorubicin and cyclosporin A in polyalkylcyanoacrylate nanoparticles. Biomaterials. 2000 Jan;21(1):1-7.

[99] Patil Y, Sadhukha T, Ma L, Panyam J. Nanoparticle-mediated simultaneous and targeted delivery of paclitaxel and tariquidar overcomes tumor drug resistance. J Control Release. 2009 May 21;136(1):21-9.

[100] Duan X, Xiao J, Yin Q, Zhang Z, Yu H, Mao S, Li Y. Smart pH-Sensitive and TemporalControlled Polymeric Micelles for Effective Combination Therapy of Doxorubicin and Disulfiram. ACS Nano. 2013 Jul 23;7(7):5858-5869

[101] Ganta S, Amiji M. Coadministration of Paclitaxel and Curcumin in Nanoemulsion Formulations To Overcome Multidrug Resistance in Tumor Cells. Mol Pharm. 2009 May-Jun;6(3):928-939.

[102] Misra R, Sahoo SK. Coformulation of Doxorubicin and Curcumin in Poly(D,L-lactide-co-glycolide) Nanoparticles Suppresses the Development of Multidrug Resistance in K562 Cells. Mol Pharm. 2011 Jun 6;8(3):852-866.

[103] Ye MX, Zhao YL, Li Y, Miao Q, Li ZK, Ren XL, Song LQ, Yin H, Zhang J. Curcumin reverses cis-platin resistance and promotes human lung adenocarcinoma A549/DDP cell apoptosis through HIF-1α and caspase-3 mechanisms. Phytomedicine. 2012 Jun 15;19(8-9):779-787.

[104] Meng H, Liong M, Xia T, Li Z, Ji Z, Zink JI, Nel AE. Engineered Design of Mesoporous Silica Nanoparticles to Deliver Doxorubicin and Pgp siRNA to Overcome Drug Resistance in a Cancer Cell Line. ACS Nano. 2010 Aug 24;4(8):4539-50.

[105] Patil YB, Swaminathan SK, Sadhukha T, Ma L, Panyam J. The use of nanoparticle-mediated targeted gene silencing and drug delivery to overcome tumor drug resistance. Biomaterials. 2010 Jan;31(2):358-365.

[106] Zheng C, Zheng M, Gong P, Deng J, Yi H, Zhang P, Zhang Y, Liu P, Ma Y, Cai L. Polypeptide cationic micelles mediated co-delivery of docetaxel and siRNA for synergistic tumor therapy. Biomaterials. 2013 Apr;34(13):3431-8.

[107] Wang H, Wu Y, Zhao R, Nie G. Engineering the Assemblies of Biomaterial Nanocarriers for Delivery of Multiple Theranostic Agents with Enhanced Antitumor Efficacy. Adv Mater. 2013 Mar 20;25(11):1616-22.

[108] Alakhova DY, Kabanov AV. Pluronic and MDR reversal; an update. Mol Pharm. 2014 Aug 4;11(8):2566-2578.

[109] I.R. Schmolka, Poloxamers in the Pharmaceutical Industry, CRC Press, Boca Ratin, FL, 1991.

[110] Batrakova EV, Li S, Brynskikh AM, Sharma AK, Li Y, Boska M, Gong N, Mosley RL, Alakhov VY, Gendelman HE, Kabanov AV. Effects of pluronic and doxorubicin on drug uptake, cellular metabolism, apoptosis and tumor inhibition in animal models of MDR cancers. J Control Release. 2010 May 10;143(3):290-301.

[111] Alakhov VYu, Moskaleva EYu, Batrakova EV, Kabanov AV.. Hypersensitization of multidrug resistant human ovarian carcinoma cells by Pluronic P85 block copolymer. Bioconjug Chem. 1996 Mar-Apr;7(2):209-216.

[112] Venne A, Li S, Mandeville R, Kabanov A, Alakhov V. Hypersensitizing Effect of Pluronic L61 on Cytotoxic Activity, Transport, and Subcellular Distribution of Doxorubicin in Multiple Drug-resistant Cells. Cancer Res. 1996 Aug 15;56(16):3626-3629.

[113] Kamboj VK and Verma PK. Poloxamers based nanocarriers for drug delivery system. Der Pharmacia Lettre, 2015, 7 (2):264-269

[114] Kadam Y, Yerramilli U, Bahadur A. Solubilization of poorly water-soluble drug carbamezapine in pluronic micelles: effect of molecular characteristics, temperature and added salt on the solubilizing capacity. Colloids Surf B Biointerfaces. 2009 Aug 1;72(1):141-147.

[115] Kabanov AV, Batrakova EV, Alakhov VY. Pluronic block copolymers for overcoming drug resistance in cancer. Adv Drug Deliv Rev. 2002 Sep 13; 54(5):759-79.

[116] Pitto-Barry, A.; Barry, N. P. E. Pluronic® block-copolymers in medicine: from chemical and biological versatility to rationalisation and clinical advances. Polym.Chem. 2014, 5, 3291-3297.

[117] Kabanov AV, Nazarova IR, Astafieva IV, Batrakova EV, Alakhov VW, Yaroslavov AA, Kabanov VA. Micelle Formation and Solubilization of Fluorescent Probes in Poly(oxyethylene-*b*-oxypropylene-*b*-oxyethylene) Solutions. Macromolecules, 1995, 28 (7), 2303–2314

[118] Kabanov AV, Batrakova EV, Alakhov VY. Pluronic block copolymers as novel polymer therapeutics for drug and gene delivery. J Control Release. 2002 Aug 21; 82(2-3):189-212.

[119] Batrakova EV, Kabanov AV. Pluronics block copolymers: evolution of drug delivery concept from inert nanocarriers to biological response modifiers. J Control Release. 2008 Sep 10;130(2):98-106.

[120] Nagarajan R.Solubilization of hydrocarbons and resulting aggregate shape transitions in aqueous solutions of Pluronic (PEO-PPO-PEO) block copolymers. Colloids Surf B Biointerfaces, 1999 Nov, 16: 55–72

[121] Foster B, Cosgrove T, Hammouda B. Pluronic Triblock Copolymer Systems and Their Interactions with Ibuprofen. Langmuir. 2009 Jun 16;25(12):6760-6766.

[122] Lavasanifar A[1], Samuel J, Kwon GS. Poly(ethylene oxide)-block-poly(L-amino acid) micelles for drug delivery. Adv Drug Deliv Rev. 2002 Feb 21;54(2):169-190.

[123] Wang L, Peng M, Zhu Y, Tong SS, Cao X, Xu XM, Yu JN. Preparation of Pluronic/Bile salt/Phospholipid Mixed Micelles as Drug Solubility Enhancer and Study the Effect of the PPO Block Size on the Solubility of Pyrene. Iran J Pharm Res. 2014 Fall;13(4):1157-1163.

[124] Danson S, Ferry D, Alakhov V, Margison J, Kerr D, Jowle D, Brampton M, Halbert G, Ranson M. Phase I dose escalation and pharmacokinetic study of pluronic polymer-bound doxorubicin (SP1049C) in patients with advanced cancer. Br J Cancer. 2004 Jun 1;90(11):2085-91.

[125] Zhang W, Shi Y, Chen Y, Ye J, Sha X, Fang X. Multifunctional Pluronic P123/F127 mixed polymeric micelles loaded with paclitaxel for the treatment of multidrug resistant tumors. Biomaterials. 2011 Apr;32(11):2894-906.

[126] Chen, Y, Sha, X, Zhang, W, Zhong, W, Fan, Z, Ren, Q, Chen, L, Fang, X. Pluronic mixed micelles overcoming methotrexate multidrug resistance: in vitro and in vivo evaluation. Int. J. Nanomed. 2013, 8, 1463−1476.

[127] Chen, L, Sha, X, Jiang, X, Chen, Y, Ren, Q, Fang, X. Pluronic P105/F127 mixed micelles for the delivery of docetaxel against Taxol-resistant non-small cell lung cancer: optimization and in vitro, in vivo evaluation. Int. J. Nanomed. 2013, 8, 73−84.

[128]Wang L, Peng M, Zhu Y, Tong SS, Cao X, Xu XM, Yu JN. Preparation of Pluronic/Bile salt/Phospholipid Mixed Micelles as Drug Solubility Enhancer and Study the Effect of the PPO Block Size on the Solubility of Pyrene. Iran J Pharm Res. 2014 Fall;13(4):1157-1163.

[129] Tao Y, Han J, Wang X, Dou H. Nano-formulation of paclitaxel by vitamin E succinate functionalized pluronic micelles for enhanced encapsulation, stability and cytotoxicity. Colloids Surf B Biointerfaces. 2013 Feb 1;102:604-610.

[130] Yang TF, Chen CN, Chen MC, Lai CH, Liang HF, Sung HW. Shell-crosslinked Pluronic L121 micelles as a drug delivery vehicle. Biomaterials. 2007 Feb;28(4):725-34.

[131] Arranja A, Schroder AP, Schmutz M, Waton G, Schosseler F, Mendes E. Cytotoxicity and internalization of Pluronic micelles stabilized by core cross-linking. J Control Release. 2014 Dec 28;196:87-95.

[132] Sun CZ, Lu CT, Zhao YZ, Guo P, Tian JL, Zhang L, Li XK, Lv HF, Dai DD, Li X. Characterization of the Doxorubicin-Pluronic F68 Conjugate Micelles and Their Effect on Doxorubicin Resistant Human Erythroleukemic Cancer Cells. J Nanomedic Nanotechnol 2:114.

[133] Liang YC, Su ZH, Yao Y, Zhang N. Preparation of pH Sensitive Pluronic-Docetaxel Conjugate Micelles to Balance the Stability and Controlled Release Issues. Materials 2015, *8*(2), 379-391.

[134] Alakhov V, Klinski E, Li S, Pietrzynski G, Venne A, Batrakova EV, Bronitch T, Kabanov A. Block copolymer-based formulation of Doxorubicin. From cell screen to clinical trials. Colloids Surf. B: Biointerfaces 1999;16:113–134.

[135] Ron ES, Bromberg LE.Temperature-responsive gels and thermogelling polymer matrices for protein and peptide delivery. Adv Drug Deliv Rev. 1998 May 4;31(3):197-221.

[136] Wang W, Liu Z, Sun P, Fang C, Fang H, Wang Y, Ji J, Chen J. RGD Peptides-Conjugated Pluronic Triblock Copolymers Encapsulated with AP-2α Expression Plasmid for Targeting Gastric Cancer Therapy in Vitro and in Vivo. Int J Mol Sci. 2015 Jul 17;16(7):16263-16274.

[137] Wang M, Wu B, Lu P, Tucker JD, Milazi S, Shah SN, Lu QL.Pluronic-PEI copolymers enhance exon-skipping of 2'-O-methyl phosphorothioate oligonucleotide in cell culture and dystrophic mdx mice. Gene Ther. 2014 Jan;21(1):52-59.

[138] Simon T, Potara M, Gabudean AM, Licarete E, Banciu M, Astilean S. Designing Theranostic Agents Based on Pluronic Stabilized Gold Nanoaggregates Loaded with Methylene Blue for Multimodal Cell Imaging and Enhanced Photodynamic Therapy. ACS Appl Mater Interfaces. 2015 Aug 5;7(30):16191-16201.

[139] Kabanov AV, Batrakova EV, Miller DW. Pluronic block copolymers as modulators of drug efflux transporter activity in the blood-brain barrier. Adv Drug Deliv Rev. 2003 Jan 21;55(1):151-164.

[140] Spitzenberger TJ, Heilman D, Diekmann C, Batrakova EV, Kabanov AV, Gendelman HE, Elmquist WF, Persidsky Y. Novel delivery system enhances efficacy of antiretroviral therapy in animal model for HIV-1 encephalitis. J Cereb Blood Flow Metab. 2007 May;27(5):1033-1042.

[141] Huang Y, Liu W, Gao F, Fang X, Chen Y. c(RGDyK)-decorated Pluronic micelles for enhanced doxorubicin and paclitaxel delivery to brain glioma. Int J Nanomedicine. 2016 Apr 19;11:1629-1641

[142] Batrakova EV, Han HY, Alakhov VYu, Miller DW, Kabanov AV. Effects of pluronic block copolymers on drug absorption in Caco-2 cell monolayers. Pharm Res. 1998 Jun;15(6):850-855.

[143] Kwon SH, Kim SY, Ha KW, Kang MJ, Huh JS, Im TJ, Kim YM, Park YM, Kang KH, Lee S, Chang JY, Lee J, Choi YW. Pharmaceutical evaluation of genistein-loaded pluronic micelles for oral delivery. Arch Pharm Res. 2007 Sep;30(9):1138-1143.

[144] Andrade F, das Neves J, Gener P, Schwartz S Jr, Ferreira D, Oliva M, Sarmento B. Biological assessment of self-assembled polymeric micelles for pulmonary administration of insulin. Nanomedicine. 2015 Oct;11(7):1621-1631.

[145] Nguyen DH, Bae JW, Choi JH, Lee JS, Park KD. Bioreducible cross-linked Pluronic micelles: pH-triggered release of doxorubicin and folate-mediated cellular uptake. J. Bioact. Compat. Polym., 2013 July; 28: 341–354

[146] Wei Z, Hao J, Yuan S, Li Y, Juan W, Sha X, Fang X. Paclitaxel-loaded Pluronic P123/F127 mixed polymeric micelles: formulation, optimization and in vitro characterization. Int J Pharm. 2009 Jul 6;376(1-2):176-185

[147] Valle JW, Armstrong A, Newman C, Alakhov V, Pietrzynski G, Brewer J, Campbell S, Corrie P, Rowinsky EK, Ranson M. A phase 2 study of SP1049C, doxorubicin in Pglycoprotein-

targeting Pluronics, in patients with advanced adenocarcinoma of the esophagus and gastroesophageal junction. Invest New Drugs. 2011 Oct;29(5):1029-1037.

[148] Alakhova DY, Zhao Y, Li S, Kabanov AV. Effect of Doxorubicin/Pluronic SP1049C on tumorigenicity, aggressiveness, DNA methylation and stem cell markers in murine leukemia, PLoS One. 2013 Aug 19;8(8):e72238.

[149] Chen Y, Zhang W, Huang Y, Gao F, Fang X. Dual-functional c(RGDyK)-decorated Pluronic micelles designed for antiangiogenesis and the treatment of drug-resistant tumor. Int J Nanomedicine. 2015 Jul 30;10: 4863-4881.

[150] Belenkov AI, Alakhov VY, Kabanov AV, Vinogradov SV, Panasci LC, Monia BP, Chow TY. Polyethyleneimine grafted with pluronic P85 enhances Ku86 antisense delivery and the ionizing radiation treatment efficacy in vivo. Gene Ther. 2004 Nov;11(22):1665-1672.

[151] Shen J, Yin Q, Chen L, Zhang Z, Li Y. Co-delivery of paclitaxel and survivin shRNA by pluronic P85-PEI/TPGS complex nanoparticles to overcome drug resistance in lung cancer. Biomaterials. 2012 Nov;33(33):8613-8624.

[152] Batrakova E, Lee S, Li S, Venne A, Alakhov V, Kabanov A. Fundamental Relationships Between the Composition of Pluronic Block Copolymers and Their Hypersensitization Effect in MDR Cancer Cells. Pharm Res. 1999 Sep;16(9):1373-1379.

[153] Batrakova EV, Li S, Alakhov VY, Miller DW, Kabanov AV. Optimal Structure Requirements for Pluronic Block Copolymers in Modifying P glycoprotein Drug Efflux Transporter Activity in Bovine Brian Microvessel Endothelial Cells. J Pharmacol Exp Ther. 2003 Feb;304(2):845-854.

[154]Batrakova EV, Li S, Alakhov VY, Elmquist WF, Miller DW, Kabanov AV. Sensitization of cells overexpressing multidrug-resistant proteins by pluronic p85. Pharm Res. 2003 Oct;20(10):1581-1590.

[155] Batrakova EV, Li S, Elmquist WF, Miller DW, Alakhov VY, Kabanov AV. Mechanism of sensitization of MDR cancer cells by Pluronic block copolymers: Selective energy depletion Br J Cancer. 2001 Dec 14;85(12):1987-1997.

[156] Alakhova DY, Rapoport NY, Batrakova EV, Timoshin AA, Li S, Nicholls D, Alakhov VY, Kabanov AV. Differential metabolic responses to pluronic in MDR and non-MDR

cells: A novel pathway for chemosensitization of drug resistant cancers. J Control Release. 2010 Feb 25;142(1):89-100.

[157] Minko T, Batrakova EV, Li S, Li Y, Pakunlu RI, Alakhov VY, Kabanov AV. Pluronic block copolymers alter apoptotic signal transduction of doxorubicin in drug-resistant cancer cells. J Control Release. 2005 Jul 20;105(3):269-278.

[158] Batrakova EV, Li S, Vinogradov SV, Alakhov VY, Miller DW, Kabanov AV. Mechanism of Pluronic Effect on P-Glycoprotein Efflux System in Blood-Brain Barrier: Contributions of Energy Depletion and Membrane Fluidization. J Pharmacol Exp Ther. 2001 Nov;299(2):483-493.

[159] Batrakova EV, Li S, Li Y, Alakhov VY, Kabanov AV. Effect of pluronic P85 on ATPase activity of drug efflux transporters. Pharm Res. 2004 Dec;21(12):2226-2233.

[160]Batrakova EV, Li S, Miller DW, Kabanov AV. Pluronic P85 Increases Permeability of a Broad Spectrum of Drugs in Polarized BBMEC and Caco-2 Cell Monolayers. Pharm Res. 1999 Sep;16(9):1366-1372.

[161] Batrakova EV, Han HY, Miller DW, Kabanov AV. Effects of pluronic P85 unimers and micelle on drug permeability in polarized BBMEC and Caco-2 cells. Pharm Res. 1998 Oct;15(10):1525-1532.

[162] Batrakova EV, Miller DW, Li S, Alakhov VY, Kabanov AV, Elmquist WF. Pluronic P85 enhances the delivery of digoxin to the brain: in vitro and in vivo studies. J Pharmacol Exp Ther. 2001 Feb;296(2):551-557.

[163] Batrakova EV, Vinogradov SV, Robinson SM, Niehoff ML, Banks WA, Kabanov AV. Polypeptide point modifications with fatty acid and amphiphilic block copolymers for enhanced brain delivery. Bioconjug Chem. 2005 Jul-Aug;16(4):793-802.

[164] Harper ME, Antoniou A, Villalobos-Menuey E, Russo A, Trauger R, Vendemelio M, George A, Bartholomew R, Carlo D, Shaikh A, Kupperman J, Newell EW,Bespalov IA, Wallace SS, Liu Y, Rogers JR, Gibbs GL, Leahy JL, Camley RE, Melamede R, Newell MK. Characterization of a novel metabolic strategy used by drug-resistant tumor cells. FASEB J. 2002 Oct;16(12):1550-1557.

[165] Meyer dos Santos S[1], Weber CC, Franke C, Müller WE, Eckert GP. Cholesterol: Coupling between membrane microenvironment and ABC transporter activity. Biochem Biophys Res Commun. 2007 Mar 2;354(1):216-221.

[166] Lala P, Ito S, Lingwood CA. Retroviral transfection of Madin-Darby canine kidney cells with human MDR1 results in a major increase in globotriaosylceramide and 10(5)-to 10(6)-fold increased cell sensitivity to verocytotoxin. Role of p-glycoprotein in glycolipid synthesis. J Biol Chem. 2000 Mar 3;275(9):6246-6251.

[167] Munteanu E, Verdier M, Grandjean-Forestier F, Stenger C, Jayat-Vignoles C, Huet S, Robert J, Ratinaud MH. Mitochondrial localization and activity of P-glycoprotein in doxorubicin-resistant K562 cells. Biochem Pharmacol. 2006 Apr 14;71(8):1162-1174.

[168] Poljsak B, Šuput D, Milisav I.Achieving the balance between ROS and antioxidants: when to use the synthetic antioxidants. Oxid Med Cell Longev. 2013;2013:956792.

[169] Circu ML, Aw TY. Glutathione and modulation of cell apoptosis. Biochim Biophys Acta. 2012 Oct;1823(10):1767-1777.

[170] Chao CC, Huang YT, Ma CM, Chou WY, Lin-Chao S. Overexpression of glutathione S-transferase and elevation of thiol pools in a multidrug-resistant human colon cancer cell line. Mol Pharmacol. 1992 Jan;41(1):69-75.

[171] Ruiz-Gómez MJ, Souviron A, Martínez-Morillo M, Gil L.P-glycoprotein, glutathione and glutathione S-transferase increase in a colon carcinoma cell line by colchicine. J Physiol Biochem. 2000 Dec;56(4):307-312.

[172] Batrakova EV, Kelly DL, Li S, Li Y, Yang Z, Xiao L, Alakhova DY, Sherman S, Alakhov VY, Kabanov AV. Alteration of genomic responses to doxorubicin and prevention of MDR in breast cancer cells by a polymer excipient: pluronic P85. Mol Pharm. 2006 Mar-Apr;3(2):113-123.

[173] Sharma AK, Zhang L, Li S, Kelly DL, Alakhov VY, Batrakova EV, Kabanov AV. Prevention of MDR development in leukemia cells by micelle-forming polymeric surfactant. J Control Release. 2008 Nov 12;131(3):220-227.

[174] Tang DG. Understanding cancer stem cell heterogeneity and plasticity. Cell Res. 2012 Mar;22(3):457-472.

[175] Singh A, Settleman J. EMT, cancer stem cells and drug resistance: an emerging axis of evil in the war on cancer. Oncogene. 2010 Aug 26;29(34):4741-4751.

[176] Harris L, Batist G, Belt R, Rovira D, Navari R, Azarnia N, Welles L, Winer E; TLC D-99 Study Group. Liposome-encapsulated doxorubicin compared with conventional doxorubicin in a randomized multicenter trial as first-line therapy of metastatic breast carcinoma. Cancer. 2002 Jan 1;94(1):25-36.

[177]Erukova VY, Krylova OO, Antonenko YN, Melik-Nubarov NS. Effect of ethylene oxide and propylene oxide block copolymers on the permeability of bilayer lipid membranes to small solutes including doxorubicin. Biochim Biophys Acta. 2000 Sep 29;1468(1-2):73-86.

[178] Zhao Y, Alakhova DY, Kim JO, Bronich TK, Kabanov AV. A simple way to enhance Doxil® therapy: drug release from liposomes at the tumor site by amphiphilic block copolymer. J Control Release. 2013 May 28;168(1):61-69.

[179] Hong W, Chen D, Zhang X, Zeng J, Hu H, Zhao X, Qiao M. Reversing multidrug resistance by intracellular delivery of Pluronic® P85 unimers. Biomaterials. 2013 Dec;34(37):9602-14.

[180] Weinberg BD, Krupka TM, Haaga JR, Exner AA.Combination of sensitizing pretreatment and radiofrequency tumor ablation: evaluation in rat model.Radiology. 2008 Mar;246(3):796-803.

[181] Krupka TM, Exner AA. Structural parameters governing activity of Pluronic triblock copolymers in hyperthermia cancer therapy. Int J Hyperthermia. 2011;27(7):663-671.

[182] Dynlacht JR, Fox MH. The effect of 45 degrees C hyperthermia on the membrane fluidity of cells of several lines. Radiat Res. 1992 Apr;130(1):55-60.

[183] Reshani H. Perera, Tianyi M. Krupka, Hanping Wu, Bryan Traughber, David Dremann, Ann-Marie Broome, and Agata A. Exner Role of Pluronic block copolymers in modulation of heat shock protein 70 expression Int J Hyperthermia. 2011; 27(7): 672–681.

[184] Kabanov AV, Lemieux P, Vinogradov S, Alakhov V. Pluronic block copolymers: novel functional molecules for gene therapy. Adv Drug Deliv Rev. 2002 Feb 21;54(2):223-233.

[185] Lemieux P, Guérin N, Paradis G, Proulx R, Chistyakova L, Kabanov A, Alakhov V. A combination of poloxamers increases gene expression of plasmid DNA in skeletal muscle. Gene Ther. 2000 Jun;7(11):986-991.

[186] Yang Z, Zhu J, Sriadibhatla S, Gebhart C, Alakhov V, Kabanov A. Promoter- and strain-selective enhancement of gene expression in a mouse skeletal muscle by a polymer excipient Pluronic P85. J Control Release. 2005 Nov 28;108(2-3):496-512.

[187] Wang F, Li K, Chen Y. Gene transfection medicated by ultrasound and Pluronic P85 in HepG2 cells. J Huazhong Univ Sci Technolog Med Sci. 2007 Dec;27(6):700-2.

[188] Meletios A. Dimopoulos, et al. Emerging therapies for the treatment of relapsed or refractory multiple myeloma. Eur J Haematol 2011,86(1):1-15.

[189] Roberto Castelli et al. Current and Emerging Treatment Options for Patients with Relapsed Myeloma. Clinical Medicine Insights: Oncology 2013,7: 209-219.

[190] Andrzej Jakubowiak. Management Strategies for Relapsed/Refractory Multiple Myeloma: Current Clinical Perspectives. Seminars in Hematology.2012, 3(49): S16-S32.

[191] Buac D, Shen M, Schmitt S, Kona FR, Deshmukh R, Zhang Z, Neslund-Dudas C, Mitra B, Dou QP. From Bortezomib to other Inhibitors of the Proteasome and Beyond. Curr Pharm Des. 2013; 19(22): 4025–4038.

[192] Lü S, Wang J. The resistance mechanisms of proteasome inhibitor bortezomib. Biomark Res. 2013 Mar 1;1(1):13.

[193] Meads MB, Hazlehurst LA, Dalton WS. The bone marrow microenvironment as a tumor sanctuary and contributor to drug resistance. Clin Cancer Res. 2008 May 1;14(9):2519-2526.

[194] Abdi J, Chen G, Chang H. Drug resistance in multiple myeloma: latest findings and new concepts on molecular mechanisms. Oncotarget. 2013 Dec;4(12):2186-2207.

CHAPTER II: SP1017 SENSITIZE BOTH SENSITIZE AND RESISTANT MM CELLS BUT NOT NORMAL HEMATOLOGICAL CELLS OR NON-HEMATOLOGICAL CANCER CELLS

2.1 Introduction

MM is a complex and heterogeneous neoplastic disorder due to the proliferation of clonal plasma cells in BM with production of monoclonal protein, which is associated with a spectrum of clinical symptoms including bone destruction, anemia, hypercalcemia, and renal failure [1]. It has a prevalence of 70,000 patients in the United States, occurring in approximately 20,000 new individuals each year [2], with the median overall survival of patients estimated at 5 to 7 years [3] and with median age at diagnosis being 66 years [4]. In the last decade, the introduction of IMIDs, and of new front-line agents such as the proteasome inhibitors have significantly improved overall survival [5]. Among the proteasome inhibitors, BTZ, a reversible inhibitor with the boronic acid group binding and forming a complex with the active site of threonine hydroxyl group in the β5-subunit, is the first proteasome inhibitor approved by U.S.FDA for treatment of relapsed/refractory MM in 2003 [6, 7]. However, not all patients respond to BTZ -based therapies and relapse occurs in many patients who initially responded. Only about 30 – 40% of mantle cell lymphoma patients and 35% multiple myeloma patients are sensitive to BTZ, indicating that more than half of patients possess intrinsic resistance to proteasome inhibition, which is a critical

limitation of BTZ therapy [8, 9,10]. Several clinical studies showed that the median duration of response to BTZ treatment ranged from half a year to a year, supporting the theory that in most of cases of continuous BTZ treatment, MM eventually acquired BTZ resistance within a year [11]. Although real mechanisms of acquired resistance to BTZ in MM patients are not yet deciphered, mutation in PSMB5 which impair BTZ binding, alterations of gene and protein expression in stress response, cell survival and antiapoptotic pathways and MDR have been indicated to be involved [12]. Moreover, BTZ treatment is often limited by BTZ-induced, dose-limiting side effects, mostly consequent to peripheral neuropathy [13]. CFZ, the second generation epoxyketone-based irreversible proteasome inhibitor, was approved by U.S. FDA in 2012 for patients with MM who had relapsed and were refractory to BTZ and at least one thalidomide derivative, associated with less peripheral neuropathy compared to BTZ [14]. CFZ However, acquired CFZ-resistance has been observed by increased resistance to CFZ in sensitive MM cells following drug selection, which was associated with up-regulation of P-glycoprotein, suggesting that drug transport may contribute to resistance [15]. Due to the development of drug resistance, MM remains an incurable disease and almost all patients eventually relapse or become refractory to current treatment regimens [16,17]. So the current challenge of MM treatments is to maintain treatment response (or even improve it), to prevent relapse and eventually to prolong survival [18]. In the clinical, BTZ is combined with several other classes of drugs used in the treatment of MM, including alkylating agents, anthracyclines and immunomodulatory drugs to achieve synergistic anti-myeloma activity by targeting

different apoptotic pathways and/or alleviate side effects [14, 19] .

Previous studies demonstrated that Pluronic® block copolymer (PEO-PPO-PEO) sensitize MDR cancer cells resulting in increased cytotoxic activity of Dox, paclitaxel, and other drugs by 2-3 orders of magnitude [20, 21]. Improved treatment of drug resistant and metastatic cancers with Dox/Pluronic formulations was also reported using several *in vivo* tumor models [22,23].SP1049C, a solution of Dox with a mixture of SP1017 (0.25% Pluronic L61 and 2% Pluronic F127) in isotonic buffered saline, has completed Phase II clinical trial and demonstrated safety and efficacy in patients with advanced adenocarcinoma of the esophagus and gastroesophageal junction [24]. Relatively hydrophobic Pluronics at concentrations below the CMC with intermediate length of PEO units from 30 to 60 and HLB <20 [25, 26] can sensitize MDR cancer cells mainly by Pgp inhibition and selective ATP depletion, which is accompanied with generation of ROS and simultaneously inhibition of GSH/GST detoxification [27, 28, 29]. On the other hand, the Pluronic-caused impairment of respiration in mitochondria decreased the mitochondrial membrane potential, promoted release of cytochrome c and overall enhanced pro-apoptotic signaling (Bax, p53, APAF1, caspase 9 and caspase 3) and mitigated anti-apoptotic cellular defense (Bcl-2 and Bcl-xl) of MDR cells [30].

Based on the promising previous results of Pluronic® block copolymers in MDR cells, we explored the synergistic effect of SP1017 and proteasome inhibitors on both BTZ/CFZ-resistant MM cell lines which are selected by drug exposure for a period of time. In addition, previous studies indicated that Pluronic® block copolymers

did not have a pronounced sensitization effect in sensitive cells compared to resistant cells or non-MDR cells require significantly higher doses of Pluronic® copolymers to achieve similar functions [27, 29]. So here our studies also examined the effect of SP1017 at the inert concentration on different sensitive MM cells to explore the way SP1017 works on non-MDR cells. Furthermore, we examined the cytotoxicity of the combination of BTZ with SP1017 in normal hematological cells (PBMC) to ensure the safety and in several non-hematological cancer cells to explore its specificity.

2.2 Materials and Methods

2.2.1 Cell culture

RPMI 8226 human MM cell line and ARH-77 human MM cell line were generous gifts from Dr. Sagar Lonial (Emory University, Atlanta, GA, USA). U266 human MM cell line and NCI-H929 human MM cell line were generous gifts from Dr. Adriana Zingone (Multiple Myeloma Section/Metabolism Branch, NCI/NIH, Bethesda, MD, USA). BTZ/CFZ-resistant RPMI 8226 MM cell lines were selected and established by exposure to sensitive RPMI 8226 MM cells of gradually increasing concentrations of BTZ /CFZ starting at 0.2nM. Consequently, the BTZ/CFZ-resistant RPMI 8226 cell lines stably growing in the presence of 40nM of BTZ or CFZ within 6 months. Peripheral Blood Mononuclear Cells (PBMC) were provided by the Elutriation Core Facility in the Department of Pharmacology and Experimental Neuroscience (UNMC, Omaha, NE, USA). MCF-7 human breast adenocarcinoma cell line,

ADR-resistant cancer cell line MCF-7/ADR, HepG2 human liver carcinoma cell line and Hela human cervix adenocarcinoma cell line were from our own lab. All MM cell lines were grown in Roswell Park Memorial Institute (RPMI)-1640 medium with 100 I.U/ml penicillin, 100ug/ml streptomycin and 10% of fetal bovine serum (FBS). MCF-7, HepG2 and Hela cells were grown in Dulbecco's Modified Eagle Medium (DMEM) with 100 I.U/ml penicillin, 100ug/ml streptomycin and 10% of FBS. MCF-7/ADR cells was grown in DMEM with 100 I.U/ml penicillin, 100ug/ml streptomycin and 10% of FBS in the presence of free DOX at 1 μg/ml.

2.2.2 Materials

Bortezomib was purchased from Selleck Chemicals (Houston, TX, USA). Carfizomib was purchased from Chemie Tek (Indianapolis, IN, USA). SP1017 was kindly provided by Supratek Pharma. Inc (Montreal, Canada). Cell counting kit-8 (CCK-8) was purchased from Dojindo Molecular Technologies (Kumamoto, Japan). MTT reagent (3-(4,5-Dimethylthiazol-2-yl)-2,5-diphenyltetrazolium bromide) was purchased from Research Products International (Prospect, IL). Annexin V-FITC/ propidium iodide (PI) Apoptosis Kit was purchased from Biovision (Milpitas, CA, USA). Rhodamine 123 was purchased from Fisher Scientific (Waltham, MA). Verapamil and Dulbecco's phosphate buffered saline solution (PBS) was purchased from Sigma-Aldrich (St. Louis, MO). Anti-P-Glycoprotein mouse mAb (C219) was purchased from EMD Millipore (Darmstadt, Germany). Cleaved caspase-8 and -9 rabbit antibodies, anti-rabbit IgG HRP-linked antibody, cell Lysis Buffer (10×) and protease inhibitor cocktail (100×) were purchased from cell signaling technology

(Danvers, MA, USA). Anti-mouse IgG HRP-linked antibody was purchased from Santa Cruz Biotechnology (Santa Cruz, CA, USA). FBS, RPMI 1640 medium, DMEM medium, penicillin, streptomycin, Trypsin–ethylenediaminetetraacetic acid (EDTA) (0.5% trypsin, 5.3 mM EDTA tetra-sodium) were purchased from Invitrogen (Carlsbad, CA, USA).

2.2.3 Cytotoxicity in human MM cell lines by CCK-8 assay

Cytotoxicity of SP1017 alone was assessed in sensitive RPMI 8226 human MM cell line and cytotoxicity of BTZ/ CFZ ± 0.005% SP1017 was assessed in sensitive RPMI 8226 human MM cell line, ARH-77 human MM cell line, H929 human MM cell line and BTZ/CFZ-resistant RPMI 8226 cell lines by a standard CCK-8 assay. Briefly, cells were seeded in a 96-well microtiter plates with 10^4 of cells per well and exposed to various doses of SP1017 alone or BTZ/CFZ± 0.005% SP1017 for 24h at 37 ℃ in a humidified, 5% CO_2 atmosphere. 10ul of CCK-8 was added to each well and the cells were incubated for 1-4 h (when the absorption value ranges from 0.2-0.8, which shows better linearity) at 37 ℃ in the dark. Absorption was measured at 450nm in a microplate reader (SpectraMax M5, Molecular Devices Co., Sunnyvale, CA, USA) using wells without cells as blanks. The net absorbance was taken as index of cell viability. The reading taken from the wells with cells cultured with control medium was used as 100% viability value. The cell viability was calculated as $A_{sample}/A_{control}$ ×100%. Each concentration point was determined from samples from eight separate wells. Based on the results of the test, the IC_{50} values (the concentration which kill 50%

of cells) were calculated by using GraphPad Prism Software (Version 5.0, GraphPad Software, San Diego, CA, USA).

2.2.3 Overall apoptosis in human MM cell lines by Annexin V/PI assay

Cytotoxicity of BTZ ± 0.005% SP1017 was accessed in normal hematologic cells (PBMC) by Annexin V/PI assay. Briefly, 2×10^5 of PBMC and RPMI 8226 MM cells were seeded in 24-well plate per well and treated with Media as control, 0.005% SP1017, 10nM of BTZ and 10nM of BTZ+ 0.005% SP1017 for 20h. After treatment, cells were washed twice with PBS and treated with Annexin V-FITC and PI in 1X Binding Buffer according to the manufacturer's instructions. The labeled cells were analyzed using Becton Dickinson FACSCalibur™ flow cytometer in Fluorescence Activated Cell Sorting (FACS) cell analysis core facility and FACSDiva software (Version 8.0, Becton Dickinson, San Jose, CA).

2.2.4 Rhodamine 123 (Rh 123) uptake in both sensitive and resistant MM cell lines

Determination of the function of Pgp was assessed by the efflux of *Rh123, the Pgp substrate*. Briefly, 10^5 of RPMI 8226 human MM cells, ARH 77 human MM cells, H929 human MM cell line BTZ/CFZ-resistant RPMI 8226 human MM cells were exposed to 3.2 uM Rh123, 3.2uM Rh123+5uM Verapamil (Pgp inhibitor), 3.2uM Rh123+0.005%SP1049 for1h, 2h, 4h respectively. After the incubation, the suspension cells were centrifuged, washed three times with PBS and solubilized in 100 ul M-PER® Mammalian Protein Extraction Reagent. After 5-10mins, 70ul of lysed cell solutions were taken for determination of the cellular dye content using

fluorescent spectrophotometer with λex=505nm and λem=540nm. The results were normalized by protein content determined by BCA assay.

2.2.5 Western blot

Determination of Pgp expression levels, cleaved caspase 8 and cleaved caspase 9 were assessed by immunoblot technique. Briefly, 1.5×10^6 of RPMI 8226 human MM cells, ARH 77 human MM cells, BTZ/CFZ-resistant RPMI 8226 human MM cells were lysed with 100ul of Cell Lysis Buffer supplemented with protease inhibitor cocktail for Pgp detection. 1.5×10^6 of RPMI 8226 human MM cells treated with different concentrations of SP1017 for 24h were lysed in lysis buffer for caspases detection. Supernatant were collected after removing cell debris by centrifugation (14000 rpm for 10 min) and protein content was determined by BCA assay. 30μg of proteins were resolved by 10% sodium dodecyl sulfate-polyacrylamide gel electrophoresis (SDS-PAGE) and transferred onto PVDF membranes. The membranes were blocked by incubation in 5% dry milk in TBST (0.1% Tween-20 in Tris-buffered saline, TBS) and probed with the relative monoclonal antibodies were used at 1:100 dilutions. The secondary horseradish peroxide anti-mouse Ig antibody was used at 1:5000 dilutions. Blots were then visualized by enhanced chemiluminescence (ECL) substrates. To correct for loading differences, the levels of protein expression were normalized to a constitutively expressed GAPDH. Intensity of the bands was quantified by Image J software.

2.2.6 Cytotoxicity in non-hematological cancer cells by MTT assay

Cytotoxicity of BTZ ± 0.005% SP1017 was accessed in different non-hematologic tumor cells by MTT assay. Briefly, 10^4 of MCF-7 human breast adenocarcinoma cells, HepG2 human liver carcinoma cells, Hela human cervix adenocarcinoma cells per well were seeded in a 96-well microtiter plates, respectively. After 24h of attachment, cells were treated with various doses of BTZ ± 0.005% SP1017 for 24h at 37 ℃ in a humidified, 5% CO_2 atmosphere. Following treatment, the medium was removed and the cells were rinsed three times by PBS. 20ul of MTT (5mg/ml) was added to each well and the cells were incubated for 2h at 37℃ in the dark to form insoluble formazan, which was then solubilized by 100ul of 20% SDS in 50% Dimethylformamide (DMF), and the absorbance was determined by at 570 nm using a microplate reader (SpectraMax M5, Molecular Devices Co., Sunnyvale, CA, USA) using wells without cells as blanks. The net absorbance was taken as index of cell viability. The reading taken from the wells with cells cultured with control medium was used as 100% viability value. The cell viability was calculated as $A_{sample}/A_{control}$ ×100%. Each concentration point was determined from samples from eight separate wells. Based on the results of the test, IC_{50} values were calculated by using GraphPad Prism 5 Software (GraphPad Software, San Diego, CA).

2.2.7 Cytotoxicity in normal hematological cells by Annexin V/PI assay

Cytotoxicity of BTZ ± 0.005% SP1017 was accessed in normal hematologic cells (PBMC) by Annexin V/PI assay. Briefly, 2×10^5 of PBMC and RPMI 8226 MM cells were seeded in 24-well plate per well and treated with Media as control, 0.005% SP1017, 10nM of BTZ and 10nM of BTZ+ 0.005% SP1017 for 20h. After treatment,

cells were washed twice with PBS and treated with Annexin V-FITC and PI in 1X Binding Buffer according to the manufacturer's instructions. The labeled cells were analyzed using Becton Dickinson FACSCalibur™ flow cytometer and FACSDiva software (Version 8.0, Becton Dickinson, San Jose, CA).

2.2.8 Statistical analysis

Statistical comparisons between two groups for in vitro studies were evaluated using Student's *t*-test. Two-tailed *P* values less than 0.05 were considered significant.

2.3 Results and discussion

SP1017 alone showed dose-dependent cytotoxicity in RPMI 8226 human MM cells **(Figure 2.1A)**. 0.005% was the maximum concentration of SP1017 which showed no cytotoxicity in RPMI 8226 MM cells after 24h exposure. The concentrations above 0.005% of SP1017 induced cell death associated with apoptosis-associated caspase 9 and caspase 8 activations **(Fig 2.1B)**. We chose 0.005% as the concentration of SP1017 (below the CMC of Pluronic® L61) in the combination therapy to investigate the sensitization effect of SP1017 on MM when combined with proteasome inhibitors.

The responses to the combination of proteasome inhibitors+SP1017 in different MM cell lines (RPMI 8226 human MM cell line, ARH-99 human MM cell line and H929 human MM cell line) were evaluated. As seen in **Table.2.1**, 0.005% SP1017 triggered 2-fold of increase of cytotoxicity in three different MM cell lines when combined with the reversible proteasome inhibitor BTZ or the irreversible proteasome

A

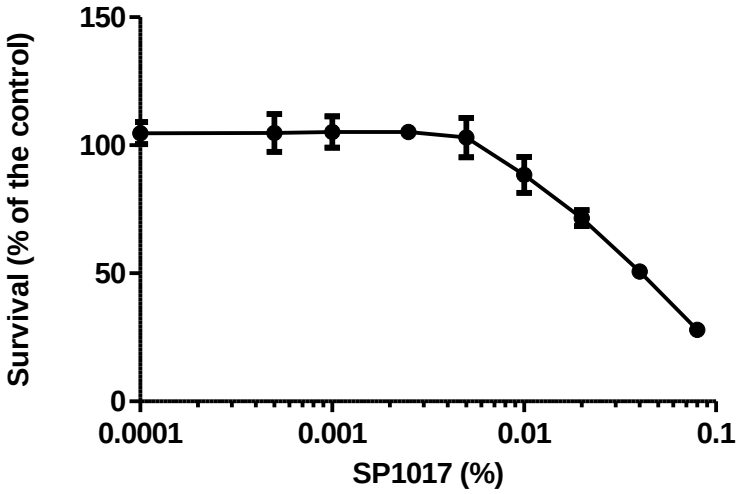

B

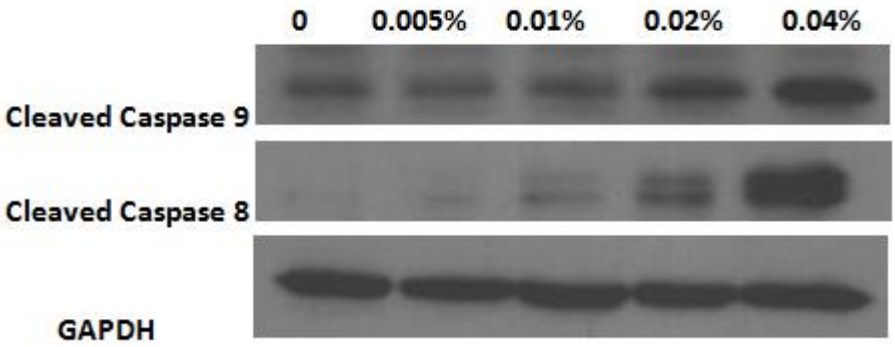

Fig.2.1. (A) Cytotoxicity of SP1017 with different concentrations to RPMI 8226 MM cells after 24h treatment. Data presented as mean ± SD. N=3. (B) Increased expression of cleaved caspase 9 and caspase 8 in RPMI 8226 MM cells after 24h treatment of different concentrations of SP1017.

Table 2.1 (A) IC_{50} of BTZ ± Pluronics in different human MM cell lines.

IC_{50}±SD (nM)	BTZ	BTZ+ 0.005%SP1017	BTZ+ 0.0006%L61	BTZ+ 0.0044%F127	BTZ+ 0.002% SP1017
RPMI 8226	14.6 ± 3.0[a]	8.1 ± 1.6 [a] ***	9.7 ± 1.5 [b] **	15.7 ± 2.2 [b]	10.5 ± 0.5 [b] *
ARH-77	17.1 ± 1.7	9.7 ± 2.3*			
H929	4.3 ± 0.6	2.4 ± 0.2**			

Table 2.1 (B) IC_{50} of CFZ ± Pluronics in different human MM cell lines.

IC_{50}±SD (nM)	CFZ	CFZ+ 0.005%SP1017	CFZ+ 0.0006% L61	CFZ+ 0.0044%F127	CFZ+ 0.002% SP1017
RPMI 8226	13.9 ± 2.4[c]	6.3 ± 1.2[c] ***	6.3 ± 1.0**	12.2 ± 2.0	8.0 ± 1.6**
ARH-77	11.7 ± 0.8	5.7 ± 1.0**	5.1 ± 2.3**	9.3 ± 2.0	
H929	16.5 ± 2.4	6.1 ± 1.0**			

Cells were treated for 24h. Data presented as mean ± SD. N=3

[a]N=10; [b]N=4; [c]N=5; *p<0.05,**p<0.01,***p<0.001;compared to drug alone.

inhibitor CFZ after 24h treatment. Lower concentration of SP1017 (0.002%) showed lower, but still significant increased cytotoxicity when combined with proteasome inhibitors compared to drugs alone. To confirm whether the decrease of MM cell viability in response to BTZ + SP1017 combination was due to apoptosis, we performed Annexin V/ PI assay by flow cytometry. BTZ+SP1017 combination showed much more early and late apoptosis compared with BTZ alone in both time- and dose-dependent manner (**Fig.2.2**), which further confirming the chemosensitizationeffect of SP1017 on MM cells when combined with proteasome inhibitors. Pluronic® L61 (HLB=3; PPO units=30; CMC=0.02%), which is more hydrophobic than Pluronic® F127 (HLB=22, PPO units=65; CMC=0.0035%) [31], played the major role in the chemosensitization effect (**Table 2.1**). This could be explained by previous studies which demonstrated the hydrophobic PPO chains with intermediate length of PEO units from 30 to 60 and HLB <20 [25, 26] of Pluronic® unimers immerse into the membrane hydrophobic areas, resulting in alterations of the membrane structure, and triggering subsequent biological effects [32]. Different drug treatment schedules were investigated by treating RPMI 8226 MM cells with BTZ+SP1017 concomitantly or sequentially. Maximal anti-MM activity was noted when SP1017 and BTZ were given concomitantly than in other order drug treatment schedules (**Table2.2**).

Acquired BTZ and CFZ resistance have been observed in MM cells as well as clinical patients, which makes proteasome inhibitors unappealing for long-term administration and limit the efficacy to be used as anti-MM drugs [33]. According to current researches, BTZ-resistance is mainly due to the impaired BTZ binding to mutant β5 subunits or the overexpression of β5 subunits while CFZ-resistance is associated with overexpression of Pgp protein [15, 34]. Our lab developed the BTZ/CFZ resistant RPMI 8226 cell lines by the stepwise increase of BTZ/CFZ

A

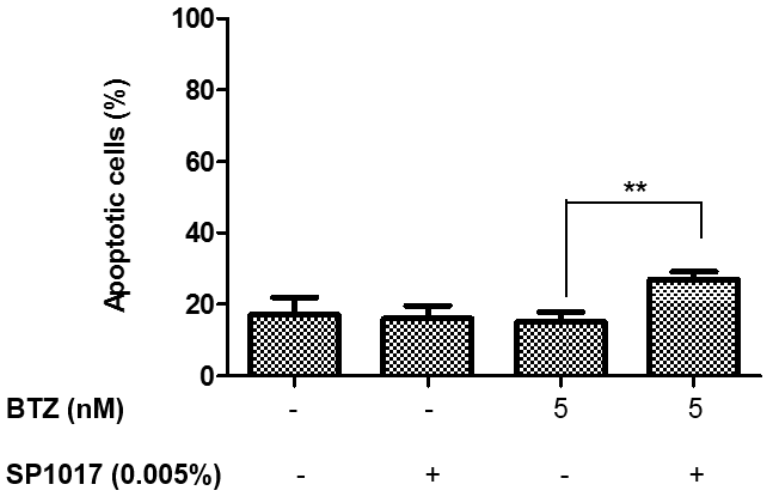

B

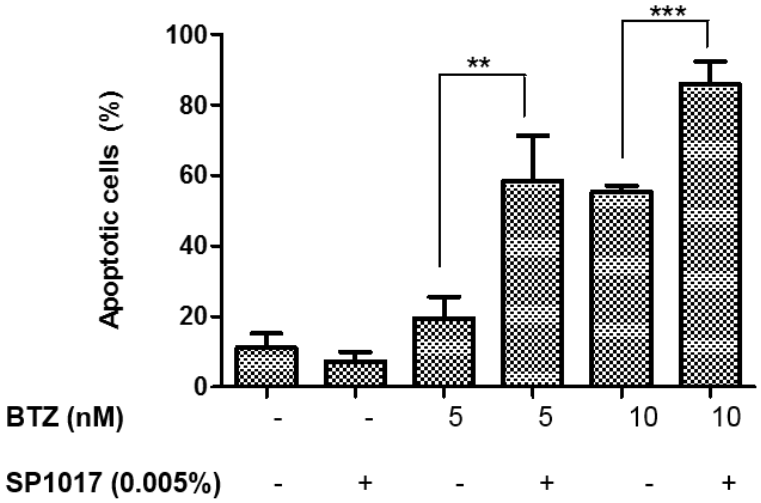

Fig.2.2 Percentage of overall cell apoptosis (early and late apoptosis) of RPMI 8226 MM cells treated with BTZ± 0.005% SP1017 for (A) 8h and (B) 24h by flow cytometric analysis using annexin V and PI staining. Data presented as mean ± SD. N=3 (*p<0.05, **p<0.01, ***p<0.001).

Table.2.2. IC_{50} of BTZ ± Pluronics in RPMI 8226 human MM cell line with different treatment schedules

IC_{50}±SD (nM)	[BFZ] 24h	[BTZ+0.005%SP1017] 24h	[0.005% SP1017] 24h+[BTZ]24h
RPMI 8226	14.6 ± 3.0[a]	8.1 ± 1.63 [a] ***	12.43 ± 1.33

Data presented as mean ± SD. N=3 ([a] N=10; ***p<0.001, compared to [BTZ] 24h).

concentration to the final concentration to 40nM by 6 months [35]. BTZ-resistant (9-fold) RPMI 8226 cells gained a marked but less pronounced cross-resistance to CFZ (5-fold) and CFZ-resistant (23-fold) RPMI 8226 cells also exhibited less cross-resistant to BTZ (6-fold). The results was in consist with previous findings that THP1 myeloid sublines with acquired resistance to BTZ (54- to 235-fold) caused by mutations in the PSMB5 gene displayed less pronounced cross-resistance to CFZ (9- to 32-fold) while MDR lymphoid CEM/VLB cells with Pgp overexpression exhibited substantial resistance to carfilzomib (114-fold) whereas less resistance to BTZ (4.5-fold) was observed [36]. Around 2.8-fold of sensitizing effect of SP1017 could be observed in BTZ-resistant cell lines when combined with BTZ or CFZ, which was comparable to that on sensitive cells. However, interestingly, we observed the significant increase of sensitizing factor (6.61±1.07) of SP1017 in CFZ resistant cell line when combined with CFZ rather than BTZ **(Table.2.3)**. The reason of higher sensitizing factor of SP1017 in CFZ- resistant cell line could be explained by the Pgp expression in CFZ-resistant cell line rather than sensitive or BTZ-resistant MM cell lines, which is confirmed by western blot **(Fig.2.3)** and functional analysis, Rh123 accumulation **(Fig.2.4)** as Pluronics inhibiting Pgp drug efflux system of MDR phenotype has been already proved [37, 38]. We found Pgp expression in selected BTZ-resistant RPMI 8226 MM cells rather than sensitive RPMI 8226 MM cells, H929 MM cells, ARH-77 MM cells or BTZ-resistant RPMI 8226 MM cells **(Fig.2.4)**, though the expression was lower than that of the positive control, MCF-7/ADR cells. Moreover, the uptake of Rh123, the Pgp substrate in sensitive RPMI 8226 MM cells,

Table.2.3. IC_{50} of BTZ/CFZ± 0.005%SP1017 in BTZ/CFZ-resistant RPMI 8226 MM cell lines (RPMI 8226/BTZ cell line and RPMI 8226/CFZ cell line)

IC_{50}±SD (nM)	BTZ	BTZ+SP	Sensitization factor[a]	CFZ	CFZ+SP	Sensitization factor[a]
Sensitive RPMI 8226	14.6 ± 3.0[a]	8.1 ± 1.6 [a] ***	1.8 ± 0.2	13.9 ± 2.4[b]	6.3 ± 1.2[b] ***	2.3 ± 0.2
RPMI 8226/BTZ	127.7 ± 29.2[b]	50.2 ± 17.1[b]***	2.7 ± 0.7	64.2 ± 20.9[b]	24.7 ± 5.9[b]**	2.6 ± 0.1
RPMI 8226/CFZ	86.0 ± 9.3	29.1 ± 8.6**	3.0 ± 0.7	324.1 ± 77.1[b]	49.4 ± 7.3[b]***	6.6 ± 1.1

Cells were treated for 24h. Data presented as mean ± SD. N=3 ([a]N=10,[b]N=5, p<0.01,***p<0.001, compared to relative drug alone). [a]Sensitization factor= [$IC_{50}$of drug] / [IC_{50} of drug+SP].

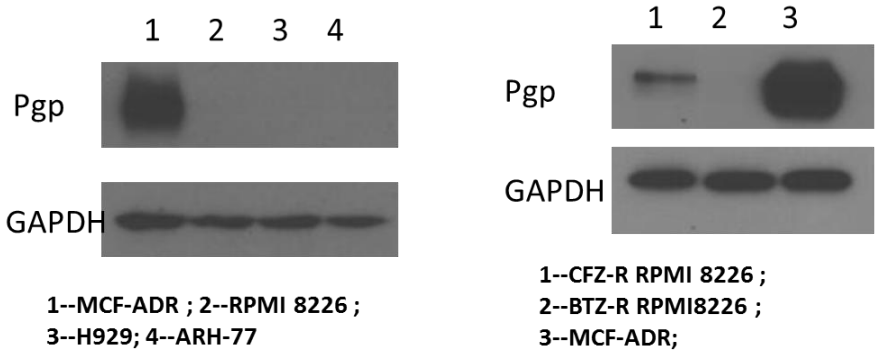

Fig 2.3 Pgp expression by western blot of Rh123 accumulation of sensitive MM cell lines and BTZ/CFZ-resistant MM cell lines.

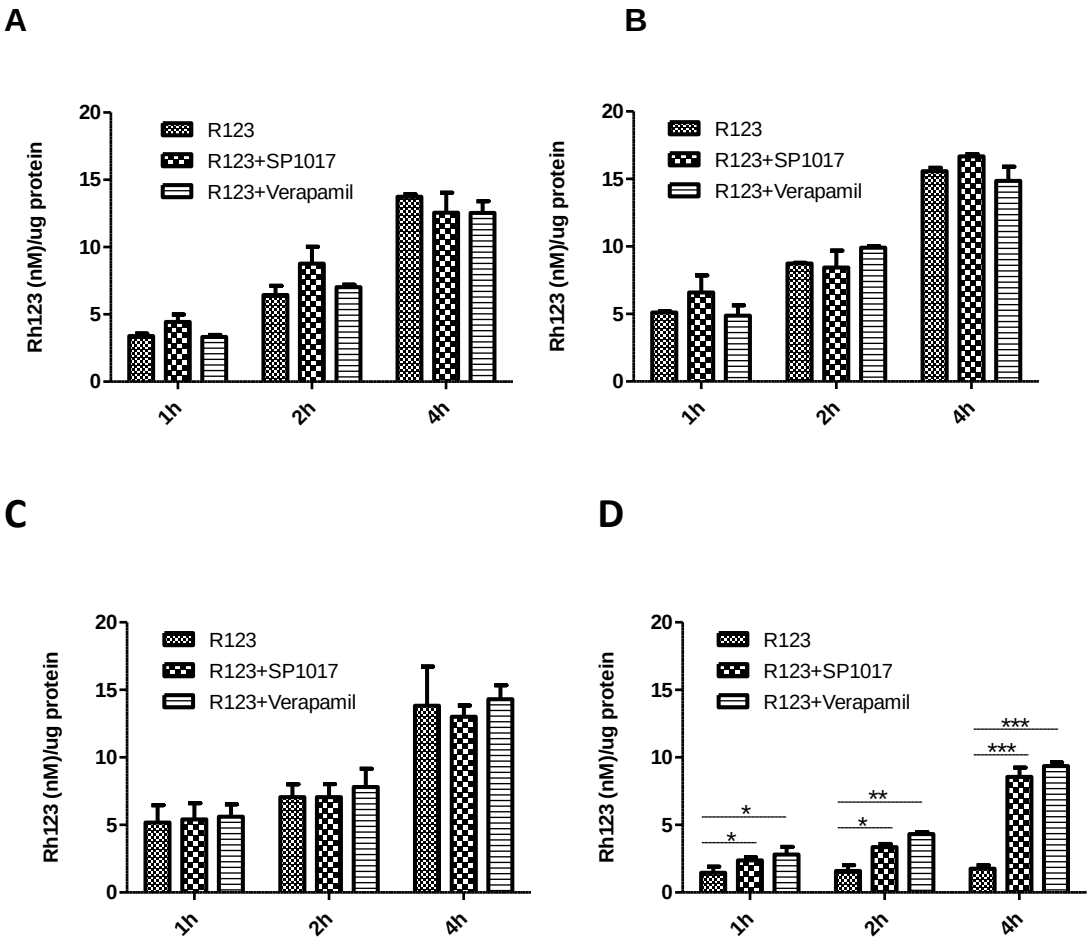

Fig.2.4 Pgp functional activity of Rh123 accumulation of (A) RPMI 8226 MM cell line, (B) ARH-77 MM cell line, (C) BTZ-resistant RPMI 8226 MM cell line and (D) CFZ-resistant RPMI 8226 MM cell line. Data presented as mean ± SD. N=3 (*P <0.05, **P<0.01, ***p<0.001).

ARH-77 MM cells and BTZ-resistant RPMI 8226 MM cells was higher than that in CFZ-resistant RPMI 8226 MM cells and was not increased in the presence of SP1017 or the Pgp inhibitor, verapamil. However, the intracellular Rh123 was much higher in CFZ-resistant RPMI 8226 MM cells in the presence of SP1017 or verapamil in a time dependent manner, indicating the inhibition of Pgp in CFZ-resistant MM cells significantly increase the uptake of Pgp substrate. Therefore, Pgp upregulation plays a major role in the development of CFZ resistance in MM exposed to prolonged CFZ therapy. Since CFZ received U.S.FDA approval in 2012, the Pluronics have greater potential to work in a combination regimen in clinical for treatment of patients with MM who were refractory to CFZ. The sensitization effect of SP1017 in CFZ-resistant MM cells when combined with BTZ was comparable to that in BTZ-resistant MM cells. Though previous studies indicated that BTZ is a substrate for Pgp and the most synergy of BTZ combined with Pgp inhibitor, elacridar was found the cells with highest Pgp level [39], BTZ exhibited as a poor Pgp substrate and that Pgp upregulation may be not the overwhelming mechanism of BTZ resistance, which was mainly related with point mutation or overexpression of PSMB5 gene and alterations of gene and protein expression in stress response, cell survival and antiapoptotic pathways[12]. For example, Pgp-expressing leukemic cells (CEM/VLB) are markedly resistant to CFZ (114-fold increase in IC_{50}) yet only a slight (4.5-fold) increase in IC_{50} was observed for BTZ. Furthermore, the Pgp inhibtor completely reversed carfilzomib resistance with little to no effect on BTZ sensitivity [36]. Despite of the chemosensitization effects with anticancer drugs, Pluronic® block copolymer was

reported to prevent the development of multidrug resistance in the cells exposed to drug in the selection as MDR cells selected in the presence of Pluronic® P85 tolerated a 1000 times less concentration of the drug compared with that selected in the absence of Pluronic® P85 [40]. Thus, the co-administration of SP1017 with anti-MM drugs might prevent or delay the emergence of acquired resistance, showed the great potential the combination of Pluronic® block copolymers with anticancer drugs. The detailed molecular mechanisms of sensitization effect of SP1017 on both BTZ and CFZ resistant MM cells need further investigation and elucidation.

Hematologic toxicity is commonly encountered in patients with MM owing to the nature of the disease and the adverse effects related to myeloma treatment. BTZ has been proved to be associated with increased rates of anemia, neutropenia, and thrombocytopenia, as well as greater incidences of infection caused by associated immunosuppression [41]. To ensure the safety of the BTZ+SP1017 combination, the cytotoxicity of the combined therapy to normal hematological cells (PBMC) was examined by Annexin V/PI assay. Though previous studies indicated that normal PBMC cell viability was relatively less affected by proteasome inhibitors as compared with that of myeloma cells [42,43], we found 10nM BTZ induced similar toxicity to RPMI 8226 MM cells and normal hematological cells after 20h treatment. However, the combination was not more toxic than single drug in PBMC while significant increase of the overall apoptosis of RPMI 8226 MM cells was induced by BTZ in the presence of SP1017 **(Fig.2.5)**. Therefore, SP1017 showed its potential to be used as a sensitizer in the combination therapy.

The ubiquitin-proteasome pathway (UPP) plays a critical role of intracellular protein degradation and cellular homeostasis maintenance. More than 80% of cellular proteins are degraded through this pathway including those involved in a broad array

of processes such as cell cycle, apoptosis, transcription, DNA repair, protein quality control and antigen presentation [44]. As the essential role of the proteasome in cell function (up-regulation of cell proliferation and down-regulation of cell death in human cancer cells), proteasome becomes the drug target for anti-cancer agents. There are two types of proteasomes, the constitutive form (20S), expressed in most cell types, and the immunoproteasome (i20S), a unique target found in lymphoid-derived cells [45]. Both BTZ and CFZ have been validated to target both the constitutive and immunoproteasomes indiscriminately in myeloma and other model systems [46]. By selectively inhibiting the i20S, it may be possible to maintain anti-myeloma and anti-lymphoma efficacy while reducing these toxicities, thereby increasing the therapeutic index. Researches also indicated cell lines representing hematologic cancers were more sensitive to immunoproteasome-specific inhibitors, which retained its preferential i20S activity in cytotoxicity assays, than a panel of solid tumor cell lines that were tested [46]. Clinical trials of BTZ also indicated the unsatisfied efficacy in treatment of solid tumors such as metastatic breast cancer, metastatic neuroendocrine tumors and advanced renal cell carcinoma [7]. For instance, from their clinical trials on 12 enrolled metastatic breast cancer patients, no objective responses were observed. One patient had stable disease, and 11 others experienced disease progression. The median survival time was only 4.3 months [47].To ensure the specificity of the BTZ+SP1017 combination to MM, we also examined the cytotoxicity of the BTZ+/-SP1017 to other non-hematologic tumor cells, such as MCF-7 human breast adenocarcinoma cells, HepG2 human liver carcinoma cells and Hela human cervix adenocarcinoma cells. BTZ alone giving less than encouraging results in non-hematologic tumor cells compared with that to RPMI 8226 MM cells and SP1017 did not showed the significant sensitization effect on non-hematological tumor cells as what showed in MM cells **(Fig.2.6)**. Therefore, the chemosensitization effect of SP1017 was proved to be specific to MM cells rather than non-hematologic tumor cells, showing the promising potential of

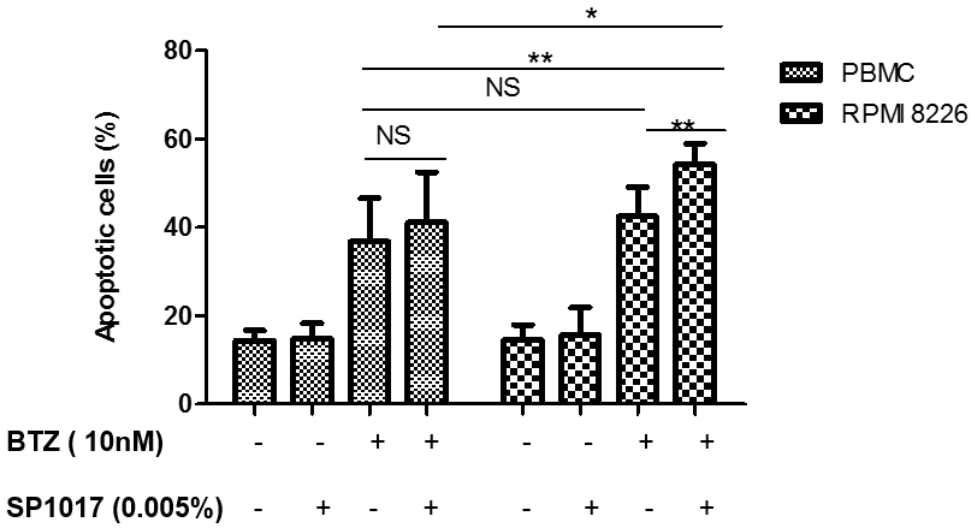

Fig.2.5. PBMC and RPMI 8226 MM cells were exposed to 10nM BTZ ± 0.005% SP1017 for 20h and assessed for apoptosis by flow cytometric analysis using annexin V and PI staining. Data presented as mean ± SD. N=6. (*p<0.05, **p<0.01, NS=no significant difference).

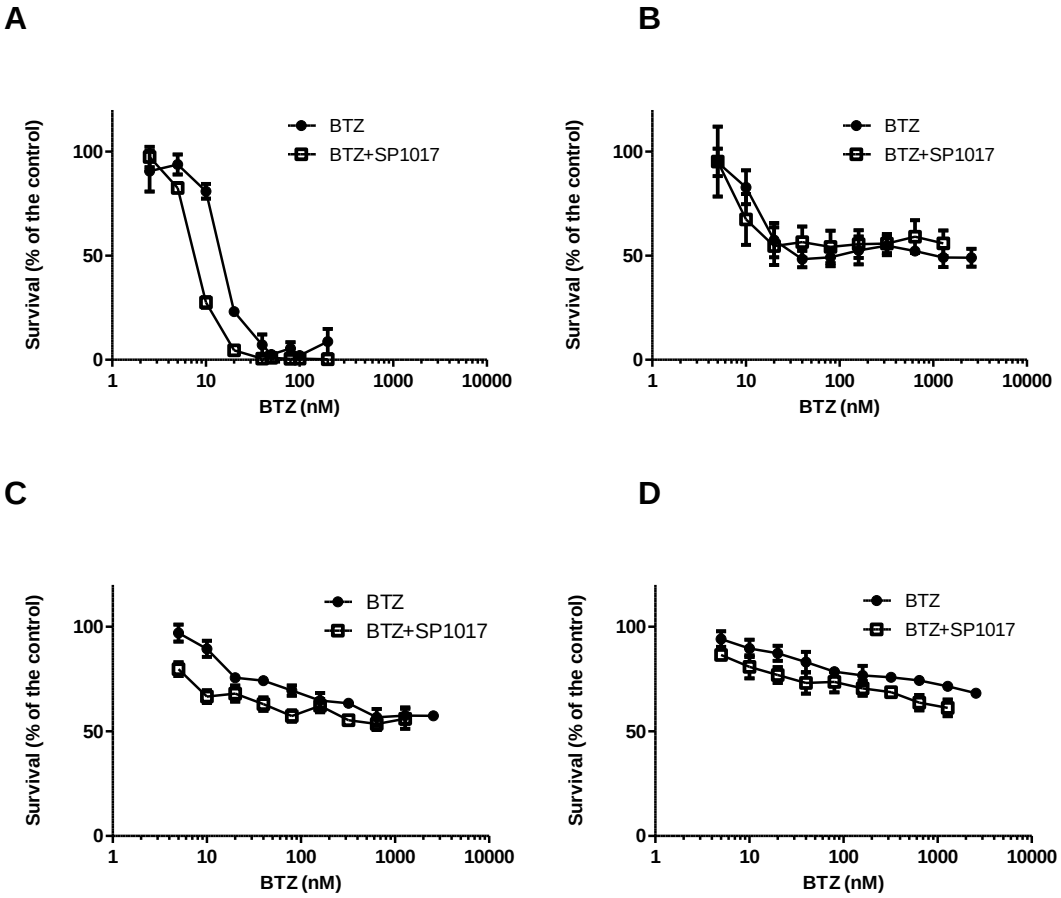

Fig.2.6. Cytotoxicity of BTZ± 0.005% SP1017 in (A) RPMI 8226 human MM cell line, (B) MCF-7 human breast adenocarcinoma cell line, (C) Hela human cervix adenocarcinoma cell line, and (D) HepG2 human liver carcinoma cell line. Cells were treated for 24h. Data presented as mean ± SD. N=6.

using the combination of BTZ+SP1017 in hematologic malignancies.

2.4 Conclusions

SP1017 is the mixed micelles formed by Pluronic® L61 which exhibited the biological effects due to its relative hydrophobicity and Pluronic® F127 as a stabilizer due to its relative hydrophilicity. 0.005% SP1017 (below the CMC of Pluronic® L61) potentiated 2-fold of both the reversible proteasome inhibitor (BTZ)- and irreversible proteasome inhibitor (CFZ)- induced cell cytotoxicity of three different MM cell lines. The increased cytotoxicity in response to BTZ + SP1017 combination was due to apoptosis analyzed by annexin V/ PI assay. Lower concentration of SP1017 (0.002%) showed lower, but still significant sensitization effect on RPMI 8226 MM cells when combined with proteasome inhibitors compared to drugs alone. BTZ-resistant RPMI 8226 cells gained a marked but less pronounced cross-resistance to CFZ and CFZ-resistant RPMI 8226 cells also exhibited less cross-resistant to BTZ. SP1017 remained the comparable sensitization effect in BTZ-resistant RPMI 8226 cells while gained significant higher sensitization factor in CFZ-resistant RPMI 8226 cells. The reason of higher sensitization effect in CFZ-resistant RPMI 8226 cell line was attributed to the Pgp expression in CFZ-resistant MM cells, which indicated that Pgp upregulation plays a major role in the development of CFZ resistance in multiple myeloma exposed to prolonged CFZ therapy while not contribute to BTZ resistance. Interestingly, SP1017 did not sensitize BTZ-induced apoptosis of normal hematological cell (PBMC), which indicates the potential of maintaining the anti-MM efficacy of the

combination therapy while reducing hematological toxicities. Moreover, BTZ alone exhibiting less than encouraging results in non-hematologic tumor cells compared with that to RPMI 8226 MM cells. The BTZ-induced cytotoxicity of non-hematological cells was not increase in the presence of SP1017, indicating the specificity of the combination therapy in dealing with hematologic malignancies.

2.5 References

[1] Laubach JP, Voorhees PM, Hassoun H, Jakubowiak A, Lonial S, Richardson PG. Current strategies for treatment of relapsed/refractory multiple myeloma. Expert Rev Hematol. 2014 Feb;7(1):97-111.

[2]Howlader N,et,al. SEER Cancer Statistics Review, 1975-2010, National Cancer Institute. Bethesda, MD, http://seer.cancer.gov/csr/1975_2010/, based on November 2012 SEER data submission, posted to the SEER web site, April 2014.

[3] Raab MS, et al, Multiple myeloma. Lancet 2009: 324–39.

[4] Kyle RA, et al. Review of 1027 patients with newly diagnosed multiple myeloma. Mayo Clin Proc 2003,78:21-33.

[5] Meletios A. Dimopoulos, et al. Emerging therapies for the treatment of relapsed or refractory multiple myeloma. Eur J Haematol 2011,86(1):1-15.

[6] Twombly R. First proteasome inhibitor approved for multiple myeloma. J Natl Cancer Inst. 2003 Jun 18;95(12):845.

[7] Chen D, Frezza M, Schmitt S, Kanwar J, Dou QP. Bortezomib as the first proteasome inhibitor anticancer drug: current status and future perspectives. Curr Cancer Drug Targets. 2011 Mar;11(3):239-253.

[8] Fisher RI, Bernstein SH, Kahl BS, Djulbegovic B, Robertson MJ, de Vos S, Epner E, Krishnan A, Leonard JP, Lonial S, Stadtmauer EA, O'Connor OA, Shi H,Boral AL, Goy A. Multicenter phase II study of bortezomib in patients with relapsed or refractory mantle cell lymphoma. J Clin Oncol. 2006 Oct 20;24(30):4867-4874.

[9] Richardson PG, Barlogie B, Berenson J, Singhal S, Jagannath S, Irwin D, Rajkumar SV, Srkalovic G, Alsina M, Alexanian R, Siegel D, Orlowski RZ, Kuter D,Limentani SA, Lee S, Hideshima T, Esseltine DL, Kauffman M, Adams J, Schenkein DP, Anderson KC. A phase 2 study of bortezomib in relapsed, refractory myeloma. N Engl J Med. 2003 Jun 26;348(26):2609-2617.

[10] Goy A, Younes A, McLaughlin P, Pro B, Romaguera JE, Hagemeister F, Fayad L, Dang NH, Samaniego F, Wang M, Broglio K, Samuels B, Gilles F, Sarris AH, Hart S, Trehu E, Schenkein D, Cabanillas F, Rodriguez AM. Phase II study of proteasome inhibitor bortezomib in relapsed or refractory B-cell non-Hodgkin's lymphoma. J Clin Oncol. 2005 Feb 1;23(4):667-675.

[11] Jagannath S, Barlogie B, Berenson J, Siegel D, Irwin D, Richardson PG, Niesvizky R, Alexanian R, Limentani SA, Alsina M, Adams J, Kauffman M,Esseltine DL, Schenkein DP, Anderson KC. A phase 2 study of two doses of bortezomib in relapsed or refractory myeloma. Br J Haematol. 2004 Oct;127(2):165-172.

[12] Lü S, Wang J. The resistance mechanisms of proteasome inhibitor bortezomib. Biomark Res. 2013 Mar 1;1(1):13.

[13] Meregalli C. An overview of bortezomib-induced neurotoxicity Toxics 2015 July 27, 3, 294-303.

[14] Dou QP, Zonder JA. Overview of proteasome inhibitor-based anti-cancer therapies: perspective on bortezomib and second generation proteasome inhibitors versus future generation inhibitors of ubiquitin-proteasome system. Curr Cancer Drug Targets. 2014;14(6):517-536.

[15] Hawley TS, Riz I, Yang W, Wakabayashi Y, Depalma L, Chang YT, Peng W, Zhu J, Hawley RG. Identification of an ABCB1 (P-glycoprotein)-positive carfilzomib-resistant myeloma subpopulation by the pluripotent stem cell fluorescent dye CDy1. Am J Hematol. 2013 Apr;88(4):265-272.

[16] Castelli R, Gualtierotti R, Orofino N, Losurdo A, Gandolfi S, Cugno M. Current and Emerging Treatment Options for Patients with Relapsed Myeloma. Clin Med Insights Oncol. 2013 Aug 19;7:209-219.

[17] Jakubowiak A.. Management Strategies for Relapsed/Refractory Multiple Myeloma: Current Clinical Perspectives. Semin Hematol. 2012 Jul;49 Suppl 1:S16-32.

[18] Vande Broek I, Jacobs P. Continuous treatment in multiple myeloma: The future? Transfus Apher Sci. 2013 Oct;49(2):147-50.

[19] Kapoor P, Ramakrishnan V, Rajkumar SV. Bortezomib combination therapy in multiple myeloma. Semin Hematol. 2012 Jul;49(3):228-242.

[20] Alakhov VYu, Moskaleva EYu, Batrakova EV, Kabanov AV.. Hypersensitization of multidrug resistant human ovarian carcinoma cells by Pluronic P85 block copolymer. Bioconjug Chem. 1996 Mar-Apr;7(2):209-16.

[21] Venne A, Li S, Mandeville R, Kabanov A, Alakhov V. Hypersensitizing Effect of Pluronic L61 on Cytotoxic Activity, Transport, and Subcellular Distribution of

Doxorubicin in Multiple Drug-resistant Cells. Cancer Res. 1996 Aug 15;56(16):3626-3629.

[22] Batrakova EV, Dorodnych TY, Klinskii EY, Kliushnenkova EN, Shemchukova OB, Goncharova ON, Arjakov SA, Alakhov VY, Kabanov AV. Anthracycline antibiotics non-covalently incorporated into the block copolymer micelles: in vivo evaluation of anti-cancer activity. Br J Cancer. 1996 Nov;74(10):1545-52.

[23] Alakhov V, Klinski E, Li S, Pietrzynski G, Venne A, Batrakova EV, Bronitch T, Kabanov A. Block copolymer-based formulation of Doxorubicin. From cell screen to clinical trials. Colloids Surf. B: Biointerfaces 1999;16:113–134.

[24] Valle JW, Armstrong A, Newman C, Alakhov V, Pietrzynski G, Brewer J, Campbell S, Corrie P, Rowinsky EK, Ranson M. A phase 2 study of SP1049C, doxorubicin in P-glycoprotein-targeting pluronics, in patients with advanced adenocarcinoma of the esophagus and gastroesophageal junction. Invest New Drugs. 2011 Oct;29(5):1029-1037

[25] Batrakova E, Lee S, Li S, Venne A, Alakhov V, Kabanov A. Fundamental Relationships Between the Composition of Pluronic Block Copolymers and Their Hypersensitization Effect in MDR Cancer Cells. Pharm Res. 1999 Sep;16(9):1373-1379.

[26] Batrakova EV, Li S, Alakhov VY, Miller DW, Kabanov AV.. Optimal Structure Requirements for Pluronic Block Copolymers in Modifying P glycoprotein Drug Efflux Transporter Activity in Bovine Brian Microvessel Endothelial Cells. J Pharmacol Exp Ther. 2003 Feb;304(2):845-854.

[27] Batrakova EV, Li S, Alakhov VY, Elmquist WF, Miller DW, Kabanov AV.. Sensitization of cells overexpressing multidrug-resistant proteins by pluronic p85. Pharm Res. 2003 Oct;20(10):1581-1590.

[28] Batrakova EV, Li S, Elmquist WF, Miller DW, Alakhov VY, Kabanov AV. Mechanism of sensitization of MDR cancer cells by Pluronic block copolymers: Selective energy depletion. Br J Cancer. 2001 Dec 14;85(12):1987-1997.

[29] Alakhova DY, Rapoport NY, Batrakova EV, Timoshin AA, Li S, Nicholls D, Alakhov VY, Kabanov AV. Differential metabolic responses to pluronic in MDR and non-MDR cells: A novel pathway for chemosensitization of drug resistant cancers . J Control Release. 2010 Feb 25;142(1):89-100.

[30] Minko T, Batrakova EV, Li S, Li Y, Pakunlu RI, Alakhov VY, Kabanov AV., Pluronic block copolymers alter apoptotic signal transduction of doxorubicin in drug-resistant cancer cells. J Control Release. 2005 Jul 20;105(3):269-278

[31] Kabanov AV, Batrakova EV, Alakhov VY. Pluronic block copolymers as novel polymer therapeutics for drug and gene delivery. J Control Release. 2002 Aug 21;82(2-3):189-212.

[32] Batrakova EV, Kabanov AV. Pluronic Block Copolymers:Evolution of Drug Delivery Concept from Inert Nanocarriers to Biological Response Modifiers. J Control Release. 2008 Sep 10;130(2):98-106.

[33] Laubach JP[1], Mitsiades CS, Roccaro AM, Ghobrial IM, Anderson KC, Richardson PG. Clinical challenges associated with bortezomib therapy in multiple myeloma and WaldenströmsMacroglobulinemia. Leuk Lymphoma. 2009 May;50(5):694-702.

[34] Franke NE, Niewerth D, Assaraf YG, van Meerloo J, Vojtekova K, van Zantwijk CH, Zweegman S, Chan ET, Kirk CJ, Geerke DP, Schimmer AD, Kaspers GJ,Jansen G, Cloos J. Impaired bortezomib binding to mutant β5 subunit of the proteasome is the underlying basis for bortezomibresistance in leukemia cells.Leukemia. 2012 Apr; 26(4):757-768.

[35] Oerlemans R, Franke NE, Assaraf YG, Cloos J, van Zantwijk I, Berkers CR, Scheffer GL, Debipersad K, Vojtekova K, Lemos C, van der Heijden JW, Ylstra B,Peters GJ, Kaspers GL, Dijkmans BA, Scheper RJ, Jansen G.. Molecular basis of bortezomib resistance: proteasome subunit beta5 (PSMB5) gene mutation and overexpression of PSMB5 protein. Blood. 2008 Sep 15;112(6):2489-2499.

[36] Verbrugge SE, Assaraf YG, Dijkmans BA, Scheffer GL, Al M, den Uyl D, Oerlemans R, Chan ET, Kirk CJ, Peters GJ, van der Heijden JW, de Gruijl TD,Scheper RJ, Jansen G. Inactivating PSMB5 mutations and P-glycoprotein (multidrug resistance-associated protein/ATP-binding cassette B1) mediate resistance to proteasome inhibitors: ex vivo efficacy of (immuno)proteasome inhibitors in mononuclear blood cells from patients with rheumatoid arthritis. J Pharmacol Exp Ther. 2012 Apr;341(1):174-182.

[37] Batrakova EV, Li S, Vinogradov SV, Alakhov VY, Miller DW, Kabanov AV. Mechanism of pluronic effect on P-glycoprotein efflux system in blood-brain barrier: contributions of energy depletion and membrane fluidization. J Pharmacol Exp Ther. 2001 Nov;299(2):483-493

[38] Batrakova EV, Li S, Li Y, Alakhov VY, Kabanov AV. Effect of pluronic P85 on ATPase activity of drug efflux transporters. Pharm Res. 2004 Dec;21(12):2226-2233.

[39] O'Connor R, Ooi MG, Meiller J, Jakubikova J, Klippel S, Delmore J, Richardson P, Anderson K, Clynes M, Mitsiades CS, O'Gorman P. The interaction of bortezomib with multidrug transporters: implications for therapeutic applications inadvanced multi ple myeloma and other neoplasias. Cancer Chemother Pharmacol. 2013 May;71(5): 1357-68.

[40] Elena Batrakova et al. Alternation of Genomic Responses to Doxorubicin and Prevention of MDR in Breast Cancer Cells by a Polymer Excipient: Pluronic P85. Molecular Pharmaceutics. 2006, 3 (2): 113-123.

[41] Lonial S, Richardson PG, San Miguel J, Sonneveld P, Schuster MW, Bladé J, Cavenagh J, Rajkumar SV, Jakubowiak AJ, Esseltine DL, Anderson KC,Harousseau JL. Characterisation of haematological profiles and low risk of thromboembolic events with bortezomib in patients with relapsed multiple myeloma. Br J Haematol. 2008 Oct;143(2):222-229.

[42] Hideshima T, Richardson P, Chauhan D, Palombella VJ, Elliott PJ, Adams J, Anderson KC. The proteasome inhibitor PS-341 inhibits growth, induces apoptosis, and overcomes drug resistance in human multiple myeloma cells. Cancer Res. 2001 Apr 1;61(7):3071-3076.

[43] Nooka AK. Management of hematologic adverse events in patients with relapsed and/or refractory multiple myeloma treated with single-agent carfilzomib. Oncology (Williston Park). 2013 Dec;27 Suppl 3:11-18.

[44] Crawford LJ, Walker B, Irvine AE. Proteasome inhibitors in cancer therapy. J Cell Commun Signal. 2011 Jun;5(2):101-110.

[45] Kuhn DJ, Orlowski RZ. The immunoproteasome as a target in hematologic malignancies. Semin Hematol. 2012 Jul;49(3):258-262.

[46] Kuhn DJ, Hunsucker SA, Chen Q, Voorhees PM, Orlowski M, Orlowski RZ. Targeted inhibition of the immunoproteasome is a potent strategy against models of multiple myeloma thatovercomes resistance to conventional drugs and nonspecific pr oteasome inhibitors. Blood. 2009 May 7;113(19):4667-4676

[47] Yang CH, Gonzalez-Angulo AM, Reuben JM, Booser DJ, Pusztai L, Krishnamurthy S, Esseltine D, Stec J, Broglio KR, Islam R, Hortobagyi GN, Cristofanilli M. Bortezomib (VELCADE) in metastatic breast cancer: pharmacodynamics, biological effects, and prediction of clinical benefits. Ann Oncol. 2006 May;17(5):813-817.

CHAPTER III: THE MOLECULAR MECHANISM OF THE SENSITIZATION EFFECT OF THE COMBINATION THERAPY TO MM.

3.1 Introduction

MM is a neoplastic proliferation of plasma cell within the BM in association with abnormal production of monoclonal immunoglobulin, also called M-protein or paraprotein detected in either serum and/or urine, decreased normal immunoglobulin levels and lytic bone disease. Over the past ten years, proteasome inhibition has emerged as an effective therapeutic strategy for treating MM and some lymphomas. Two typical examples of proteasome inhibitors used in MM are BTZ, the reversible inhibitor of the 20S proteasome and CFZ, the irreversible inhibitor of the 20S proteasome, which are U.S.FDA approved for relapsed or refractory MM [1].

The UPP degrades the majority of damaged/mutated/misfolded proteins in the cell to maintain the protein homeostasis [2]. Conversely, blockade of protein degradation by proteasome inhibitors causes accumulation of ubiquitinated damaged/mutated/misfolded proteins, which in turn up-regulates heat-shock response and cell death [3]. Degradation of a protein via UPP involves two discrete and successive steps: 1) tagging of the substrate protein by the covalent attachment of multiple ubiquitin molecules (conjugation); 2) the subsequent degradation of the tagged protein and free ubiquitin for recycling by the barrel-shaped 26S proteasome, composed of two 19S regulatory complex, separated in lid and base, and the 20s proteasome core, separated in 2 flanking α rings and 2 central β rings (degradation) [4,5]. Specifically, protein is first marked with a chain of small polypeptides called ubiquitin; ubiquitin-activating enzyme E1 then activates ubiquitin and links it to the ubiquitin-conjugating

enzyme E2 in an ATP-dependent manner; ubiquitin protein ligase E3 then links the ubiquitin molecule to the protein; a long polypeptide chain of ubiquitin moieties is formed; and finally, the 19S regulatory complexes recognize the poly-ubiquitinated proteins , unfold the protein substrates and assist in their translocation through a narrow gate into the 20S core particle where degradation takes place **(Fig 3.1)** [6, 7]. The 20S (or constitutive) catalytic core is barrel-shaped by 4 stacked rings, 2 outer α and 2 inner β rings, each formed by 7 subunits with an overall architecture of $\alpha_{1-7}\beta_{1-7}\beta_{1-7}\alpha_{1-7}$ **(Fig.3.2)**.The α rings serve as "gatekeepers" for the "proteolytic core" that is composed of the β rings. The active sites reside in three β subunits, β1, β2, and β5, exhibiting chymotrypsin-like, trypsin-like, and peptidyl-hydrolase (caspase)-like activities respectively [5]. Another form of the proteasome that is primarily expressed in cells of hematopoietic origin and cells exposed to inflammatory cytokines, known as the immunoproteasome (i20s) , is composed of iβ1 (LMP2), iβ2 (MECL-1), and iβ5 (LMP7) subunits which replace the constitutive β1, β2, and β5 subunits in the 20S core proteasome [8]. BTZ, a boronic dipeptide, reversibly inhibit the chymotrypsin-like (ChT-L) activity at the β5-subunit or LMP7 subunit with high potency and to a lesser extent (approximately 10-fold lower affinity) inhibit the caspase-like activity at the β1-subunit, thus leading to the accumulation of ubiquitinated proteins [9, 10]. CFZ, irreversible epoxomicin-related proteasome inhibitor, has been demonstrated sustained inhibition of proteasomal ChT-L activity and greater selectivity for the β5 subunit and LMP7 than BTZ, which contributes to its greater cytotoxic response and improved tolerability profile relative to BTZ [11, 12].

The imbalance of cellular protein homeostasis can lead to proteotoxic stress due to accumulation of misfolded proteins in the (endoplasmic reticulum) ER lumen and cytosol, resulting in harmful cellular effects known as proteotoxicity [13]. Cells respond to

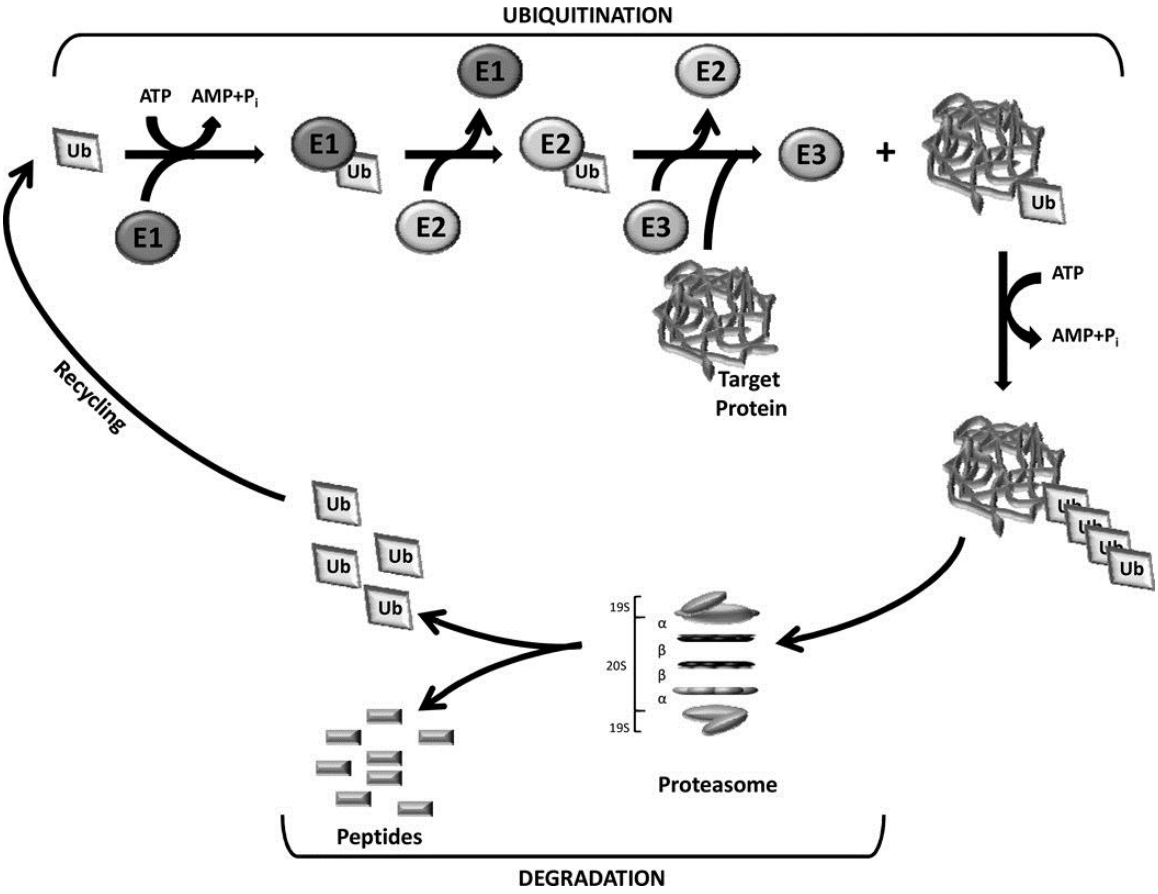

Fig.3.1 The ubiquitin-proteasome pathway. The ubiquitination of target proteins is mediated by Ub-activating (E1), Ub-conjugating (E2), and Ub-ligating (E3) enzymes. Substrate proteins tagged with a multiple-ubiquitin chain are then degraded by the 26S proteasome which is composed of a 20S catalytic core and two 19S subunits. (Adapted from [7])

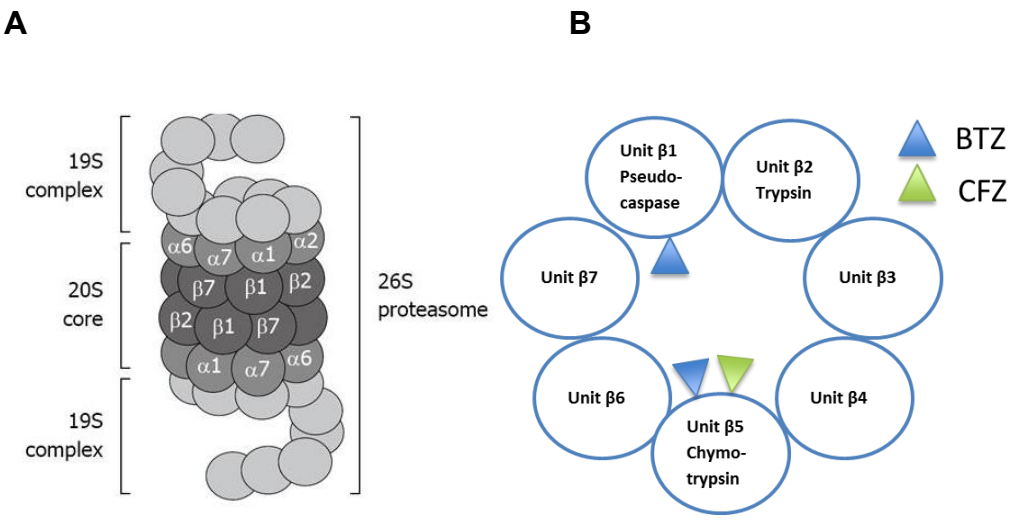

Fig.3.2 (A) The 26S proteasome consists of the 20S core capped with the 19S regulatory complexes that recognize ubiquitinated protein substrates designated for proteolysis. (Adapted from Bardag-Gorce F. Effects of ethanol on the proteasome interacting proteins. World J Gastroenterol. 2010 Mar 21; 16 (11): 1349-1357). (B) One of the constitutive 20S proteasome core β rings which has seven nonidentical subunits. BTZ binds slowly and reversibly inhibits the chymotrypsin-like activity and with lower affinity targets the caspase-like activity. CFZ irreversibly binds and inhibits predominantly the chymotrypsin-like activity. In the immunoproteasome, BTZ binds the β5i and β1i subunits while CFZ binds the β5i subunit. (Adapted from Orlowski RZ, Kuhn DJ. Proteasome inhibitors in cancer therapy: lessons from the first decade. Clin Cancer Res. 2008 Mar 15; 14 (6): 1649-1657).

proteotoxic stress in a compartment-specific manner. For example, the heat-shock response is triggered by proteotoxic stress in the cytosol, and the unfolded protein response (UPR) is activated by misfolded proteins in the ER, a condition referred to as ER stress [14]. The cellular heat-shock response is manifested by increased expression of heat-shock proteins (HSPs) , represents a basic defense mechanism employed by cells to protect themselves against stressors such as cold, UV light, and environmental toxins [15]. Most of the major HSPs function as molecular chaperones serve a wide variety of functions in cellular processes, but are primarily involved in the folding, assembly, and/or degradation of proteins and therefore appear to prevent the accumulation of aggregated, misfolded, or damaged proteins in the affected cell [16, 17] . Upregulation of heat shock protein expression by proteasome inhibition has been explored in the previous studies. A marked increase in HSP70 and a more than two-fold increase in HSP27 and HSP90 were observed in cells treated by the proteasome inhibitor, MG132 [18]. BTZ induced a pronounced upregulation of HSP 27, HSP70 and HSP90 in MM.1S cells, which reflected a stress response. The functional significance of up-regulation of HSPs in conferring a protective effect against BTZ is confirmed by the fact that HSPs inhibitors sensitized MM cells to BTZ-mediated apoptosis. The HSP90 inhibitor 17-AAG showed in vitro synergistic apoptotic effect on MM cells when combined with BTZ [19]. Another Hsp90 inhibitor IPI-504, overcame BTZ resistance in mantle cell lymphoma when combined with BTZ in vitro and in vivo by down-regulation of pro-survival ER chaperone Grp 78/Bip [20]. The ER is arranged in a dynamic tubular network involved in metabolic processes, which serves several important functions, including the post-translational modification and folding and assembly of newly synthesized secretory proteins. The accumulation of unfolded and/or misfolded proteins in ER lumen causes the failure of the ER to cope with the excess protein load, which is termed ER stress [21]. ER stress may elicit a series of complementary adaptive

mechanisms collectively referred to as the UPR activation, which results in a transient attenuation in the rate of protein synthesis, an upregulation of genes encoding chaperones and other proteins that prevent polypeptide aggregation and participate in polypeptide folding, and retro-translocation and degradation of ER-localized proteins, in order to maintains the protein-folding homeostasis within the ER [22]. Activation of the UPR depends on three ER stress sensors, including protein kinase RNA-like ER kinase (PERK), inositol-requiring protein 1α (IRE1α) and activating transcription factor 6 (ATF6). Under basal conditions these proteins are bound by the ER chaperone immunoglobulin heavy-chain-binding protein (Grp 78/Bip) and maintained in an inactive state. When ER stress develops, Grp 78/Bip is sequestered by the misfolded peptides and, as a consequence, released from the three sensor proteins, which triggers activation of the UPR branch [23]. For instance, PERK, a transmembrane serine/threonine kinase localized in the ER membrane, is activated by ER stress via dimerization and autophosphorylation, leading to phosphorylation of eIF2α and resulting in a global inhibition of translation [24]. However, if ER stress persists or is aggravated, ER stress signaling appears to switch from pro-survival to pro-apoptosis which is initiated through the activation of CCAAT/enhancer-binding homologous protein (CHOP), also known as growth arrest- and DNA damage-inducible gene 153 (GADD153), whose expression is low under non-stressed conditions, but markedly increases in response to ER stress through IRE1-, PERK- and ATF6-dependent transcriptional induction [25]. CHOP has been proved to play an important role in ER stress-induced apoptosis [26, 27]. Moreover, elevated CHOP expression results in the down-regulation of anti-apoptotic Bcl-2 expression, translocation of Bax protein from the cytosol to the mitochondria and perturbation of the cellular redox state by depletion of cellular glutathione and exaggerated production of reactive oxygen species, which functions as an integrator and amplifier of the death pathway [28].

The involvement of oxidative stress, an imbalance in the ratio of pro- and antioxidants has been observed in cells treated with proteasome inhibitors. The proteasome inhibitor, MG 132 induced calf pulmonary artery endothelial cells death via caspase-dependent apoptosis and GSH (an important buffering agent that maintains redox homeostasis) depletion [29]. Pretreatment with GSH or N-acetyl-L-cysteine (NAC, a precursor of glutathione and elevates glutathione contents) significantly suppressed BTZ-induced ROS generation and provided significant protection against apoptosis caused by BTZ in thyroid cancer cells [30]. BTZ treatment decreases intracellular GSH both in MM cell lines and in malignant plasma cells obtained from MM patients. Decreasing intracellular glutathione through buthionine sulfoximine treatment strongly enhanced BTZ toxicity while antioxidant NAC protected MM cells from BTZ-mediated cell death [31]. All of the above evidences indicate that oxidative stress is involved in BTZ-induced cell apoptosis

It is suggested a dual apoptotic mechanism induced by BTZ in MM cells: one is the intrinsic apoptotic pathway (mitochondrial mediated), and the other is extrinsic apoptotic pathway (death receptor mediated) [3]. The two apoptotic pathways showed in (**Fig.3.3)**. The intrinsic stimuli, such as DNA damage or ER stress, activate BH3-only proteins leading to BAX and BAK activation, which insert into the mitochondrial membrane, compromising its integrity. Mitochondrial membrane permeabilization results in the release of cytochrome c. In the cytoplasm, cytochrome c interacts with APAF-1, inducing its oligomerization and thereby forming a structure termed the apoptosome that recruits and activates an initiator caspase, caspase 9. Caspase 9 cleaves and activates executioner caspases, caspase 3 and caspase 7, leading to apoptosis. The extrinsic apoptotic pathway is initiated by the ligation of death receptors with their cognate ligands, leading to the recruitment of adaptor molecules such as FAS-associated

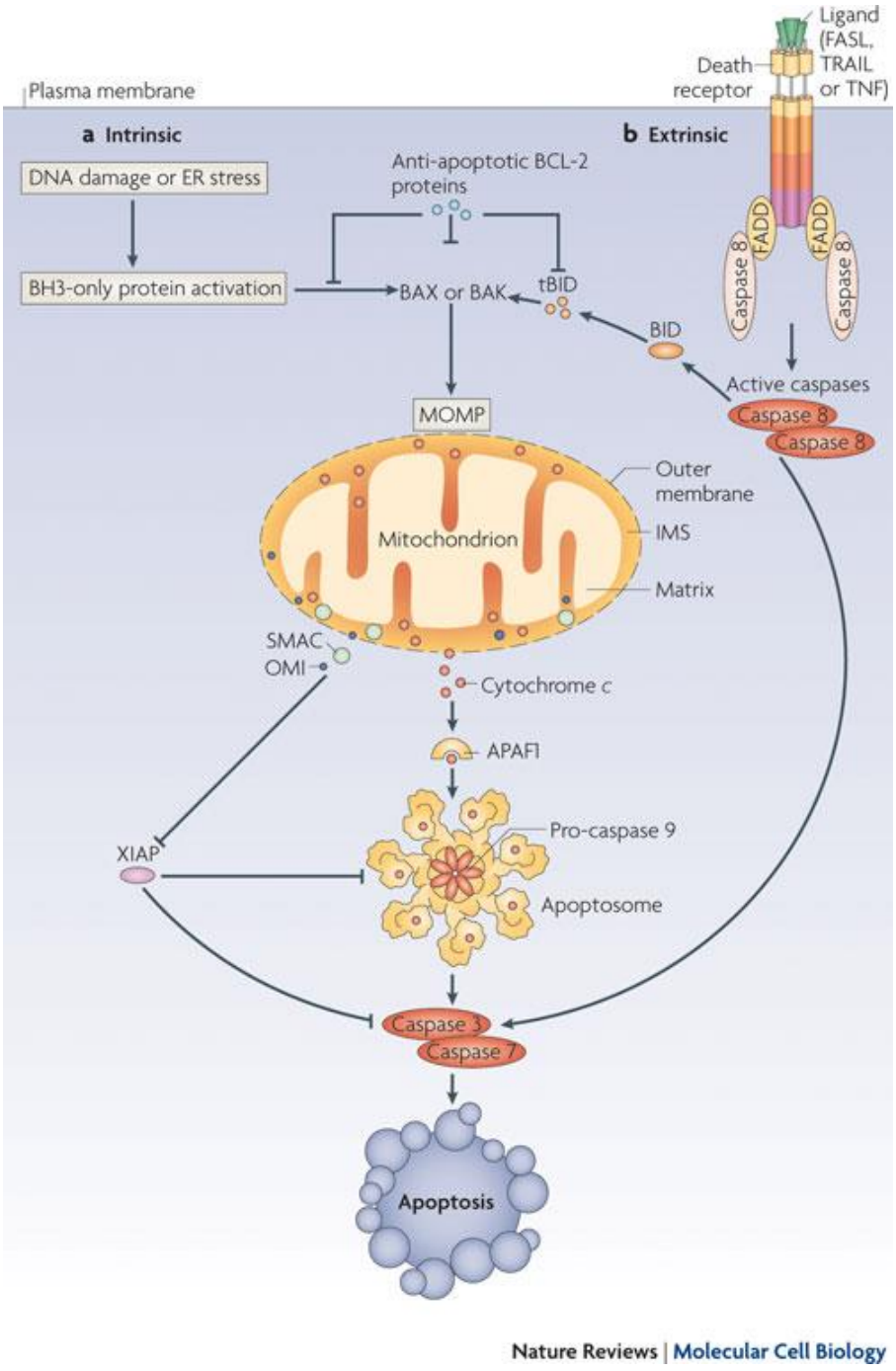

Fig.3.3 Intrinsic and extrinsic apoptotic pathways. (Adapted from Tait SW, Green DR. Mitochondria and cell death: outer membrane permeabilization and beyond. Nat Rev Mol Cell Biol. 2010 Sep;11(9):621-632).

death domain (FADD) protein and then caspase 8. The dimerization and activation of caspase 8 directly cleave and activate caspase 3 and caspase 7, leading to apoptosis. Caspase 8 can cleave and activate BH3-only protein BH3-interacting domain death agoinst (BID), the resulting truncated BID (tBID) lead to mitochondrial membrane permeabilization [32]. BTZ was explored to elevate ROS generation, increase in mitochondrial membrane potential ($\Delta\psi_{m)}$, and release of cytochrome c into the cytosol in a time-dependent manner. Co-incubation with rotenone and antimycin A, inhibitors of mitochondrial electron transport chain complexes I and III, or with cyclosporine A, an inhibitor of mitochondrial permeability transition pore, resulted in inhibition of BTZ-induced ROS generation, increase in $\Delta\psi_m$, and cytochrome *c* release. Tiron, an antioxidant agent, blocked the BTZ-induced ROS production, $\Delta\psi_m$ increase, and cytochrome *c* release [33]. In primary chronic lymphocytic leukemia (CLL) cells, BTZ induced Bax accumulation, translocation to mitochondria, conformational change, and oligomerization [34], which can lead to inhibition of anti-apoptotic Bcl-2, release of cytochrome c/Smac from mitochondria and activation of caspase-9 [35]. Further, it was elucidated that BTZ induced caspase-dependent apoptosis by down-regulation of apoptosis inhibitors, such as Bcl-2, A1, cIAP-2, and (at higher concentration) FLIP and XIAP, but did not change the protein levels of cIAP-1 and Bcl-XL [3]. Another mechanism of BTZ-mediated apoptosis is via activation of extrinsic apoptotic pathway, as was demonstrated by an increased activity of c-Jun N-terminal kinase (JNK) and increase in death-inducing receptors Fas and DR5 and the death ligand FasL that further enhanced Fas-mediated signalling and caspase-8 activation [3].

BM microenvironment, which is composed of a cellular compartment (stromal cells, osteoblasts, osteoclasts, endothelial cells, and immune cells) and a noncellular compartment including the extracellular matrix (ECM) and the liquid milieu (cytokines,

growth factors, and chemokines), appears to be responsible for homing of specific cells in the BM niche, their proliferation, survival, and in the case of MM cells, resistance to chemotherapy [36]. The interaction of MM and bone marrow stromal cells (BMSCs) triggers cell-adhesion-medicated drug resistance and cytokine-mediated drug resistance **(Fig.3.4)**. Specifically, MM cells adhere ECM proteins, such as type I collagen and fibronectin via syndecan 1 and very late antigen 4 on MM cells and to BMSC vascular cell adhesion molecule 1 via VLA-4 on MM cells [37]. MM cells bind to fibronectin, which in turn induces G1 arrest associated with elevated levels of $p27^{kip1}$ protein levels, which could potentially be causative for resistance [38]. Adhesion of MM to BMSC induces the activation of p42/44 mitogen-activated protein kinase (MAPK) and nuclear factor NF-κB in BMSCs, which upregulates adhesion molecules on both MM cells and BMSCs. Moreover, the adhesion of tumor cells to BMSCs further upregulates the transcription and secretion of the cytokines by BMSCs and/or MM cells [39,40]. Cytokines secreted from MM cells induce interleukin-6(IL-6) secretion, tumor-necrosis factor-α (TNF-α), vascular endothelia growth factor and NF-κB activation in BMSCs, which activate the main signaling pathways (p42/44 MAPK, Janus kinase (JAK)/signal transducer and activator of transcription 3 (STAT3) and/or phosphatidylinositol 3-kinase (PI3K/AKT)) and induces the intracellular expression of downstream inhibitor of apoptosis proteins (IAPs), FLICE-inhibitory protein (FLIP), survival, cellular inhibitor of apoptosis-2 (cIAP2), A1/BFL1, and XIAP in MM cells, associated with MM cell proliferation and survival [41]. It has been proved that BTZ inhibited MM cells growth by downregulating the expression of adhesion molecules on MM cells and BMSCs and their related adherence and NF-κB-dependent induction of IL-6 secretion and/or BMSC/MM cell adherence-induced p42/p44 MAPK activation [42]. Therefore, BTZ not only acts directly on MM cells, but alters cellular interactions and cytokine secretion in the BM milieu to inhibit tumor cell growth, induce apoptosis,

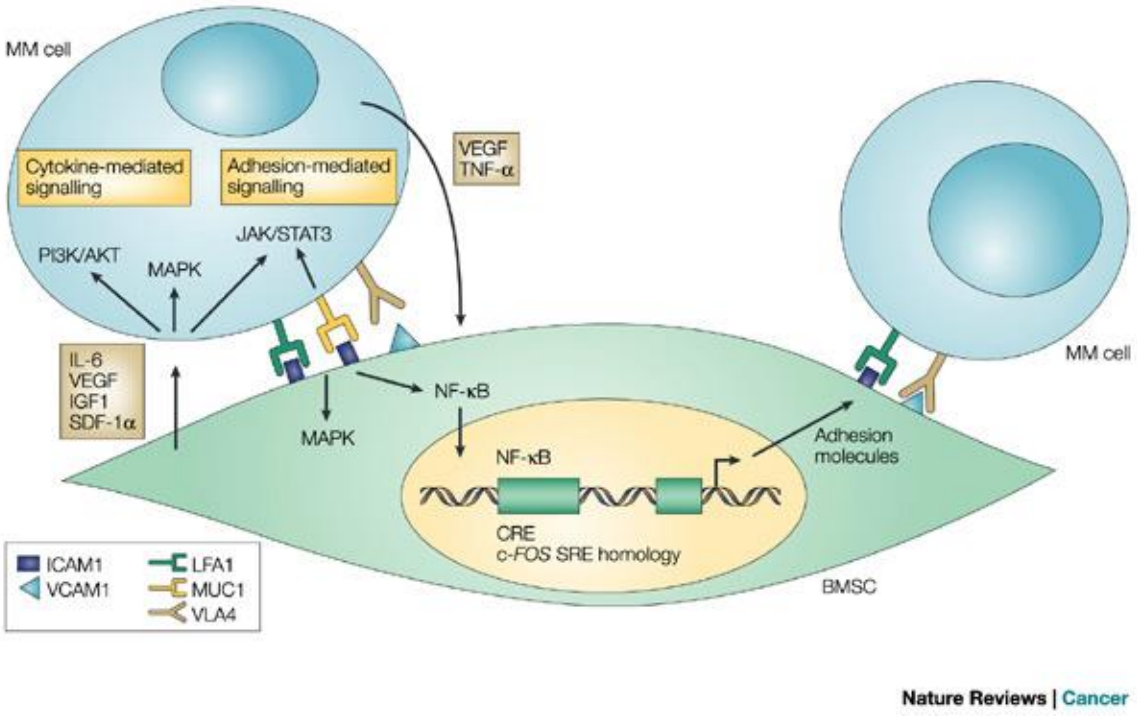

Fig.3.4 The binding of MM cells to the BMSCs triggers adhesion- and cytokine-mediated MM cell growth, survival and migration. (Adapted from [41]).

and overcome drug resistance.

Based on the sensitization effect of SP1017 on MM cells combined with the proteasome inhibitor BTZ as discussed in Chapter II, we explored the molecular mechanisms of the sensitization effect of the combination of SP1017 and BTZ on RPMI 8226 MM cells, including the proteasome inhibition, accumulation of poly-ubiquitinated proteins, proteotoxic stress, ER stress, Golgi fragmentation, oxidative stress and the downstream apoptotic signaling cascades. We also explored the role of SP1017 played in the BM microenvironment to conquer environment-induced drug resistance.

3.2 Materials and Methods

3.2.1 Cell culture

RPMI 8226 human MM cell line was generous gifts from Dr. Sagar Lonial (Emory University, Atlanta, GA, USA). BTZ/CFZ-resistant RPMI 8226 MM cell lines were selected and established by exposure to sensitive RPMI 8226 MM cells of gradually increasing concentrations of BTZ /CFZ starting at 0.2nM. Consequently, the BTZ/CFZ-resistant RPMI 8226 cell lines stably growing in the presence of 40nM of BTZ or CFZ within 6 months. OMA-AD BM stromal cell line was a kind gift from Dr Shantaram Joshi (UNMC, Omaha, NE, USA). All MM cell lines were grown in Roswell Park Memorial Institute (RPMI)-1640 medium with 100 I.U/ml penicillin, 100ug/ml streptomycin and 10% of fetal bovine serum (FBS). MCF 7, HepG2 and Hela cells were grown in Dulbecco's Modified Eagle Medium (DMEM) with 100 I.U/ml penicillin, 100ug/ml streptomycin and 10% of FBS. OMA-AD BM stromal cell line was grown in Roswell Park Memorial Institute (RPMI)-1640 medium with 100 I.U/ml penicillin, 100ug/ml streptomycin and 20% of FBS.

3.2.2 Materials

Bortezomib was purchased from Selleck Chemicals (Houston, TX, USA). Carfizomib was purchased from Chemie Tek (Indianapolis, IN, USA). SP1017 was kindly provided by Supratek Pharma. Inc (Montreal, Canada). Cell counting kit-8 (CCK-8) was purchased from Dojindo Molecular Technologies (Kumamoto, Japan). Proteasome-Glo™ Chymotrypsin-Like Cell-Based assay kit was purchased from Promega (Madison, WI, USA). Bioxytech GSH-400 kit was purchased from Oxis International Inc. (Portland, OR, USA). Caspase-3 Fluorogenic substrate (AD-DEVD-AMC), Caspase-8 Fluorogenic substrate (Ac-IETD-AFC), APC annexin V and anti-GRP 78/BiP were purchased from BD Bioscience (San Jose, CA, USA). Caspase-9 Fluorogenic substrate (Ac-LEHD-AFC), Anti-P-Glycoprotein (C219) mouse antibody and the mouse IL-6 enzyme linked immunosorbent assay (ELISA) kit were purchased from EMD Millipore (Darmstadt, Germany). Human lambda EILSA kit was purchased from Bethyl Laboratories Inc (Montgomery, TX, USA). Mitoprobe JC-1 assay kit was purchased from Life technologies (Grand Island, NY, USA). Cyanine 5 NHS ester was obtained from Lumiprobe (Hallandale Beach, FL, USA). Annexin V-FITC/ propidium iodide (PI) Apoptosis Kit was purchased from Biovision (Milpitas, CA, USA). Mitochondria Isolation Kit for Cultured Cells, enhanced chemilumescent (ECL) substrates and M-PER® Mammalian Protein Extraction Reagent were purchased from Thermo Scientific Inc. (Waltham, MA, USA). Cleaved Caspase-3 (Asp175), Cleaved Caspase-8 (Asp391), Cleaved Caspase-9 (Asp330), Cytochrome c (D18C7), Hsp 70, XIAP(3B6), Bxl-xL (54H6), Survivin (71G4B7), GAPDH (14C10) rabbit antibodies, CHOP(L63F7), Ubiquitin (P4D1) mouse antibodies, anti-rabbit IgG HRP-linked antibody, cell Lysis Buffer (10×) and protease inhibitor cocktail (100×) were purchased from cell signaling technology (Danvers, MA, USA). Anti-mouse IgG HRP-linked antibody was purchased from Santa Cruz Biotechnology (Santa Cruz, CA, USA). 1,1′-carbonildiimidazole (CDI), ethylenediamine, N-Acetyl-L-cysteine (NAC) and other chemicals were purchased from

Sigma-Aldrich (St Louis, MO, USA) and were used without further purification. MitoTracker® Red CMXRos, ProLong Gold antifade reagent with DAPI, Fetal bovine serum (FBS), RPMI 1640 medium, DMEM medium, penicillin, streptomycin, Trypsin–ethylenediaminetetraacetic acid (EDTA) (0.5% trypsin, 5.3 mM EDTA tetra-sodium) and other chemicals were purchased from Invitrogen (Carlsbad, CA, USA).

3.2.3 Cytotoxicity in human MM cell line by CCK-8 assay

Cytotoxicity of BTZ ±0.005% SP1017 in the presence with 10mM NAC or BTZ ±0.005% SP1017 in the presence with 1uM Dexamethasone (DEX) or DEX alone was assessed in different MM cell lines by a standard CCK-8 assay. Briefly, cells were seeded in a 96-well microtiter plates with 10^4 of cells per well and exposed to various doses BTZ ± 0.005% SP1017 in the presence with 10mM NAC or various doses BTZ ± 0.005% SP1017 in the presence with 1uM DEX or various doses of DEX alone for 24h at 37 ℃ in a humidified, 5% CO_2 atmosphere. 10ul of CCK-8 was added to each well and the cells were incubated for 1-4 h (when the absorption value ranges from 0.2-0.8, which shows better linearity) at 37 ℃ in the dark. Absorption was measured at 450nm in a microplate reader (SpectraMax M5, Molecular Devices Co., Sunnyvale, CA, USA) using wells without cells as blanks. For the experiments in the presence of NAC, cells were collected, washed with PBS twice and resuspended in the fresh RPMI 1640 medium before added the CCK-8 to prevent the effect of NAC on dye in the CCK-8. The net absorbance was taken as index of cell viability. The reading taken from the wells with cells cultured with control medium was used as 100% viability value. The cell viability was calculated as $A_{sample}/A_{control}$ ×100%. Each concentration point was determined from samples from eight separate wells. Based on the results of the test, the IC_{50} values (the concentration which kill 50% of cells) were calculated by using GraphPad Prism Software (Version 5.0, GraphPad Software, San Diego, CA, USA).

3.2.4 Proteasome activity

The chymotrypsin-like proteasome activity was evaluated by Proteasome-Glo Chymotrypsin-Like Cell-Based Assays. Briefly, 1.5×10^4 of RPMI 8226 cells per well in a 96-well microtiter plates were treated with Media as control, 0.005% SP1017, 10nM of BTZ and 10nM of BTZ+ 0.005% SP1017 for 1h, 2h and 4h. Cells were collected, washed with PBS and resuspended in 1ml fresh RPMI 1640 medium. 100ul of cells were taken and plated in white polystyrene, flat opaque bottom Corning® 96-well plate (Sigma-Aldrich, St Louis, MO, USA). Proteasome-Glo™ Cell-Based Reagents were prepared according to the manufacturer's instructions. 100ul reagents were added to 100ul/well drug-treated samples. Luminescence was determined as relative light units (RLU) using the SpectraMax M5 microplate reader and the results were normalized by protein content determined by BCA assay.

3.2.5 Measurement of reduced glutathione (GSH) levels

GSH levels were evaluated by Bioxytech GSH-400 kit. Briefly, 10^7 of sensitive or resistant RPMI 8226 cells per sample were treated with Media as control, SP1017, BTZ and BTZ+ SP1017 in relative dose for 12h. Cells were collected and lysed in 100ul fresh Metaphosphoric acid (MPA) working solution. Reagents were added to each of samples according to the manufacturer's instructions and the final absorbance was measured at 400 nm using the SpectraMax M5 microplate reader and the results were normalized by protein content determined by BCA assay.

3.2.6 Measurement of membrane potential in mitochondria

Measurement of the membrane potential is based on potential dependent accumulation of a dye, JC-1, in mitochondria, which is monitored by fluorescence emission shift from green (~529 nm) to red (~590 nm). Consequently, mitochondrial

depolarization is indicated by the increase of percentage of green positive cells. $5*10^5$ of RPMI 8226 MM cells were seeded in 24-well plates per well and exposed to different concentrations of BTZ± 0.005% SP1017 for 12h and 24h. After the drug treatment, 50 μM CCCP (as the positive control) and 0.75 μM JC-1 were added in each well for 20 min incubation. Cells were then collected, washed three times with PBS and analyzed by Becton Dickinson FACSCalibur™ flow cytomerter and FACSDiva software (Version 8.0, Becton Dickinson, San Jose, CA).

3.2.7 The translocation of Cyanine 5-labeled L61 Pluronic® (Cy5-L61) to subcellular organelles by confocal analysis

3.2.7.1 Preparation of Cy5-L61

Pluronic® L61 was labeled with Cyanine 5 fluorophore according to the method described before [43]. Briefly, Pluronic® L61were activated with CDI, and then modified with excess of ethylenediamine and purified by dialysis against 20% ethonal. Amino-modified L61 was conjugated with Cyanine5 NHS ester (1:1) in dimethylformamide in the presence of 1.2 eq of tertiary amine. Free Cyanine5 and Cy5-L61 were separated by Sephadex LH-20 (Sigma-Aldrich, St Louis, MO, USA) column in methonal/ dichloromethane (1:1) phase.

3.2.7.2 Mitochondria staining

$3*10^5$ of cells were seeded in 24 well plate per well, incubated with 0.00055% Cy5-L61 for 20min. Meanwhile, cells were treated for 20 min with a staining solution containing 100 nM of the mitochondrial dye, MitoTracker® Red CMXRos. Cells were then washed with PBS three times, fixed with 4% paraformaldehyde (PFA) for 10min, centrifuged onto glass slides, mounted by coverslips with Prolong Gold antifade reagent

with DAPI. Cells were visualized by confocal imaging system (Carl Zeiss LSM 510 Meta, Peabody, MA, USA).

3.2.7.3 Golgi and ER staining

Cells ($3*10^5$) were seeded in 24 well plate per well, incubated with Cy5-L61 (0.00055% L61 equivalent) for 0.5 h, 2 h and 8 h. Then, cells were washed with PBS three times, fixed with 4% PFA for 10min, and centrifuged onto glass slides. After blocking with 1% donkey serum, cells were incubated with primary antibodies at 37°C for 1 h followed by washing with PBST three times. Further, cells were stained with DyLight secondary antibodies. After the final wash in PBST, cells were mounted in ProLong Gold antifade reagent with DAPI. The following primary antibodies were used: rabbit polyclonal – giantin (ab24586), and Calreticulin (ab4) (Abcam). The secondary antibody (Jackson Immuno Research) was donkey anti-rabbit Alexa Fluor 594 (711-585-152). Colocalization was determined by Pearson's coefficient, which represents a correlation of channels inside the colocalized regions, using ImageJ JACoP plugin.

3.2.8 Caspases activation

$5*10^5$ or $3*10^6$ of RPMI 8226 MM cells per sample were treated with BTZ ±0.005% SP1017 for 24h for the measurement of caspase 3 and caspase 8/9 activity, respectively. After the drug treatment, cells were collected, washed three times with PBS and lysed in 400ul lysis buffer [10mM Tris-HCl (pH 7.5), 10mM NaH_2PO_4/Na_2HPO_4, 130mM NaCl, 1% Triton X-100, 10mM $Na_4P_2O_7 \cdot 10\ H_2O$] by sonication. 100ul of the lysed cell solution were mixed with 5ug of the fluorogenic caspase 3 substrate Ac-DEVD-AMC, caspase 9 substrate Ac-LEHD-AFC and caspase 8 substrate Ac-IETD-AFC, respectively and incubated for 1h at 37℃. The activity was evaluated by measuring the cleavage of the Ac-DEVD-AMC substrate in the Perkin Elmer luminescence spectrometer LS 50B with λex=380nm, λem=440nm and the cleavage of the Ac-LEHD-AFC and Ac-IETD-AFC

substrates in the spectrometer λex=400nm, λem=505nm. The results were normalized by protein content determined by BCA assay.

3.2.9 Western blot

Identification of cleaved caspase 3, caspase 8, and caspase 9, Pgp, ubiquitnated proteins, HSP70, CHOP, GRP78/BiP, cytochrome c, survivin, XIAP, BCL-xl was done using immunoblot technique. Briefly, Cells were treated with BTZ ±0.005% SP1017 for relative period of time and lysed with Cell Lysis Buffer supplemented with protease inhibitor cocktail. Supernatant were collected after removing cell debris by centrifugation (14000 rpm for 10 min) and protein content was determined by BCA assay. Cytoplasmic extraction for cytochrome c was separated and collected by Mitochondria Isolation Kit for Cultured Cells according to the manufacturer's instructions. 15-30µg of proteins were resolved by 10%,12% or 15% sodium dodecyl sulfate-polyacrylamide gel electrophoresis (SDS-PAGE) and transferred onto PVDF membranes. The membranes were blocked by incubation in 5% dry milk in TBST (0.1% Tween-20 in TBS) and probed with the relative monoclonal antibodies were used at 1:1000 dilutions. The secondary horseradish peroxide Ig antibodies were used at 1:5000 dilutions. Blots were then visualized by ECL substrates. To correct for loading differences, the levels of protein expression were normalized to a constitutively expressed GAPDH. Intensity of the bands was quantified by Image J software.

3.2.10 In vitro tumor microenvironment models

3.2.10.1 CM culture model

OMA-AD stromal cells were cultured in T-75 flask until they were grown to 80-90% confluence. Old medium were removed and 15ml new fresh media (RPMI 1640 medium with 20% FBS) were added. Conditioned medium (CM) from stromal cells cultures was

collected following 24h of incubation and contaminated suspended cells were removed by centrifugation. 10^4 of RPMI 8226 MM cells were seeded per well and exposed to various doses of BTZ ± 0.005% SP1017 for 24h in RPMI 1640 meidum with 10% FBS, RPMI 1640 meidum with 20% FBS and CM, respectively. Cell viabilities were analyzed by the CCK-8 method.

3.2.10.2 Adhesion model

10^5 of OMA-AD stromal cells were seeded in 12-well-plate per well and incubated for 24h for attachement at 37°C. After that, 10^5 GFP+ RPMI 8226 cells were allowed to adhere for 12h. Nonadhered cells were removed and samples were exposed to different concentration of BTZ+/-SP1017 for 24h. For a control, myeloma cells were treated in same concentrations of BTZ+/-SP1017 in suspension. Cells were stained with annexin V-APC and PI staining as per the manufacturer's instructions. Apoptotic-induced cell death was analyzed by Becton Dickinson FACSCalibur™ flow cytometer and FACSDiva software (Version 8.0, Becton Dickinson, San Jose, CA). In coculture experiments with stromal cell line, GFP+ populations were gated as tumor cells for the analysis of apoptosis.

3.2.10.3 IL-6 secretion

10^5 of OMA-AD stromal cells were seeded in 12-well-plate and incubated for 24h for attachment. Old media were removed and fresh media or fresh media containing 10^5 RPMI 8226 MM cells were added, followed by 4h or 24h of cell adhesion and another 24h BTZ ±0.005% SP1017 treatments. Supernatant were collected and IL-6 levels were analyzed by the mouse IL-6 ELISA kit according to the manufacturer's instructions.

3.2.12 Paraprotein Level

10^5 of RPMI 8226 MM cells were seeded in 24 well plate per well, treated with Medium as control, 0.005% SP1017, 5nM of BTZ and 5nM of BTZ+ 0.005% SP1017 for 2h (total media volume 2ml). Supernatant were collected and the paraprotein levels were analyzed by human Lambda ELISA kit the according to the manufacturer's instructions. The results were normalized by protein content determined by BCA assay.

3.2.13 Statistical analysis

Statistical comparisons between two groups for in vitro studies were evaluated using Student's *t*-test. Two-tailed *P* values less than 0.05 were considered significant.

3.3 Results and discussion

3.3.1 SP1017 potentiate BTZ-induced proteasome inhibition

The ubiquitin-proteasome pathway plays a vital role in regulating protein stability and thus normal cellular function. It involves two distinct, critical steps: covalent attachment of multiple ubiquitin molecules to a protein substrate, and degradation of the tagged substrate protein by the 26S proteasome. BTZ, a boronic dipeptide operating as a reversible inhibitor of the 26S proteasome, mainly binds and forms a complex with the active site of threonine hydroxyl group in the β5-subunit and blocks the chymotrypsin-like activity of the proteasome, thus leading to the accumulation of ubiquitinated proteins [7]. We found that BTZ effectively inhibited about 50% of chymotrypsin-like proteasome activity after 1h treatment and the inhibition increased when the treatment period extended. The combination induced significantly higher proteasome activity inhibition compared with BTZ alone after 1h, 2h and 4h treatment **(Fig.3.5A)**. As a result, BTZ+SP1017 combination further potentiated the BTZ-induced accumulation of poly-ubiquitinated proteins, proved by higher accumulation of poly-ubiquitinated proteins in

A

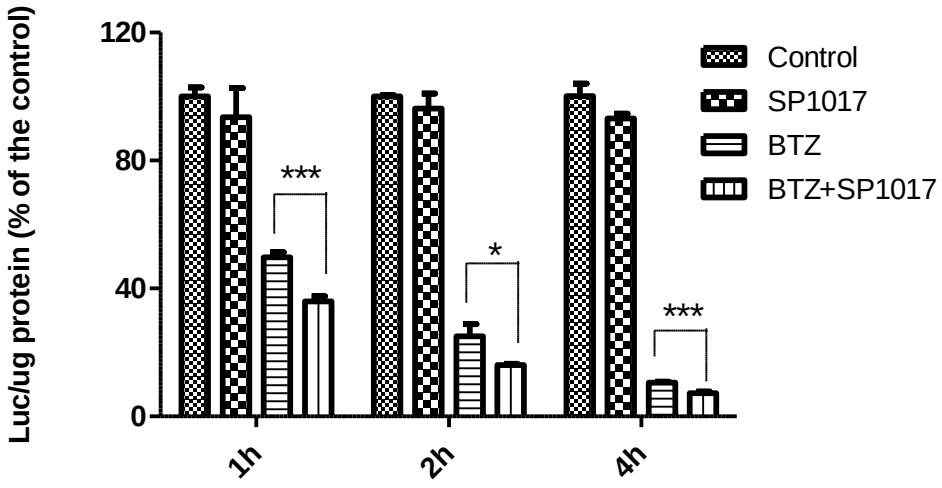

B

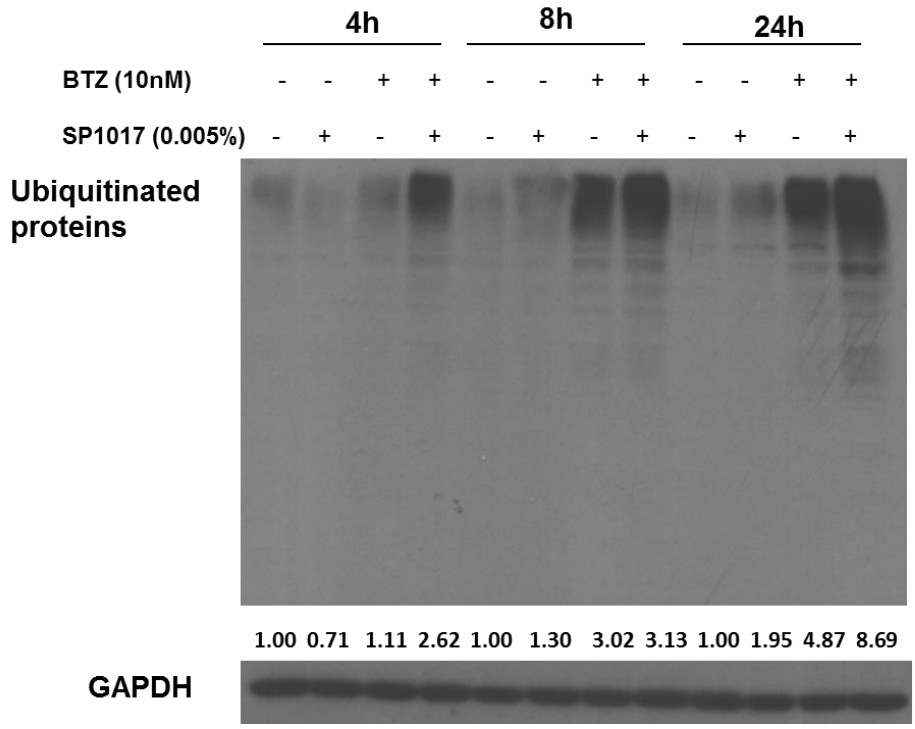

Fig.3.5 (A) Chymotrypsin-like proteasome activity of RPMI 8226 MM cells treated with BTZ± 0.005% SP1017 for 1h, 2h and 4h. Data presented as mean ± SD. N=3 (*P<0.05, ***p<0.001). (B) Accumulation of ubiquitinated proteins in RPMI 8226 MM cells treated with BTZ± 0.005% SP1017 for 4h, 8h and 24h. Data represented as a set out of three experiments.

cells treated with BTZ+SP1017 combination compared with BTZ alone after 4h, 8h and 24h **(Fig.3.5B)**.

3.3.2 SP1017 potentiate BTZ-induced Proteotoxic stress and ER stress

An imbalance of cellular protein homeostasis can lead to proteotoxic stress due to accumulation of misfolded proteins, resulting in harmful cellular effects known as proteotoxicity. Cells respond to proteotoxic stress by triggering the heat-shock response which leads to the rapid and robust expression of molecular chaperones to prevent protein misfolding and aggregation in the cytosol, and the UPR, the signaling network activated by misfolded proteins in the ER, called ER stress [14]. BTZ+SP1017 combination enhanced levels of ubiquitinated proteins compared with BTZ alone **(Fig 3.5B)**, indicating proteotoxic stress in the cytosol. Additionally, the effect of the combination on cytosolic proteotoxicity was reconfirmed by measuring protein levels of the HSP70 chaperone. HSP 70 levels of cells treated with combination were observed to be significantly higher than that treated with BTZ alone after 8h, 12h and 24h treatment, indicating the cellular response to alleviate proteotoxic stress in cytosol **(Fig.3.6A)**. Upon ER stress, GRP78/Bip, a master regulator of the UPR is released from ER transmembrane signal transducers, including PERK, IRE1 and ATF6, leading to the activation of URP signaling pathways. Release from GRP78/Bip allows ATF6 to translocate from ER to Golgi where it is cleaved. The cleaved form of ATF6 migrates into the nucleus and acts as an active transcription factor to upregulate proteins that augment ER folding capacity, including the ER chaperones GRP78/Bip [44,45]. However, under severe and prolonged ER stress, ER stress signaling appears to switch from pro-survival to pro-apoptosis which is initiated through the activation of CHOP, which plays an important role in ER stress-induced apoptosis [25]. In our study, we found CHOP levels of cells treated with combination were significantly higher than that

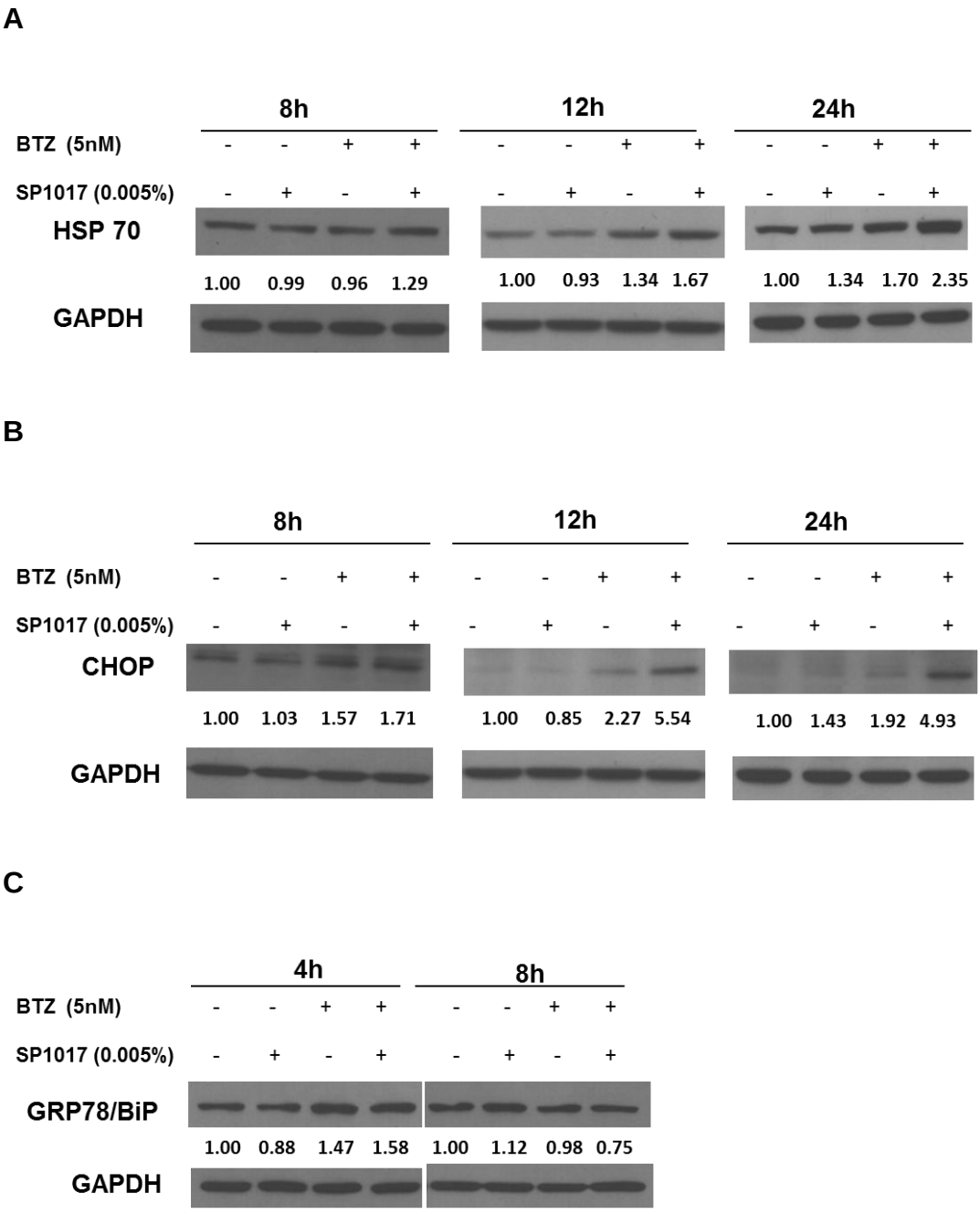

Fig.3.6 (A) HSP70 and (B) CHOP expressions of RPMI 8226 MM cells treated with BTZ± 0.005% SP1017 for 8h, 12h and 24h. (C) GRP 78/BiP expression of RPMI 8226 MM cells treated with BTZ± 0.005% SP1017 for 4h and 8h. Data represented as a set out of three experiments.

treated with BTZ alone after 8h, 12h and 24h treatment **(Fig.3.6B)**, indicating the ER stress. However, GRP78/BiP expression was slightly up-regulated by both BTZ and combination after 4h treatments, but down-regulated after 8h treatments **(Fig.3.6C)**. It may be explained by the fact that upregulation of GRP78/BiP was involved in the initial phase of UPR activation. In conditions of prolonged stress, the goal of the UPR changes from promotion of cellular survival to commitment of cellular apoptosis.

3.3.3 Pluronic® L61 translocates to ER and Golgi complex and the combination therapy reduced paraprotein associated with Golgi fragmentation

According to previous studies, hydrophobic PPO chains with intermediate length of PEO units from 30 to 60 and HLB <20 [46, 47] of Pluronic® unimers immerse into the membrane hydrophobic areas, resulting in alterations of the membrane structure, and triggering subsequent biological effects [48]. In our study we labeled Pluronic® L61, the component which played major role of chemosentization effect with dye cyanine 5 to explore its trafficking in the cells. Cy5-L61 was observed to be accumulated in both Golgi apparatus and ER after 8h treatment **(Fig. 3.7A, 3.7B)**, which could be another factor contributing to the increased ER stress and Golgi fragmentation **(Fig.3.8)** under combination treatment. Interestingly, we found 0.005% SP1017 alone at the inert concentration induced significant Golgi fragmentation **(Fig.3.8)**. The colocalization of Pluronic® L61 with subcellular membrane components, ER and Gogli and subsequent specific cellular responses, could be attributed by the interaction of the Pluronic® unimers and lipid membranes [49]. Relatively hydrophobic copolymers could insert into the membrane below the polar head groups, loosen the lipid packaging and translocate through the membrane. The immersed Pluronic® block copolymers disrupt the membrane integrity, which results in decreased membrane microviscosity and the subsequent specific cellular response [50, 51]. Newly synthesized secretory

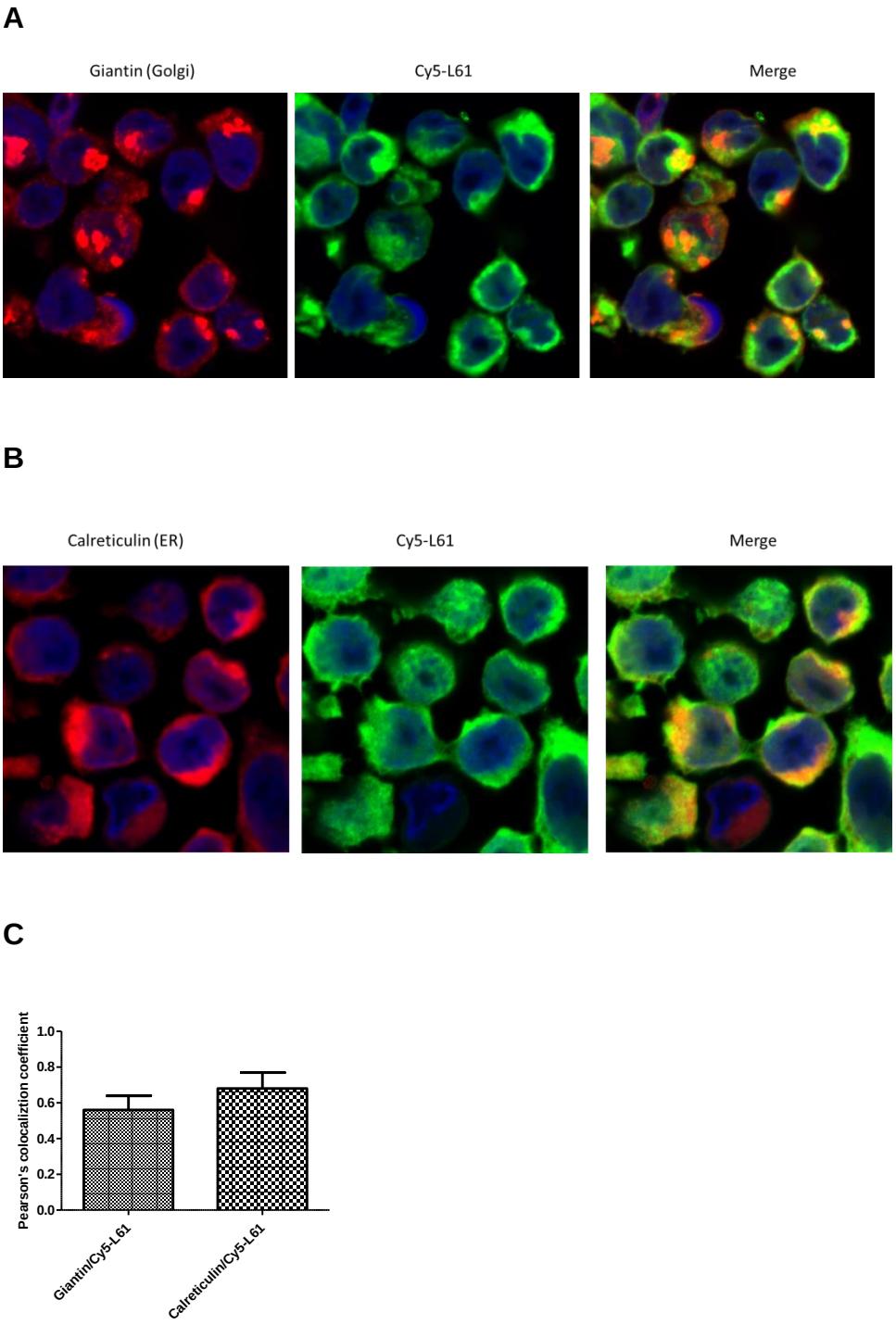

Fig.3.7 Translocation of Cy5-L61 (0.00055% L61 equivalent) into (A) the Golgi apparatus (Giantin as the Golgi marker) and (B) ER (Calreticulin as the ER marker) of RPMI 8226 MM cells after 8h incubation. Nuclei were counterstained with DAPI (blue). Quantification of Pearson's coefficient in cells presented in (C); n = 30 cells for each series of experiments; Data presented as mean ± SD.

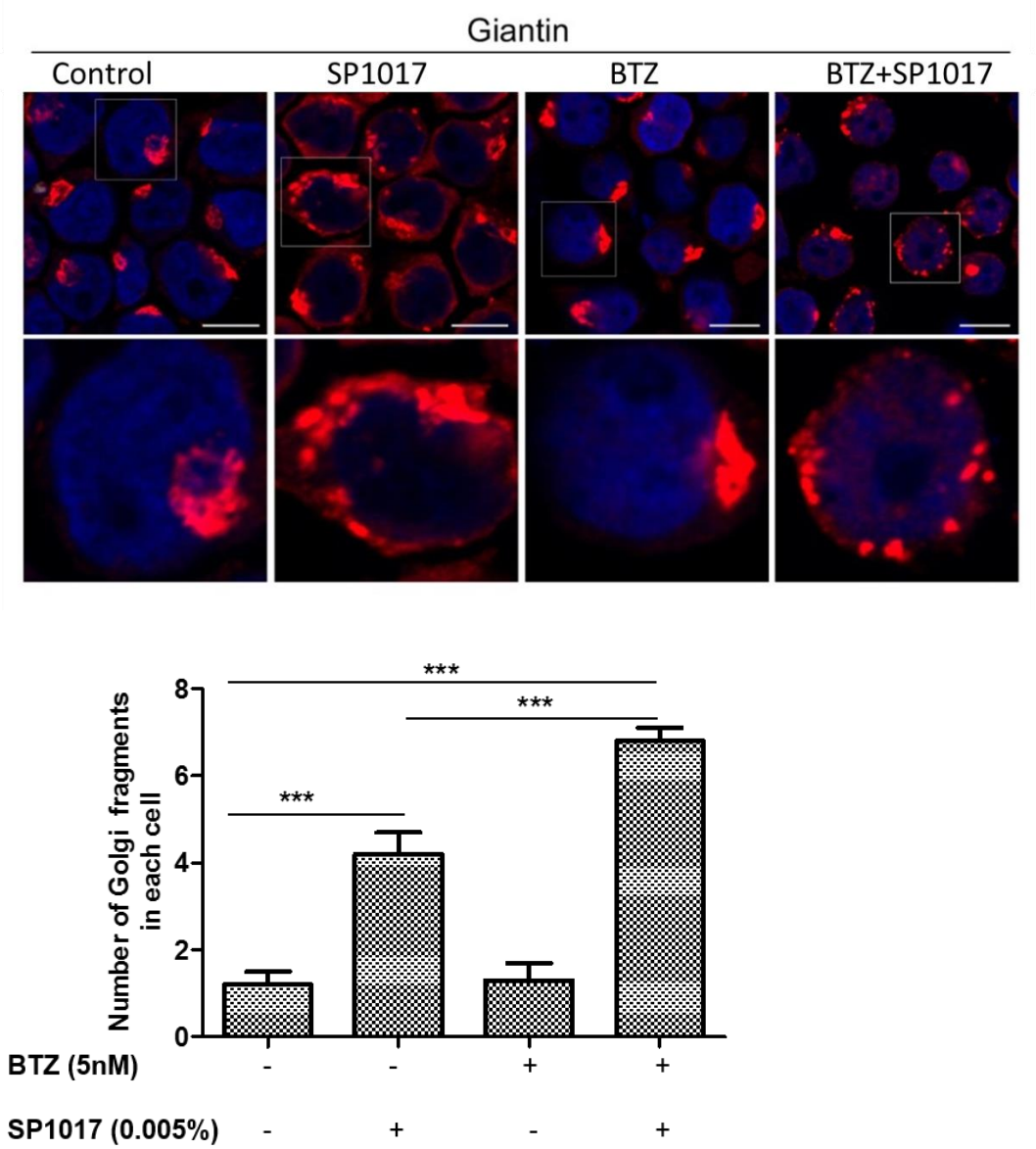

Fig.3.8 Golgi fragmentation of RPMI 8226 MM cells treated with BTZ± 0.005% SP1017 for 8h, as measured by the number of Golgi fragments stained with Giantin. The low panel shows high magnifications of the highlighted area (white boxes). Nuclei were counterstained with DAPI (blue), n = 30 cells for each series of experiments; Data presented as mean ± SD. N=10 (***P<0.001).

glycoproteins, such as the paraprotein, are transported from the ER to the plasma membrane or other destinations via the Golgi complex. In the secretory pathway, the Golgi complex is a central organelle essential for processing and sorting of lipids and proteins [52, 53]. Therefore, Golgi disorganization may block secretory traffic and plasma membrane delivery of proteins [54,55]. Indeed, here observed that there was significant reduce of paraprotein (human monoclonal immunoglobulin (Ig) lambda which is produced in excess in MM) when treated with the combination compared to drug alone or control **(Fig. 3.9)**. 0.005% SP1017 alone also induced slightly decrease of the secretion of paraprotein compared to control **(Fig. 3.9)**. As clonal expansion of the MM results in the excessive production of monoclonal Ig light chains and the deposition in the kidneys can lead to renal failure which is a clinical hallmark of MM [56], the reduction of secretion of Ig lambda from MM cells treated with combination therapy determines the potential as an anti-myeloma therapy in prevent renal failure.

3.3.4 SP1017 potentiate BTZ-induced oxidative stress

The biologically active form, GSH, plays key role in the cellular antioxidant defense system. The imbalance of intracellular GSH homeostasis could lead to oxidative stress and apoptosis [57]. SP1017 potentiated the BTZ-induced GSH depletion in sensitive RPMI 8226 MM cell line after 12h treatment (**Fig.3.10A**). In addition, the antioxidant, NAC, significantly reversed the BTZ+SP1017 induced cell death at BTZ 5nM and 10nM (**Fig.3.11**), which proved that oxidative stress was at least partially involved in the combination-induced cell death. In the Chapter II, we proved the SP1017 could still sensitize both BTZ -resistant MM cells and CFZ-resistant MM cells to proteasome inhibitors. Strikingly, SP1017 showed drastic sensitization effect (sensitization factor=6.6) on CFZ-resistant RPMI 8226 MM cell line as the MDR phenotype was only observed in CFZ-resistant MM cells rather than BTZ-resistant MM cells. The basal level

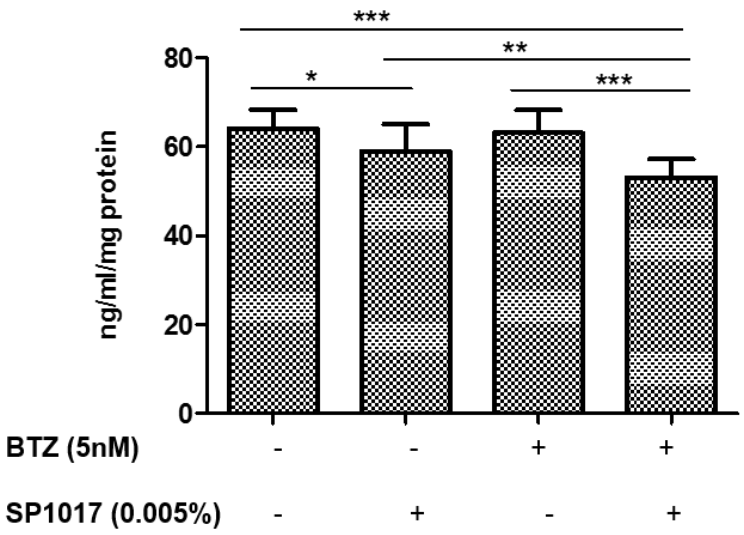

Fig.3.9 Paraprotein (human lambda) level from the supernatant of RPMI 8226 MM cells treated with BTZ± 0.005% SP1017 for 8h (statistics calculated by N=12). Data presented as mean ± SD. N=12 (*P<0.05, **P<0.01, ***P<0.001).

of GSH in BTZ-resistant RPMI 8226 MM cells was higher than that of sensitive RPMI 8226 MM cells (**Fig.3.10B**), which may contribute to the resistance to anticancer drugs. SP1017 potentiated the drug-induced GSH depletion in both BTZ- and CFZ-resistant MM cell lines **(Fig.3.10B, 3.10C)**, indicating the potential of SP1017 in overcoming acquired resistance of MM. Drug+SP1017 combination increased the GSH depletion even at quite low concentration of drug in CFZ-resistant MM cell line compared that in BTZ-resistant MM cell line, which was due to the Pgp expression in CFZ-resistant MM cell line as SP1017 is quite effective in inhibiting Pgp, thus increasing the intracellular CFZ to exhibit the anticancer effect.

3.3.5 SP1017 potentiate BTZ-induced intrinsic and extrinsic apoptotic pathways

As shown in **Fig.2.2**, MM cells underwent more apoptosis in BTZ + SP1017 combination, which was linked to activation of apoptosis signal transduction pathways such as intrinsic and/or extrinsic pathway in cancer cells [58,59]. Here we explored whether the BTZ + SP1017 combination induced the MM cells apoptosis via both intrinsic and extrinsic pathways. Cy5-L61 was found to translocate into mitochondria after 20min exposure of the copolymer to RPMI 8226 MM cells **(Fig.3.12)**, which was consistent with the previous work that Pluronic® P85 can rapidly transport to mitochondrial of both MCF7 and MCF7/ADR cells [60]. Moreover, we observed significant increased loss of mitochondrial membrane potential in cells treated with the BTZ + SP1017 combination for 12h and 24h **(Fig. 3.13A, 3.13B)** and increased release of cytochrome c into cytoplasm in cells treated with the BTZ + SP1017 combination for 12h **(Fig.3.13C)**. The caspase 9 and caspase 3 activations were proved by both functional fluorogenic assay and western blot of the expression of the active forms of caspases. Both caspase 9 and caspase 3 activities were significantly increased in cells

A

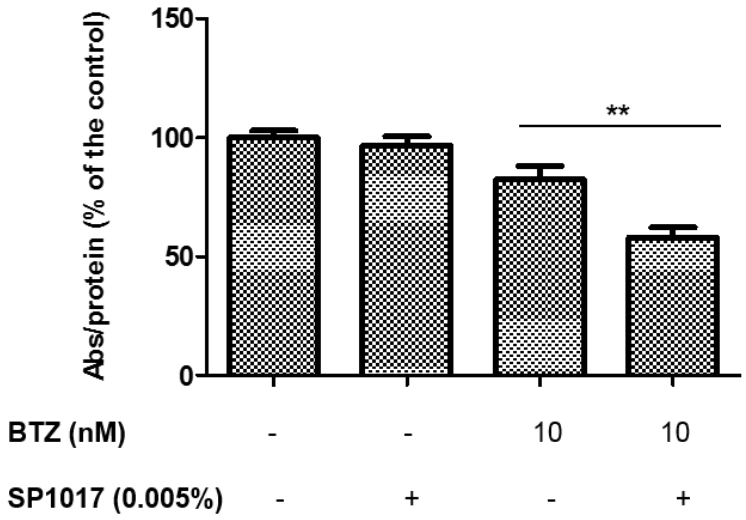

B

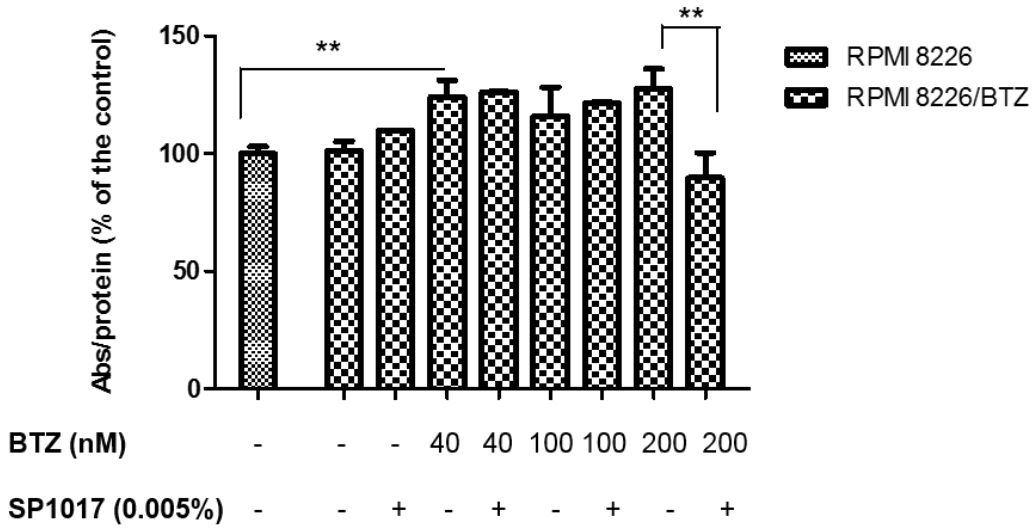

C

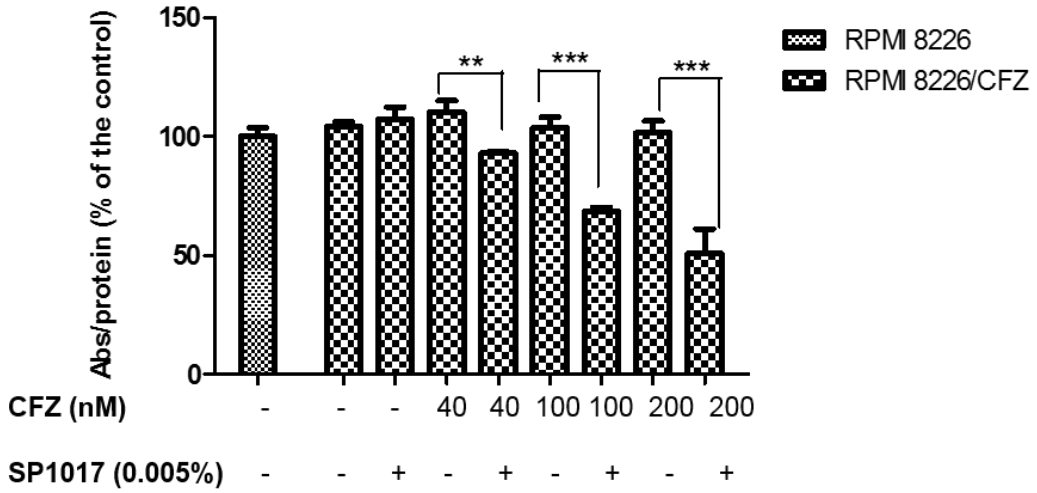

Fig.3.10. GSH level of (A) sensitive, (B) BTZ- resistant RPMI 8226 MM and (C) CFZ-resistant RPMI 8226 MM cells treated with drug ± 0.005% SP1017 for 12h. Data presented as mean ± SD. N=3 (**P<0.01, ***P<0.001).

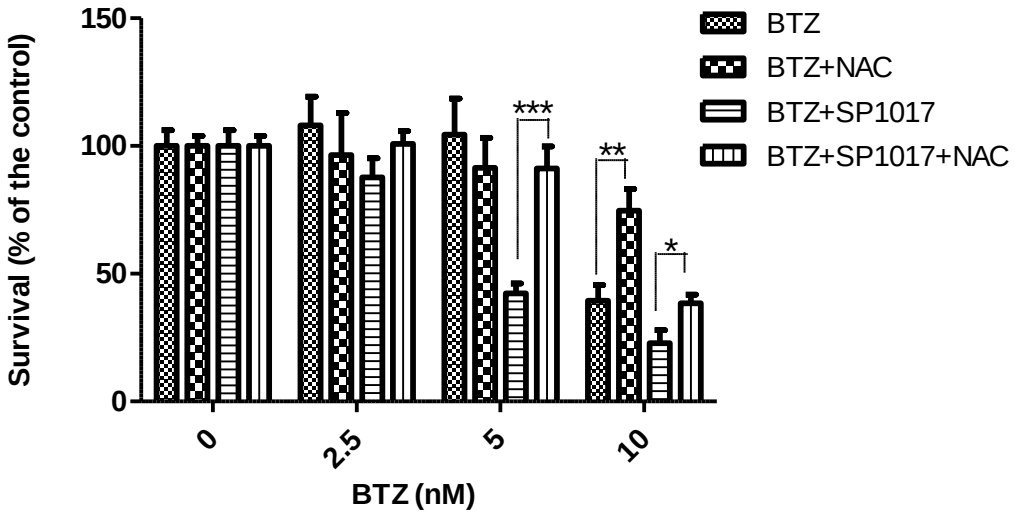

Fig.3.11 Cell survival of sensitive RPMI 8226 MM cells treated with BTZ± 0.005% SP1017 in presence of antioxidant 10mM NAC. Cells were treated for 24h. Data presented as mean ± SD. N=3 (*P<0.05, **P<0.01, ***P<0.001).

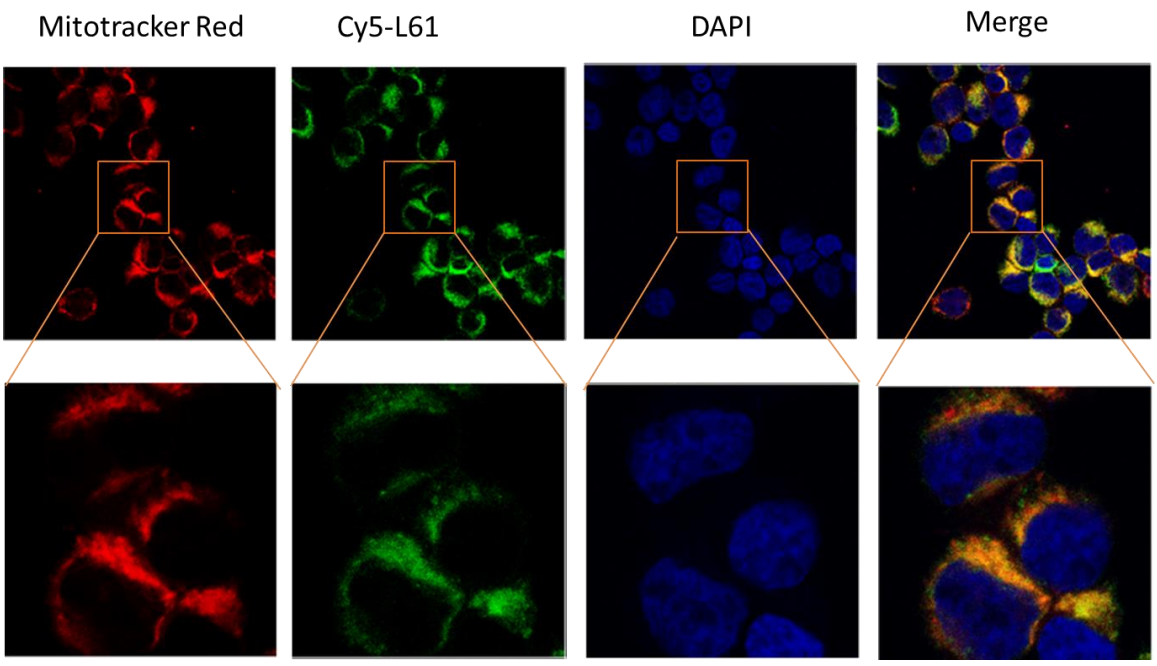

Fig.3.12. Co-localization of Cy5-L61 with mitochondria marker (MitoTracker-Red) in RPMI 8226 MM cell after 20min exposure. The low panel shows high magnifications of the highlighted area. Nuclei were counterstained with DAPI (blue).

A

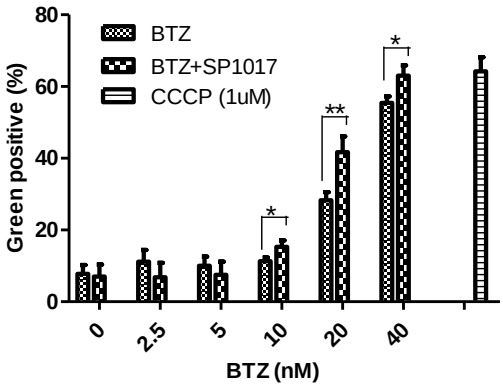

B

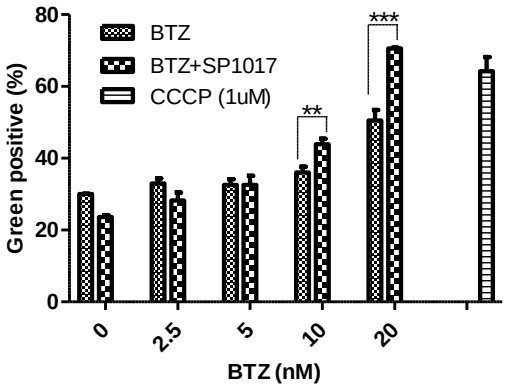

C

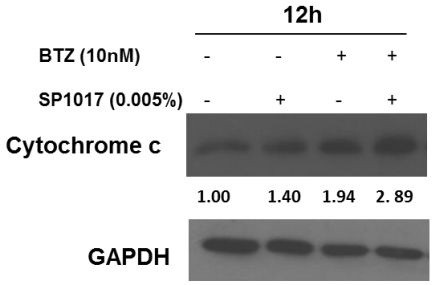

Fig 3.13 Loss of mitochondrial membrane potential (green positive %) of cells treated with BTZ± 0.005% SP1017 for (A)12h and (B) 24h, CCCP used as positive control; (C) Cytochrome c release into cytoplasm of cells were treated with BTZ+/-SP for 12h. Data presented as mean ± SD. N=3 (*P<0.05, **P<0.01, ***P<0.001) or as a set out of three experiments.

treated with the combination for 24h compared with BTZ alone **(Fig.3.14A, 3.14C)**. Significant increased expression of cleaved caspase 9 and caspase 3 were observed in the combination treatment for both 8h and 24h compared with BTZ alone (**Fig.3.15)**. All the above evidence showed SP1017 was involved in mitochondria-dependent apoptotic (intrinsic) pathway. In the previous work, Pluronic® P85 at relative low concentration can only induce inhibition of mitochondria respiration, decrease of mitochondrial membrane potential, release of cytochrome c from mitochondria in MDR cells, but not in the sensitive cells [60, 61]. Our study proved SP1017 at quite low concentration could sensitize sensitive MM cells to proteasome inhibitors via mitochondria-dependent apoptotic pathway. On the other hand, the increased activation of caspase 8 and caspase 3 proved by both functional assay and western blot in MM cells treated the combination treatment compared with BTZ alone **(Fig.3.14B, 3.14C, 3.15)** showed SP1017 was involved in mitochondria-independent (extrinsic) apoptosis pathway as well. Extrinsic apoptotic pathway is involved in stimulation of Fas/CD95 death receptor, which results in receptor aggregation and recruitment of the adaptor molecule FADD and procaspase-8 to form the so-called death-inducing signaling complex (DISC) that eventually leads to activation of downstream signaling and apoptosis [62]. It was reported that Fas/CD95 is translocated and aggregated into lipid raft clusters during Fas/CD95-mediated apoptosis and a group of lipid analogies behaved promising anti-MM activity by targeting and accumulating in lipid rafts of malignant cells, inducing raft aggregates that act as scaffolds for the recruitment of Fas/CD95 death receptor, FADD, and pro-caspase-8 into lipid rafts leading to the formation of DISC and apoptosis [63, 64, 65]. Previous studies also showed the hydrophobic PPO chains of Pluronic® unimers can immerse into the biomembrane hydrophobic areas, resulting in the alternations of the membrane structure and decreasing its microviscosity (“membrane fluidization”) [50]. More specifically, Pluronic® unimers were proved to selectively localize in particular

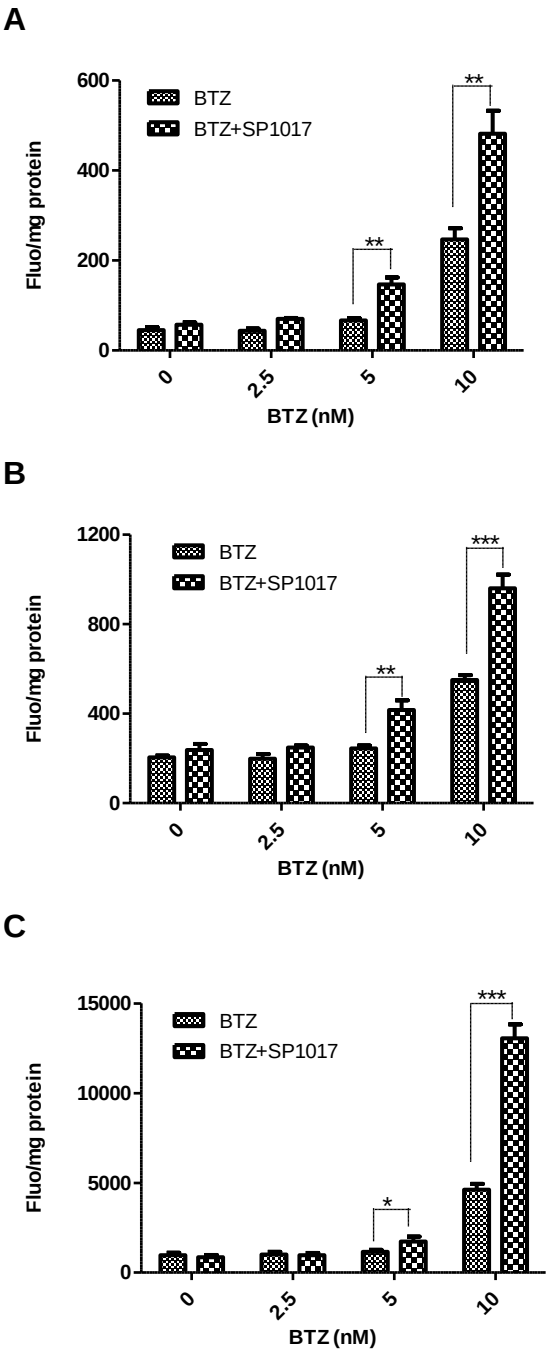

Fig 3.14 (A) caspase 9 activation, (B) caspase 8 activation and (C) Caspase 3 activation of cells treated with BTZ± 0.005% SP1017 for 24h, evaluated by measuring the cleavage of the fluorogenic substrate Ac-IETD-AFC, Ac-LEHD-AFC and Ac-DEVD-AMC, respectively. Data presented as mean ± SD. N=3 (*P<0.05, **P<0.01, ***P<0.001).

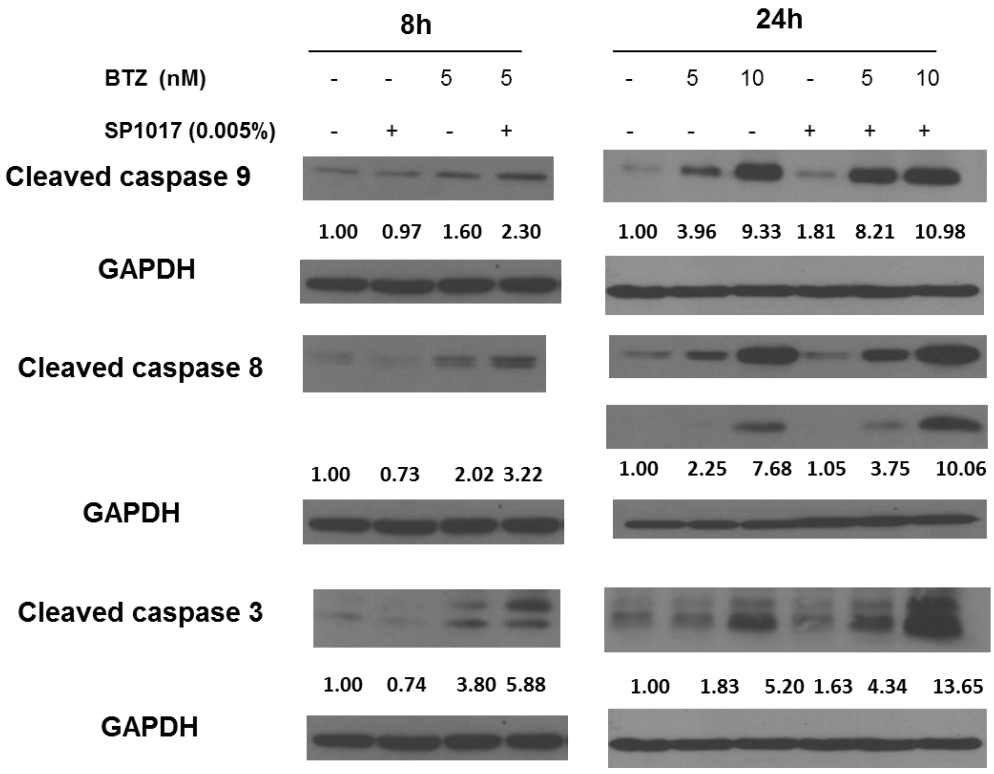

Fig 3.15. Western blot of cleaved caspase 9, cleaved Caspase 8 and cleaved caspase 3 of cells treated with BTZ± 0.005% SP1017 for 8h and 24h. Data represented as a set out of three experiments.

domains of cellular membrane called lipid rafts/caveolae [66]. So the potentiation of the activation of extrinsic apoptotic pathway by SP1017 may attribute to its ability to target lipid rafts and recruit the death receptors. Increase expressions of cleaved caspase 9/8/3 were observed in RPMI 8226 MM cells treated with CFZ+ SP1017 combination for 24h compared with CFZ alone **(Fig.3.16)**. Besides the potentiation of drug-induced pro-apoptotic signaling, SP1017 further decreased the expression of anti-apoptotic proteins when combined with BTZ. The anti-apoptotic proteins, Survivin and XIAP were significantly decreased under the BTZ+SP1017 combination treatment for both 12h and 24h compared with drug alone (**Fig.3.17**), which could be another factor inducing cell apoptosis.

3.3.6 SP1017 sensitize MM cells in tumor microenvironment

Besides triggering apoptotic signaling pathways, the combination therapy also overcomes the major chemoresistance mechanisms in MM cells. Resistance to tumor therapy can be subdivided into two broad categories: acquired and de novo. Acquired resistance develops in the course of treatment as a result of sequential genetic changes that eventually culminate in complex therapy-resistant phenotypes. In the Chapter II, we have proved that SP1017 overcome the acquired drug resistance of MM. Environment-medicated drug resistance is one form of de novo drug resistance to protect tumor cells from anticancer drugs. The interaction of MM and BMSCs triggers cell-adhesion-medicated drug resistance and cytokine-mediated drug resistance [36]. Our data showed RPMI 8226 MM cells cultured in BM stroma (OMA-AD stromal cells) -derived CM were more resistant to BTZ compared with cells in RPMI 8226 media with 10% or 20% FBS. However, SP1017 still had the ability to sensitize cells cultured in CM to BTZ (**Fig.3.18**). In cell adhesion model, GFP-labeled RPMI 8226 MM cells adhered to OMA-

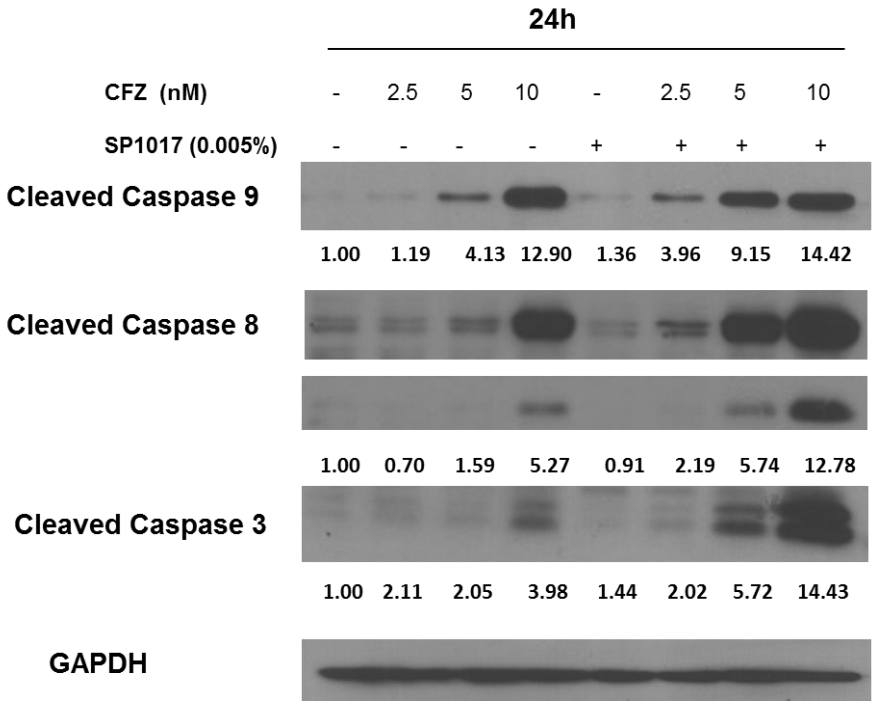

Fig.3.16. Western blot of cleaved caspase 9, cleaved Caspase 8 and cleaved caspase 3 of cells treated with CFZ ± 0.005% SP1017 for 24h.

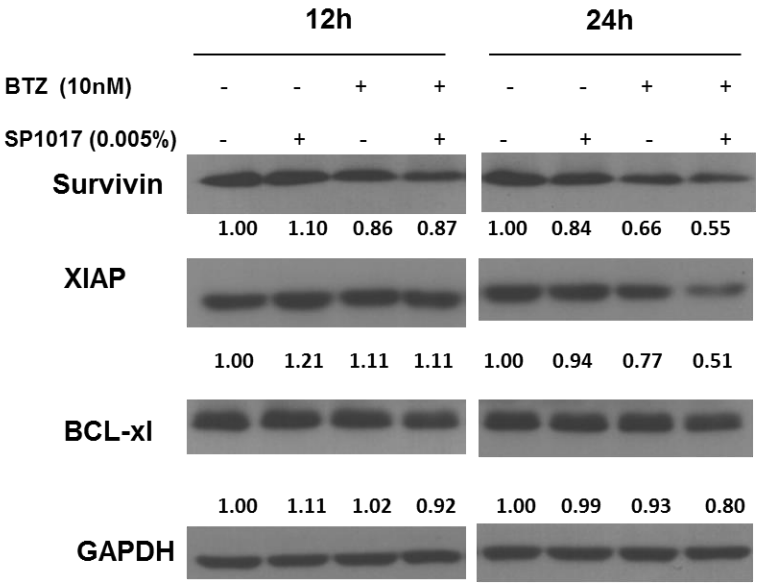

Fig 3.17. Western blot of anti-apoptotic proteins (Survivin, XIAP, BCL-xl) of cells treated with BTZ± 0.005% SP1017 for 12h and 24h. Data presented as a set out of three experiments.

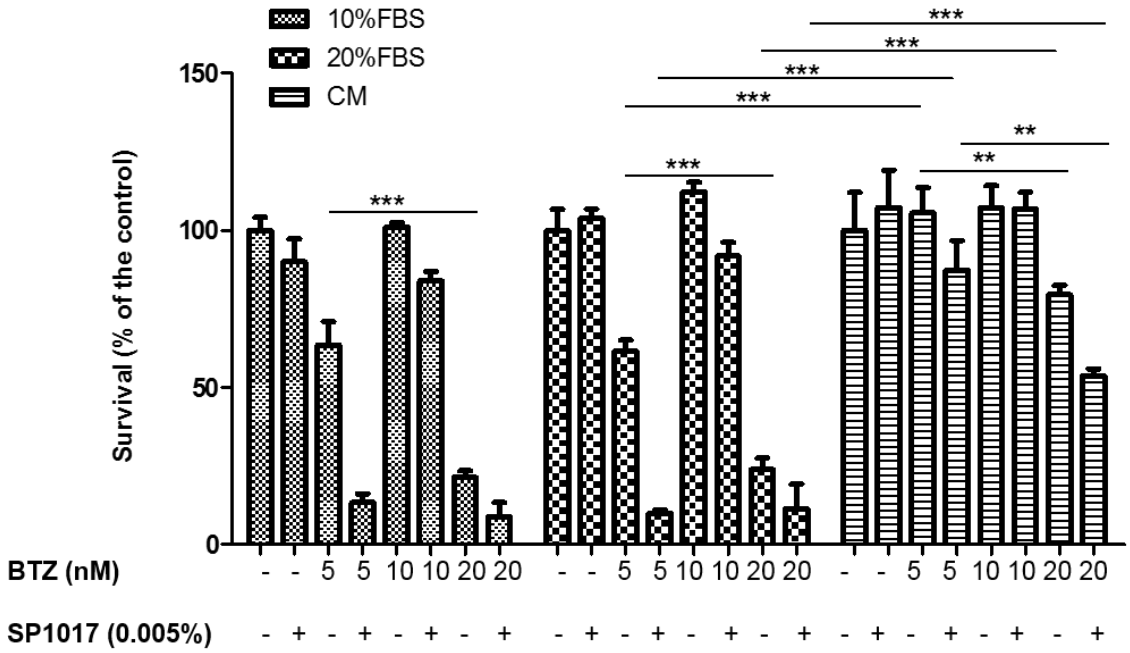

Fig.3.18. Cell survival of sensitive RPMI 8226 MM cell line treated with BTZ± 0.005% SP1017 for 24h. Tumor cells were maintained as follows: RPMI 1640 medium with 10% FBS, CM, RPMI 1640 medium with 20% FBS. Data presented as mean ± SD. N=3 (*P<0.05, **P<0.01, ***P<0.001).

AD stromal cells and exposed to BTZ +/- SP1017 for 24h. For a control, MM cells were treated in same concentrations of BTZ+/-SP1017 in suspension. Apoptotic-induced cell death was determined by Annexin V-APC/ PI assay. From the result showed in **Fig.3.19**, more cell apoptosis were observed in MM cells in suspension than MM cells in the adhesion model to both BTZ and the combination therapy. However, the combination therapy still induced more apoptosis in MM cells in the adhesion model compared with BTZ alone, indicating the sensitization of SP1017 in the BM microenvironment-mediated drug resistance. Though the BTZ+SP1017 co-treatment sensitize MM cells in stromal cell microenvironment in both models, OMA-AD stromal cells survived under treatment of BTZ+SP1017 combination even at a very high concentration, proving the combination therapy is well tolerated **(Fig.3.20)**.The adhesion of tumor cells to BMSCs is proved to upregulate the transcription and secretion of the cytokines by BMSCs, such as IL-6, a major growth and survival factor for MM cells by triggering signaling pathways that exert a pro-survival effect [40]. Here we proved that adherence of multiple myeloma cells to BM stromal cells upregulated the secretion of IL-6 compared with that secreted by OMA-AD stromal cells alone **(Fig.3.21)**. However, the BTZ +SP1017 combination significantly inhibited the IL-6 secretion from stromal cells **(Fig.3.21)**, which makes the combination therapy more promising in the treatment of MM.

3.3.6 Dexamethasone (DEX)+BTZ+SP1017 combination

Since the approval of BTZ by U.S.FDA in 2003, several BTZ-based combination therapies have emerged, including the IMiDs-BTZ-based combinations and combinations of BTZ with conventional chemotherapeutic agents such as melphalan-BTZ based combinations, cyclophosphamide-BTZ based combinations, anthracyclines-BTZ based combinations [67].Combinations should ideally take into account the different mechanisms of action, drug resistance pathways, and incorporate strategies designed to

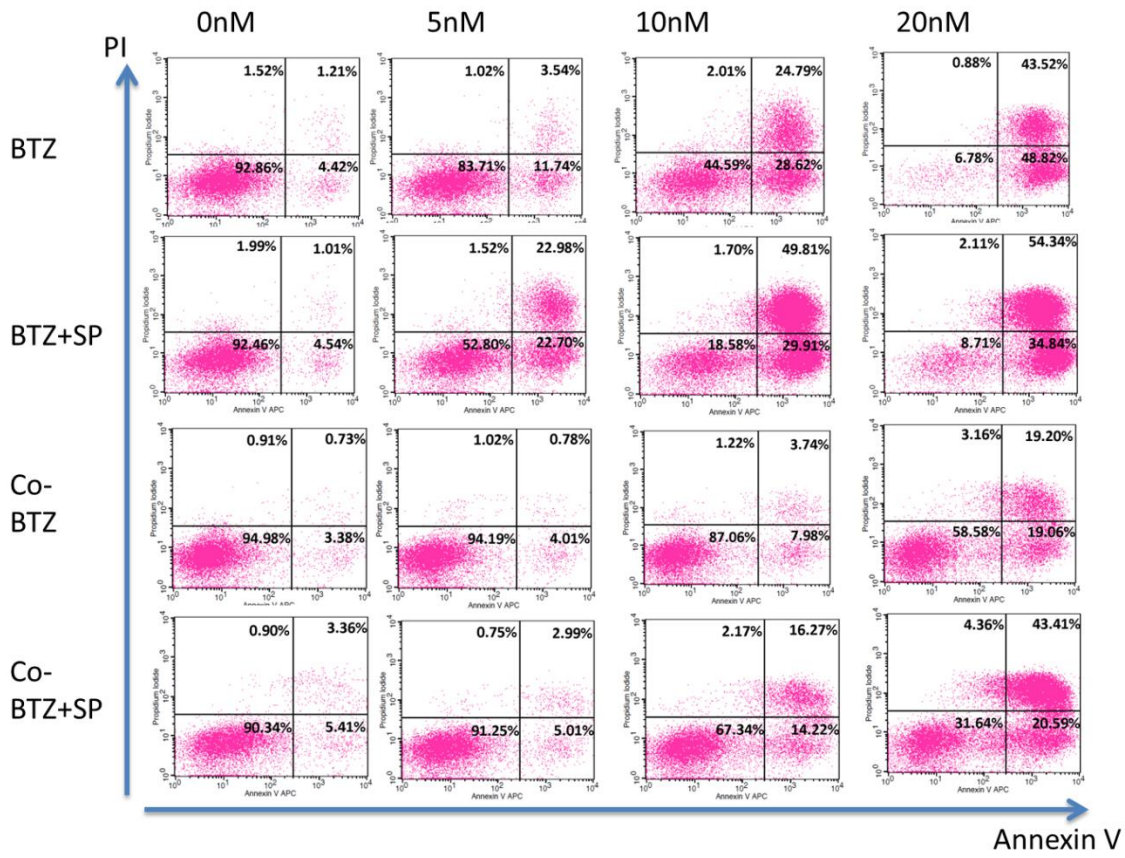

Fig 3.19. Stromal cells protect multiple myeloma cells by direct contact in Adhesion Model. GFP^{+}RPMI8226 MM cells were cultured alone (the upper two lines, BTZ and BTZ+SP) or co-cultured (the bottom two lines, Co-BTZ and Co-BTZ+SP) with stromal cells directly and exposed to BTZ ± 0.005% SP1017 for 24h and assessed for apoptosis by flow cytometric analysis using allophycocyanin (APC)-conjugated annexin V and propidium iodide (PI). Percentages of cells in each quadrant are shown and represented as a set out of three experiments. Left bottom quadrant (annexin V^{-}/PI^{-}, viable cells), right bottom quadrant (annexin V^{+}/PI^{-}, early apoptotic cells), right upper quadrant (annexin V^{+}/PI^{+}, late apoptotic cells) and left upper quadrant (annexin V^{-}/PI^{+}, necrotic cells).

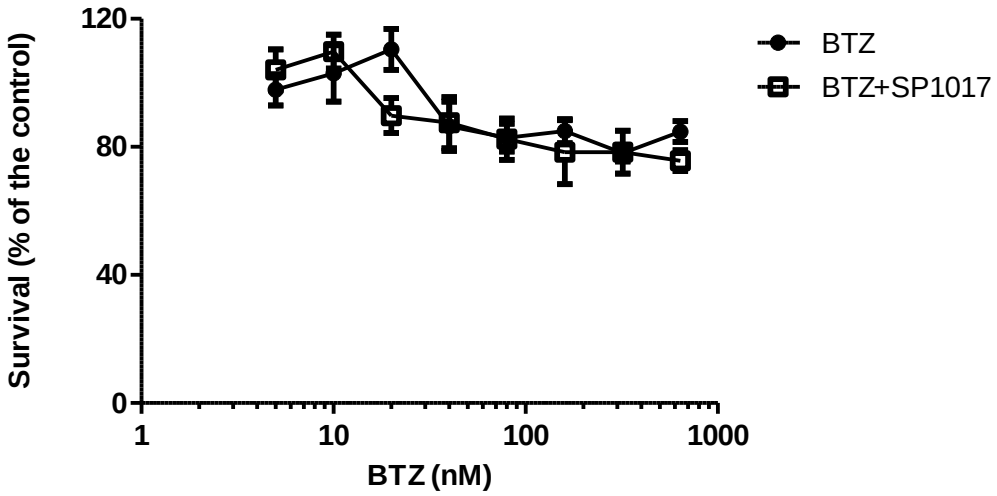

Fig.3.20. Cytotoxicity of BTZ ± 0.005%SP1017 to OMA-AD stromal cells after 24h treatment. Data presented as mean ± SD. N=3.

A

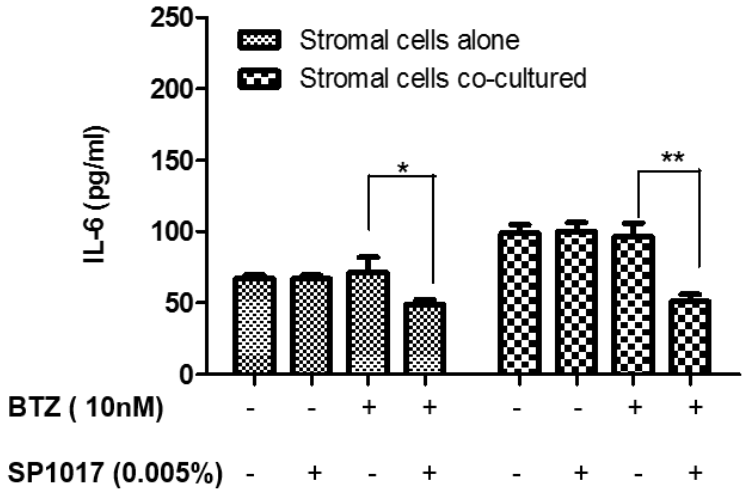

B

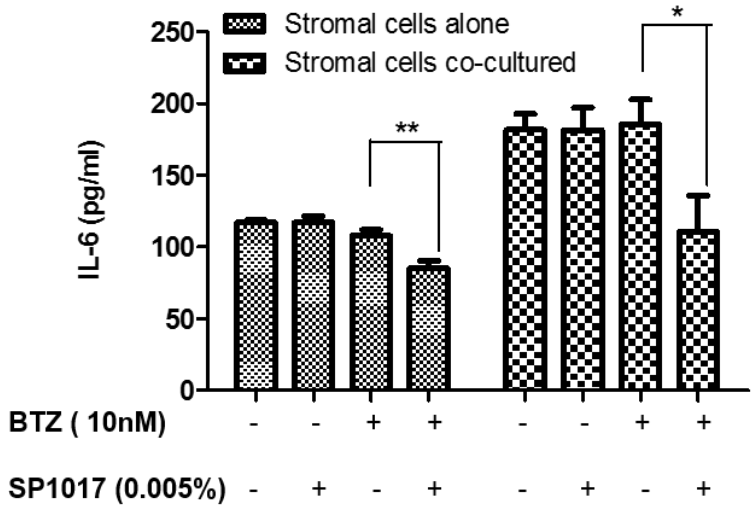

Fig 3.21. IL-6 level in the supernatant of stromal cells and stromal cells co-cultured with MM cells in Adhersion Model after (A) 4h and (B) 24h adhesion, followed by another 24h drug treatments. Data presented as mean ± SD. N=3 (*P <0.05, **P<0.01).

improve sensitivity of myeloma cells to the drug. DEX, a glucocorticoid analog, used in certain hematological malignancies, especially in the treatment of MM, in which DEX is given alone in a high dose [68] or together with other anti-MM drugs. Combination therapies with DEX plus BTZ, thalidomide, or lenalidomide have been extensively used and are among the most effective treatments for patients with relapsed or refractory MM [69, 70]. The combination of DEX with BTZ along with other drugs such as thalidomide, doxorubicin, cisplatin, cyclophosphamide, and etoposide has resulted in improvements in both response rates and long-term outcomes [69, 71]. Hematologic toxic effects are quite frequent when thalidomide, lenalidomide, or bortezomib is used together with conventional chemotherapy but are less frequent when these drugs are used with DEX alone[69]. It is widely accepted that the ability of glucocorticoids like DEX to achieve MM cell apoptosis is mediated via initial binding to their cognate receptor, the glucocorticoid receptor (GR). Ligand binding to the GR could result in inhibition of NFκB activity by ‘‘transactivation’’ via transcription of IκB and by ‘‘transrepression’’ via a reduction in transcription of the NFκB genes, thus decreasing the NFκB-dependent anti-apoptotic proteins [72,73]. Here we examined the effectiveness of the BTZ+DEX+SP1017 3-drug combination in MM. DEX itself didn’t induce any cytotoxicity to both RPMI 8226 MM cell line and ARH-77 MM cell line even at quite high concentration (**Fig.3.22a, 3.22b**). However, the addition of DEX (1uM) potentiated the BTZ- or BTZ+SP1017- induced cell death in both RPMI 8226 MM cell line and ARH-77 MM cell line (**Fig.3.23a, 3.23b**). Meanwhile, SP1017 potentiated the BTZ-induced cell death in both absence and presence of DEX. SP1017 was proved to potentiate the BTZ-induce of XIAP(one of NFκB-dependent anti-apoptotic protein) deduction **(Fig.3.17)**. Here we observed that XIAP was further reduced by the addition of DEX (**Fig.3.24**).

A

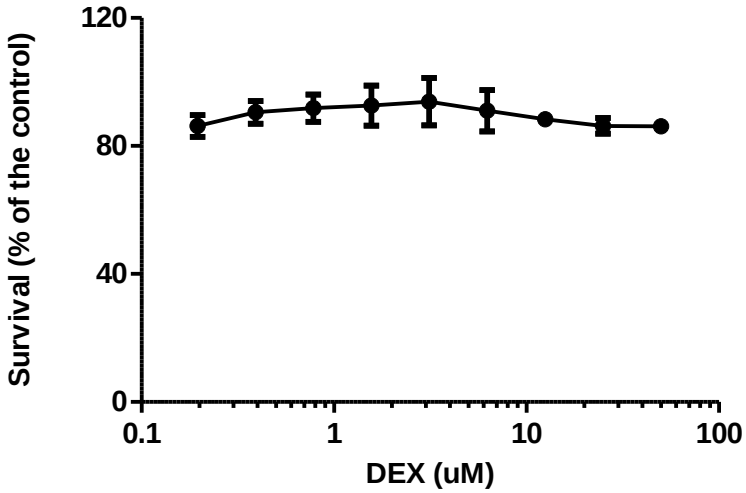

B

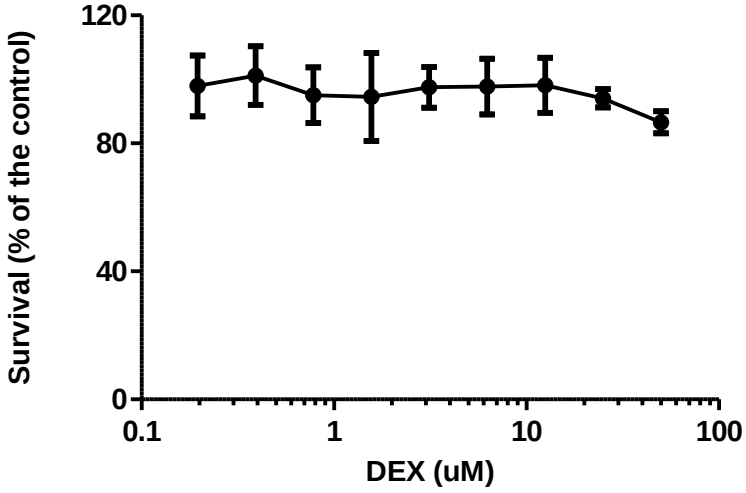

Fig.3.22. Cell survival of (A) sensitive RPMI 8226 MM cell line and (B) ARH 77 cell line treated with DEX with different doses for 24h. Data presented as mean ± SD. N=3.

A

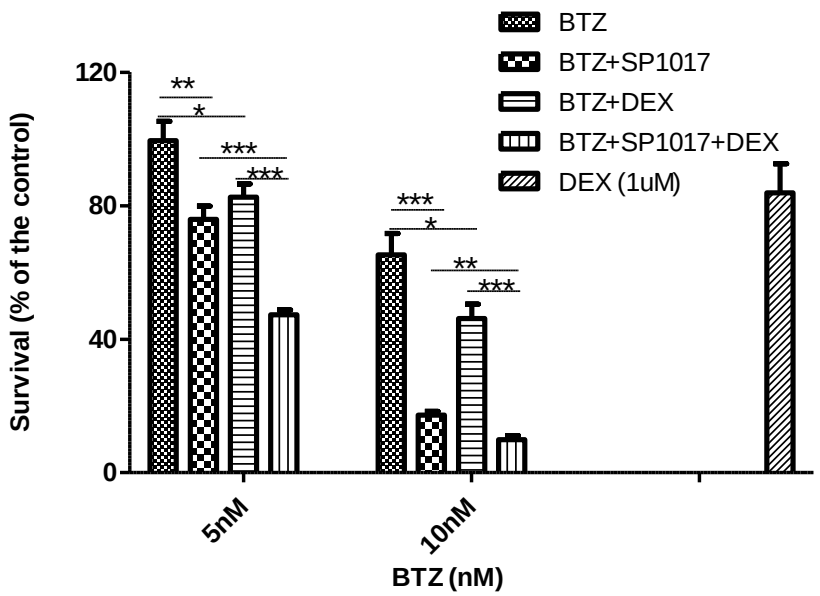

B

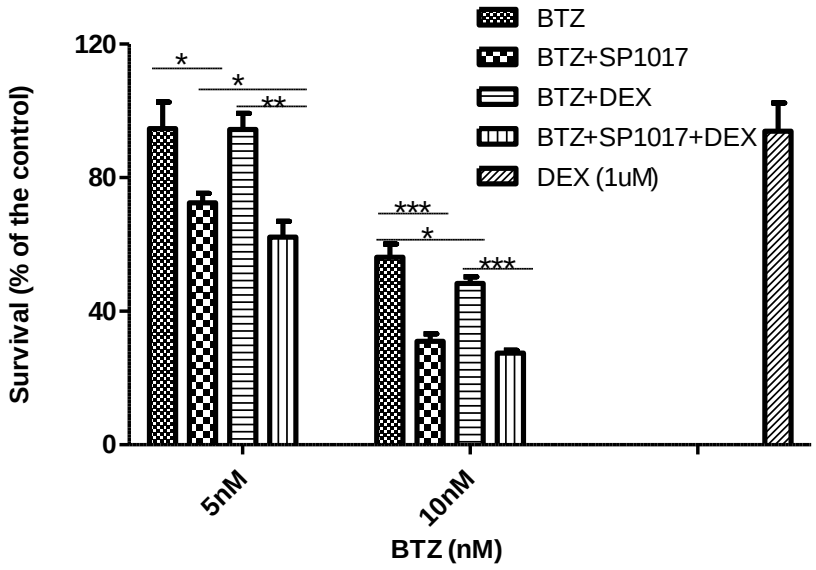

Fig 3.23. Cell survival of (A) sensitive RPMI 8226 MM cell line and (B) ARH 77 cell line treated with 3-drug combination (BTZ+0.005%SP1017+1uMDEX) for 24h. Data presented as mean ± SD. N=3 (***P<0.001,**P<0.01, and *P<0.05).

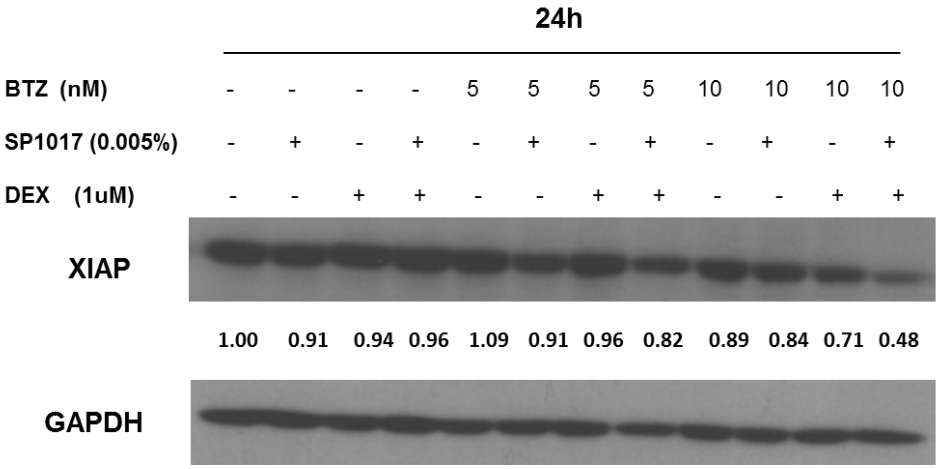

Fig.3.24. Expression of XIAP of sensitive RPMI 8226 MM cell line treated with 3-drug combination for 24h. Data represented as a set out of three experiments.

3.4 Conclusions

In the previous published work, Pluronics at relative low concentration can sensitize MDR cancer cells mainly by Pgp inhibition, selective ATP depletion, ROS generation, inhibition of GSH/GST detoxification as well as triggering mitochondria apoptotic signals, but not in sensitive cells [74, 75, 76, 77]. Here in our study we firstly proved that at quite low concentration, the mixture of Pluronics SP1017 sensitize sensitive MM cells to proteasome inhibitors discussed in Chapter II. Mechanistic studies showed that the BTZ+SP1017 combination–induced apoptosis is associated with : 1) increase of suppression of ChT-L proteolytic activity, concomitant with increased accumulation of ubiquitinated proteins and proteotoxic stress; 2) accumulation of Pluronic® L61 in ER and increase of ER stress response; 3) accumulation of Pluronic® L61 in Golgi apparatus, increase of Golgi fragmentation and reduction of secretion of paraprotein; 4) increase of GSH depletion, resulting in less ability to neutralize drug-induced oxidative stress; 5) increase of activation of both mitochondria-dependent (quick translocation of Pluronic® L61 into mitochondria, mitochondrial membrane potential loss, cytochrome c release and activation of caspase 9/3) and independent (activation of caspase 8/3) apoptotic pathways; 6) decrease of the expression of anti-apoptotic proteins. Studies in the BM microenvironment models showed that the combination of SP1017 and BTZ effectively overcame both adhesion-mediated drug resistance and cytokines-mediated drug resistance, indicating the great potential to use the combination for MM. One of the mechanisms is due to the significant reduction of secretion of IL-6, the major growth factor by BMSCs treated by the combination rather than BTZ alone. The findings provide the strong rationale for our further investigation of the treatment efficiency of the combination therapy in human myeloma/SCID mice model and the future clinical evaluation in patients with relapsed and refractory myeloma. In addition,

SP1017 in combination with BTZ and DEX leads to most pronounced anti-proliferative effect, indicating the potential of SP1017 used in corticosteroid sparing regimens to further improve the therapeutic efficacy as well as limiting significant side effects that patient with multiple myeloma often experience.

3.5 References

[1] Dou QP, Zonder JA. Overview of proteasome inhibitor-based anti-cancer therapies: perspective on bortezomib and secondgeneration proteasome inhibitors versu s future generation inhibitors of ubiquitin-proteasome system. Curr Cancer Drug Targets. 2014;14(6):517-536.

[2] Adams J. The proteasome: a suitable antineoplastic target. Nat Rev Cancer. 2004 May;4(5):349-60.

[3] Mitsiades N, Mitsiades CS, Poulaki V, Chauhan D, Fanourakis G, Gu X, Bailey C, Joseph M, Libermann TA, Treon SP, Munshi NC, Richardson PG, Hideshima T, Anderson KC. Molecular sequelae of proteasome inhibition in human multiple myeloma cells. Proc Natl Acad Sci U S A. 2002 Oct 29;99(22):14374-14379

[4]Ciechanover A, Schwartz AL. The ubiquitin-proteasome pathway: the complexity and myriad functions of proteins death.Proc Natl Acad Sci U S A. 1998 Mar 17;95(6):2727-2730.

[5] Herrmann J, Lerman LO, Lerman A. Ubiquitin and ubiquitin-like proteins in protein regulation. Circ Res. 2007 May 11;100(9):1276-1291.

[6] Chauhan D, Hideshima T, Anderson KC. Proteasome inhibition in multiple myeloma: therapeutic implication. Annu Rev Pharmacol Toxicol. 2005;45:465-476.

[7] Chen D, Frezza M, Schmitt S, Kanwar J, Dou QP.. Bortezomib as the First Proteasome Inhibitor Anticancer Drug: Current Status and Future Perspectives. Curr Cancer Drug Targets. 2011 March ; 11(3): 239–253.

[8] Kloetzel PM, Ossendorp F. Proteasome and peptidase function in MHC-class-I-mediated antigen presentation. Curr Opin Immunol. 2004 Feb;16(1):76-81.

[9] Berkers CR, Verdoes M, Lichtman E, Fiebiger E, Kessler BM, Anderson KC, Ploegh HL, Ovaa H, Galardy PJ. Activity probe for in vivo profiling of the specificity of

proteasome inhibitor bortezomib. Nat Methods. 2005 May;2(5):357-362.

[10] Chauhan D, Catley L, Li G, Podar K, Hideshima T, Velankar M, Mitsiades C, Mitsiades N, Yasui H, Letai A, Ovaa H, Berkers C, Nicholson B, Chao TH,Neuteboom ST, Richardson P, Palladino MA, Anderson KC. A novel orally active proteasome inhibitor induces apoptosis in multiple myeloma cells with mechanisms distinct from Bortezomib. Cancer Cell. 2005 Nov;8(5):407-419.

[11] Parlati F, Lee SJ, Aujay M, Suzuki E, Levitsky K, Lorens JB, Micklem DR, Ruurs P, Sylvain C, Lu Y, Shenk KD, Bennett MK. Carfilzomib can induce tumor cell death through selective inhibition of the chymotrypsin-like activity of the proteasome. Blood. 2009 Oct 15;114(16):3439-47.

[12] Kuhn DJ, Chen Q, Voorhees PM, Strader JS, Shenk KD, Sun CM, Demo SD, Bennett MK, van Leeuwen FW, Chanan-Khan AA, Orlowski RZ. Potent activity of carfilzomib, a novel, irreversible inhibitor of the ubiquitin-proteasome pathway, against preclinical models of multiple myeloma. Blood. 2007 Nov 1;110(9):3281-3290.

[13] Grant S. Enhancing proteotoxic stress as an anticancer strategy. Oncotarget. 2011 Apr;2(4):284-286.

[14] Bush KT, Goldberg AL, Nigam SK. Proteasome inhibition leads to a heat-shock response, induction of endoplasmic reticulum chaperones, andthermotolerance. J Biol Chem. 1997 Apr 4;272(14):9086-9092.

[15] Welch WJ. Mammalian stress response: cell physiology, structure/function of stress proteins, and implications for medicine and disease. Physiol Rev. 1992 Oct;72(4):1063-1081.

[16] Hartl FU. Molecular chaperones in cellular protein folding. Nature. 1996 Jun 13;381(6583):571-579.

[17]Hartl FU, Hayer-Hartl M. Molecular chaperones in the cytosol: from nascent chain to

folded protein. Science. 2002 Mar 8;295(5561):1852-1858.

[18] Awasthi N, Wagner BJ. Upregulation of heat shock protein expression by proteasome inhibition: an antiapoptotic mechanism in thelens. Invest Ophthalmol Vis Sci. 2005 Jun;46(6):2082-2091.

[19] Duus J, Bahar HI, Venkataraman G, Ozpuyan F, Izban KF, Al-Masri H, Maududi T, Toor A, Alkan S. Analysis of expression of heat shock protein-90 (HSP90) and the effects of HSP90 inhibitor (17-AAG) in multiple myeloma. Leuk Lymphoma. 2006 Jul;47(7):1369-1378.

[20] Roué G, Pérez-Galán P, Mozos A, López-Guerra M, Xargay-Torrent S, Rosich L, Saborit-Villarroya I, Normant E, Campo E, Colomer D. The Hsp90 inhibitor IPI-504 overcomes bortezomib resistance in mantle cell lymphoma in vitro and in vivo by down-regulation of the prosurvival ER chaperone BiP/Grp78. Blood. 2011 Jan 27;117(4):1270-1279.

[21] Harding HP, Calfon M, Urano F, Novoa I, Ron D. Transcriptional and translational control in the Mammalian unfolded protein response. Annu Rev Cell Dev Biol. 2002;18:575-599.

[22] Rao RV, Bredesen DE. Misfolded proteins, endoplasmic reticulum stress and neurodegeneration. Curr Opin Cell Biol. 2004 Dec;16(6):653-662.

[23] Lenna S, Trojanowska M. The role of endoplasmic reticulum stress and the unfolded protein response in fibrosis. Curr Opin Rheumatol. 2012 Nov;24(6):663-668.

[24] Harding HP, Zhang Y, Bertolotti A, Zeng H, Ron D. Perk is essential for translational regulation and cell survival during the unfolded protein response. Mol Cell. 2000 May;5(5):897-904.

[25] Nishitoh H. CHOP is a multifunctional transcription factor in the ER stress response. J Biochem. 2012 Mar;151(3):217-219

[26] Matsumoto M, Minami M, Takeda K, Sakao Y, Akira S. Ectopic expression of CHOP (GADD153) induces apoptosis in M1 myeloblastic leukemia cells. FEBS Lett. 1996 Oct 21;395(2-3):143-7.

[27] Maytin EV, Ubeda M, Lin JC, Habener JF. Stress-inducible transcription factor CHOP/ gadd153 induces apoptosis in mammalian cells via p38 kinase-dependent and-independent mechanisms. Exp Cell Res. 2001 Jul 15;267(2):193-204.

[28] McCullough KD, Martindale JL, Klotz LO, Aw TY, Holbrook NJ. Gadd153 sensitizes cells to endoplasmic reticulum stress by down-regulating Bcl2 and perturbing the cellular redox state.Mol Cell Biol. 2001 Feb;21(4):1249-1259.

[29] Han YH, Moon HJ, You BR, Yang YM, Kim SZ, Kim SH, Park WH. MG132, a proteasome inhibitor, induced death of calf pulmonary artery endothelial cells via casp ase-dependent apoptosis and GSH depletion. Anticancer Res. 2010 Mar;30(3):879-885.

[30] Du ZX, Zhang HY, Meng X, Guan Y, Wang HQ. Role of oxidative stress and intracellular glutathione in the sensitivity to apoptosis induced by proteasome inhibitor in thyroid cancer cells. BMC Cancer. 2009 Feb 16;9:56.

[31] Nerini-Molteni S, Ferrarini M, Cozza S, Caligaris-Cappio F, Sitia R. Redox homeostasis modulates the sensitivity of myeloma cells to bortezomib. Br J Haematol. 2008 May;141(4):494-503.

[32] Tait SW, Green DR. Mitochondria and cell death: outer membrane permeabilization and beyond. Nat Rev Mol Cell Biol. 2010 Sep;11(9):621-32.

[33] Ling YH, Liebes L, Zou Y, Perez-Soler R. Reactive oxygen species generation and mitochondrial dysfunction in the apoptotic response to Bortezomib, anovel proteasome inhibitor, in human H460 non-small cell lung cancer cells. J Biol Chem. 2003 Sep 5;278(36):33714-23.

[34] Liu FT, Agrawal SG, Gribben JG, Ye H, Du MQ, Newland AC, Jia L. Bortezomib blocks Bax degradation in malignant B cells during treatment with TRAIL. Blood. 2008 Mar 1;111(5):2797-805

[35] Wei MC, Zong WX, Cheng EH, Lindsten T, Panoutsakopoulou V, Ross AJ, Roth KA, MacGregor GR, Thompson CB, Korsmeyer SJ. Proapoptotic BAX and BAK: a requisite gateway to mitochondrial dysfunction and death. Science. 2001 Apr 27;292(5517):727-730.

[36] De Raeve HR, Vanderkerken K. The role of the bone marrow microenvironment in multiple myeloma. Histol Histopathol. 2005 Oct;20(4):1227-1250.

[37] Manier S, Sacco A, Leleu X, Ghobrial IM, Roccaro AM. Bone marrow microenvironment in multiple myeloma progression.
J Biomed Biotechnol. 2012;2012:157496.

[38] Hazlehurst LA, Damiano JS, Buyuksal I, Pledger WJ, Dalton WS. Adhesion to fibronectin via beta1 integrins regulates p27kip1 levels and contributes to cell adhesion mediated drug resistance (CAM-DR). Oncogene. 2000 Sep 7;19(38):4319-4327.

[39] Uchiyama H, Barut BA, Mohrbacher AF, Chauhan D, Anderson KC. Adhesion of human myeloma-derived cell lines to bone marrow stromal cells stimulates interleukin-6 secretion. Blood. 1993 Dec 15;82(12):3712-3720.

[40] Gupta D, Treon SP, Shima Y, Hideshima T, Podar K, Tai YT, Lin B, Lentzsch S, Davies FE, Chauhan D, Schlossman RL, Richardson P, Ralph P, Wu L,Payvandi F, Muller G, Stirling DI, Anderson KC. Adherence of multiple myeloma cells to bone marrow stromal cells upregulates vascular endothelial growth factor secretion: therapeutic applications.Leukemia. 2001 Dec;15(12):1950-61.

[41] Hideshima T, Anderson KC. Molecular mechanisms of novel therapeutic approaches for multiple myeloma. Nat Rev Cancer. 2002 Dec;2(12):927-937.

[42] Hideshima T, Richardson P, Chauhan D, Palombella VJ, Elliott PJ, Adams J, Anderson KC. The proteasome inhibitor PS-341 inhibits growth, induces apoptosis, and overcomes drug resistance in humanmultiple myeloma cells. Cancer Res. 2001 Apr 1;61(7):3071-3076.

[43] Batrakova EV, Li S, Alakhov VY, Miller DW, Kabanov AV. Optimal Structure Requirements for Pluronic Block Copolymers in Modifying P-glycoprotein Drug Efflux Transporter Activity in Bovine Brain Microvessel Endothelial Cells J Pharmacol Exp Ther. 2003 Feb;304(2):845-854.

[44] Wang M, Wey S, Zhang Y, Ye R, Lee AS. Role of the unfolded protein response regulator GRP78/BiP in development, cancer, and neurological disorders. Antioxid Redox Signal. 2009 Sep;11(9):2307-2316.

[45] Amy S. Lee. The ER chaperone and signaling regulator GRP78/BiP as a monitor of endoplasmic reticulum stress. Methods. 2005 Apr;35(4):373-381.

[46] Batrakova E, Lee S, Li S, Venne A, Alakhov V, Kabanov A. Fundamental Relationships Between the Composition of Pluronic Block Copolymers and Their Hypersensitization Effect in MDR Cancer Cells. Pharm Res. 1999 Sep;16(9):1373-1379.

[47] Batrakova EV, Li S, Alakhov VY, Miller DW, Kabanov AV.. Optimal Structure Requirements for Pluronic Block Copolymers in Modifying P glycoprotein Drug Efflux Transporter Activity in Bovine Brian Microvessel Endothelial Cells. J Pharmacol Exp Ther. 2003 Feb;304(2):845-854.

[48] Batrakova EV, Kabanov AV. Pluronic Block Copolymers:Evolution of Drug Delivery Concept from Inert Nanocarriers to Biological Response Modifiers. J Control Release. 2008 Sep 10;130(2):98-106.

[49] Alakhova DY, Kabanov AV. Pluronics and MDR Reversal: An Update. Mol Pharm. 2014 Aug 4;11(8):2566-78.

[50] Batrakova EV, Li S, Vinogradov SV, Alakhov VY, Miller DW, Kabanov AV. Mechanism of Pluronic Effect on P-Glycoprotein Efflux System in Blood-Brain Barrier: Contributions of Energy Depletion and Membrane Fluidization. J Pharmacol Exp Ther. 2001 Nov;299(2):483-493.

[51] Batrakova EV, Li S, Li Y, Alakhov VY, Kabanov AV. Effect of pluronic P85 on ATPase activity of drug efflux transporters. Pharm Res. 2004 Dec;21(12):2226-2233.

[52] Hicks SW, Machamer CE.. Golgi structure in stress sensing and apoptosis. Biochimica et Biophysica Acta 1744 (2005) 406 –414.

[53] Farquhar MG, Palade GE. The Golgi apparatus: 100 years of progress and controversy. Trends Cell Biol. 1998 Jan;8(1):2-10.

[54] Petrosyan A, Cheng PW, Clemens DL, Casey CA. Downregulation of the small GTPase SAR1A: a key event underlying alcohol-induced Golgi fragmentation in hepatocytes. Sci Rep. 2015 Nov 26;5:17127.

[55] Petrosyan A, Casey CA, Cheng PW. The role of Rab6a and phosphorylation of non-muscle myosin IIA tailpiece in alcohol-induced Golgi disorganization. Sci Rep. 2016 Aug 18;6:31962.

[56] Heher EC, Rennke HG, Laubach JP, and Richardson PG. Kidney Disease and Multiple Myeloma Clin J Am Soc Nephrol. 2013 Nov 7; 8(11): 2007–2017.

[57] Circu ML, Aw TY. Glutathione and modulation of cell apoptosis. Biochim Biophys Acta 2012 Oct;1823(10):1767-1777.

[58] Fulda S, Debatin KM. Targeting apoptosis pathways in cancer therapy. Curr Cancer Drug Targets. 2004 Nov;4(7):569-76.

[59] Fulda S, Debatin KM. Extrinsic versus intrinsic apoptosis pathways in anticancer chemotherapy. Oncogene. 2006 Aug 7;25(34):4798-4811.

[60] Alakhova DY, Rapoport NY, Batrakova EV, Timoshin AA, Li S, Nicholls D, Alakhov VY, Kabanov AV.Differential Metabolic Responses to Pluronic in MDR and non-MDR Cells: A Novel Pathway for Chemosensitization of Drug Resistant CancersJ Control Release. 2010 Feb 25;142(1):89-100.

[61] Batrakova EV[1], Li S, Elmquist WF, Miller DW, Alakhov VY, Kabanov AV. Mechanism of sensitization of MDR cancer cells by Pluronic block copolymers: Selective energy dep letion. Br J Cancer. 2001 Dec 14;85(12):1987-1997.

[62] Peter ME, Krammer PH. The CD95(APO-1/Fas) DISC and beyond. Cell Death Differ. 2003 Jan;10(1):26-35.

[63] Gajate C, Mollinedo F. The antitumor ether lipid ET-18-OCH_3 induces apoptosis through translocation and capping of Fas/CD95 into membrane rafts in human leukemic cells. Blood. 2001 Dec 15;98(13):3860-3863.

[64] Gajate C, Mollinedo F. Edelfosine and perifosine induce selective apoptosis in multiple myeloma by recruitment of death receptors and downstream signaling molecules into lipid rafts. Blood. 2007 Jan 15;109(2):711-719.

[65] Mollinedo F, de la Iglesia-Vicente J, Gajate C, Estella-Hermoso de Mendoza A, Villa-Pulgarin JA, Campanero MA, Blanco-Prieto MJ. Lipid raft-targeted therapy in multiple myeloma. Oncogene. 2010 Jul 1;29(26):3748-57.

[66] Sahay G, Batrakova EV, Kabanov AV. Different internalization pathways of polymeric micelles and unimers and their effects on vesicular transport. Bioconjug Chem. 2008 Oct;19(10):2023-2029.

[67] Kapoor P, Ramakrishnan V, Rajkumar SV. Bortezomib combination therapy in multiple myeloma. Semin Hematol. 2012 Jul;49(3):228-42.

[68] Friedenberg WR, Kyle RA, Knospe WH, Bennett JM, Tsiatis AA, Oken MM. High-dose dexamethasone for refractory or relapsing multiple myeloma. Am J Hematol. 1991 Mar;36(3):171-5.

[69] Palumbo A, Anderson K. Multiple myeloma. N Engl J Med. 2011;364:1046–1060.

[70] Nooka AK, Kastritis E, Dimopoulos MA, Lonial S. Treatment options for relapsed and refractory multiple myeloma. Blood. 2015 May 14;125(20):3085-99.

[71]Kapoor P, Ramakrishnan V, Rajkumar SV. Bortezomib combination therapy in multiple myeloma. Semin Hematol. 2012 Jul;49(3):228-42.

[72] Sharma S, Lichtenstein A. Dexamethasone-induced apoptotic mechanisms in myeloma cells investigated by analysis of mutant glucocorticoid receptors.Blood. 2008 Aug 15;112(4):1338-45.

[73] Salem K, Brown CO, Schibler J, Goel A. Combination chemotherapy increases cytotoxicity of multiple myeloma cells by modification of nuclear factor (NF)-κB activity. Exp Hematol. Feb 2013; 41(2): 209–218.

[74]Batrakova EV, Li S, Alakhov VY, Elmquist WF, Miller DW, Kabanov AV.. Sensitization of cells overexpressing multidrug-resistant proteins by pluronic p85. Pharm Res. 2003 Oct;20(10):1581-1590.

[75] Batrakova EV, Li S, Elmquist WF, Miller DW, Alakhov VY, Kabanov AV. Mechanism of sensitization of MDR cancer cells by Pluronic block copolymers: Selective energy depletion. Br J Cancer. 2001 Dec 14;85(12):1987-1997.

[76] Alakhova DY, Rapoport NY, Batrakova EV, Timoshin AA, Li S, Nicholls D, Alakhov VY, Kabanov AV. Differential metabolic responses to pluronic in MDR and non-MDR cells: A novel pathway for chemosensitization of drug resistant cancers . J Control Release. 2010 Feb 25;142(1):89-100.

[77] Minko T, Batrakova EV, Li S, Li Y, Pakunlu RI, Alakhov VY, Kabanov AV., Pluronic block copolymers alter apoptotic signal transduction of doxorubicin in drug-resistant cancer cells. J Control Release. 2005 Jul 20;105(3):269-278

CHAPTER IV: THE ANTI-TUMOR ACTIVITY OF THE BTZ+SP1017 COMBINATION THERAPY IN HUMAN MM/SCID MODELS.

4.1 Introduction

To further evaluate potential of SP1017+BTZ combination for treating MM, an in vivo murine model that recapitulates the characteristics of human disease condition of MM is required. An animal model that accurately reflects human MM and takes into account the protective nature of BMSCs would be powerful in confirming the efficacy of therapeutic agents in vivo. There are currently three types of MM animal models: 1) injection of pristane oil in BALB/c mice leads to intraperitoneal plasmacytomas but without BM colonization and osteolysis; 2) injection of allogeneic malignant plasma cells (5T2MM, 5T33) in the C57BL/KalwRij mouse induces BM proliferation and osteolytic lesions; 3) injection of malignant plasma cell lines in immunodeficient mice SCID or NOD/SCID [1]. The BALB /c oil-induced and transplantable plasmacytomas resemble human MM in their ability to produce a monoclonal immunoglobulin [2]. The major disadvantage of the first model is that plasma cells are restrictively localized in the peritoneum and do not extend to the BM, which does not faithfully resemble human MM [1]. The 5TMM model originates from spontaneously developed MM in aged C57BL/KalwRij mice and has since been propagated by intravenous injection of BM cells from MM bearing mice, into young naive syngeneic recipients. This model has been extensively used for studying homing mechanisms of MM cells to BM, interaction of MM cells with the BM environment, and evaluation of new therapies [3, 4]. However, the 5TMM models are limited by being solely murine-derived and representative of only one type of myeloma. Xenograft models, in which human MM cell lines are injected into immune compromised mice (for example, severe combined immunodeficient (SCID),

nude, NOD/SCID gamma (NSG) mice, etc.), can be used to establish systemic disease (via intravenous injection of MM cells) or local disease (via subcutaneous or intratibial injections) [5]. The models allow for the implantation of human MM cells, which are more relevant for investigating therapeutic targets and preclinical therapeutic testing than murine MM cells. Subcutaneous xenograft models not only fail to reflect the systemic nature of diffuse lesions of MM but also place tumor cells in the cutaneous microenvironment, which is radically different from the BM microenvironment, which appears to play an important role in differentiation, migration, proliferation, survival, and drug resistance of the malignant plasma cells [6], thus influencing the responsiveness to therapy. Several NOD/SCID MM models using intravenous injection of human MM cell lines, including U266, MM.1S, RPMI-8266 or primary human MM cells have been described [7, 8, 9, 10]. MM cells are preferentially homing into BM via selective binding of adhesion molecules on their surface to BMSCs and ECM proteins. For example, the very-late antigen 4 on MM cells binds to fibronectin and lymphocyte function-associated antigen-1 on MM cells binds to intercellular adhesion molecule-1 on BMSCs [11]. NOD/SCID IL-2Rγ(null) mice (NSG) mice, which lack the interleukin-2 (IL-2) gamma chain, have recently been used to develop models of MM [12]. Compared to the SCID and NOD/SCID strains which lack mature B and T lymphocytes, this strain lacks NK cells, characterized by defects in macrophages, complement and dendritic cell function and shows significant improvements in tumor cell engraftment associated with abolishment of residual immune function and lack of thymic lymphoma development accompanied by an extended lifespan [13, 14]. NSG mice were injected intravenously via the tail vein with U266, XG-1, OPM-2 or patient-derived MM cells, and provided MM models which feature consistent tumor burden and osteolytic bone disease including paraplegia, paraprotein in the serum, osteolytic lesions and loss of trabecular bone [15]. Though tumor growth was observed in the BM of xenograft models, some of

previous studies indicated that MM cells were found in various sites, including the lungs, liver, kidneys, spleen [9, 10, 16]. Intra-tibial inoculation of tumor cells in NSG mice has been developed as well, which exhibited typical disease symptoms exclusively without organ involvement [17, 18].

In order to evaluate therapeutic benefit of SP1017+BTZ combination for treating MM and provide more accurate preclinical evaluations of investigational therapies, we successfully established the human MM/SCID mice model by injecting Luc^+/GFP^+ RPMI 8226 MM cells (2×10^6/100ul PBS/Mouse) into NSG mice. In 4 weeks post tumor implantation, mice were treated with saline, SP1017, BTZ or combination of SP1017 and BTZ via tail vein injections twice weekly for 4 weeks. Total body bioluminescence imaging (BLI), the serum levels of human immunoglobulin lambda paraprotein, changes in the body weight and onset of hind limb paralysis at the late stages of the disease were used to monitor the treatment efficacy.

4.2 Materials and methods

4.2.1 Materials

Bortezomib was purchased from Selleck Chemicals (Houston, TX, USA). SP1017 was kindly provided by Supratek Pharma. Inc (Montreal, Canada). F-Luc-GFP Lentivirus was purchased from Capital Biosciences (Rockville, MD, USA). Human lambda EILSA kit was purchased from Bethyl Laboratories Inc (Montgomery, TX, USA). Luciferase assay system and cell culture lysis reagent were purchased from Promega (Madison, WI, USA). Hank's Balanced Salt Solution (HBSS), ACK lysing buffer were purchased from Fisher Scientific (Pittsburgh, PA, USA). Hexadimethrine bromide (Polybrene) was purchased from Sigma-Aldrich (St Louis, MO, USA). FITC anti-mouse CD 45 antibody

was purchased from Biolegend (San Diego, CA, USA). PE anti-mouse CD11b and Purified Rat Anti-Mouse CD16/CD32 was purchased from BD Biosciences (San Jose, CA, USA).

4.2.2 Labeling of RPMI 8226 MM cells with Luciferase (Luc) and GFP

To prepare stably transfected Luc^+/GFP^+ MM cells, RPMI 8226 MM cells were infected with F-Luc-GFP Lentivirus. Briefly, 10^5 of cells were seeded in one well of a 24-well plate and mixed with 100ul of F-Luc-GFP Lentivirus (10^8 TU/ml) in 1ml of the complete media in the presence of Polybrene (8 μg/mL). Cells was centrifuged at 300Xg for 1h at room temperature and incubated at 37 ℃ in a humidified, 5% CO_2 atmosphere overnight. The cells were washed with PBS, fresh culture medium was added the next morning and cells were incubated for the enlargement of the cell number. To enrich for Luc positive cells, cells were sorted by Becton Dickinson FACSAria™ flow cytometer with GFP expression.

4.2.3 The establishment of the human MM/SCID model

A three mice pilot study was conducted to establish the human MM/SCID models. MM was generated by i.v. injection of Luc^+/GFP^+ RPMI-8226 cells (2×10^6 cells suspended in 100 ul of PBS) via tail vein of NSG mice. The tumor progression was evaluated by BLI, the serum levels of human immunoglobulin lambda paraprotein, changes in the body weight and onset of hind limb paralysis. The BM of one the tumor-beaing mouse and one control mouse was extracted by ice-cold HBSS. All cells were collected and centrifuged down at 1500rpm for 10min. The supernatant was removed and cells were incubated with 2ml of ACK lysis buffer in 37°C water bath for 2min to remove the red cells. Another 25ml of HBSS was added to stop the lysis reaction. The GFP positive tumor cells were analyzed using Becton Dickinson FACSCalibur™ flow cytomerter and FACSDiva software (Version 8.0, Becton Dickinson, San Jose, CA).

4.2.4 The evaluation of the combination of SP1017+BTZ in human MM/SCID model

Female six-week old NOD/SCIDγc ^{null} (NSG) mice were obtained from The Jackson Laboratories and housed in AAALAC accredited facility. Food and reverse osmosis water were available ad libitum throughout the study. Animals were quarantined for 7 days prior to study initiation. All animal studies were conducted in accordance with the protocol approved by the University of Nebraska Medical Center Institutional Animal Care and Use Committee. MM was generated by i.v. injection of Luc^{+}/GFP^{+} RPMI-8226 cells (2 $\times 10^{6}$ cells suspended in 100 ul of PBS) via tail vein of NSG mice. After development of tumors (4 weeks after injection), animal were randomized (4 treatment groups, n=10) and treated with saline, 0.1% SP1017 (100ul), 0.5mg/kg BTZ or combination of 0.1% SP1017 (100ul) and 0.5mg/kg BTZ. Treatments were administrated via tail vein injections twice weekly for 4 weeks (On day 1, 4, 8, 11, 15, 18, 22, 25). Tumor progression was monitored by bioluminescence imaging (BLI) once weekly, the procedure of which had been detailed in [19]. Blood samples were collected twice a week prior to drug injection from each mouse from facial vein by using 4-5mm lancet for the measurement of human Igλ in murine serum using human lambda ELISA Kit according to the manufacturer's instructions. Animal body weight was monitored every second day starting from the day of malignant cell infusion and during tumor development and drug treatment. General physical conditions, clinical signs and ascending paralysis were assessed using a four-stage scale of 0-3, with "0" being clinically normal, "1" being decreased tail tone or weak tail only, "2" being hind limb weakness and "3" being hind limb paralysis. Upon initial stages of disease progression, animals were monitored for clinical signs every second day. When initial clinical signs are noticed (score 1-2), animals were monitored on daily basis. The paralyzed mice or

non-paralyzed mice with 20% of body weight loss or those becoming moribund were euthanized via CO_2 asphyxiation.

4.2.5 Preparation of Cy5-L61

Pluronic® L61 was labeled with Cyanine 5 fluorophore according to the method described before[20]. Briefly, Pluronic® L61were activated with CDI, and then modified with excess of ethylenediamine and purified by dialysis against 20% ethonal. Amino-modified L61 was conjugated with Cyanine5 NHS ester (1:1) in dimethylformamide in the presence of 1.2 eq of tertiary amine. Free Cyanine5 and Cyanine5-labeled L61 were separated by Sephadex LH-20 (Sigma-Aldrich, St Louis, MO, USA) column using methonal/ dichloromethane (1:1) as elution phase.

4.2.6 Biodistribution of Cy5-L61 in both tumor-bearing mice and control mice

5 Female six-week old NOD/SCIDγc ^{null} (NSG) mice were inoculated with Luc^+/GFP^+ RPMI-8226 cells as described above. In 6 weeks post MM cell inoculation, saline (100ul as control) and Cy5-L61 (0.011% L61 equivalent) mixed with 0.089% F127 in saline (100ul), which compose 0.1% SP1017 were injected into both tumor-bearing mice and control mice without tumor. After 24h, the images of the whole body, skeleton as well as organs were taken using IVIS imaging system to track the distribution of Cy5-L61. In addition, the BM of the tumor-bearing mice and control mice were extracted by ice-cold HBSS. All cells were collected and centrifuged down at 1500rpm for 10min. The supernatant was removed and cells were incubated with 2ml of ACK lysis buffer in 37°C water bath for 2min to remove the red cells. Another 25ml of HBSS was added to stop the lysis reaction. The Cy5-positive cells were analyzed using Becton Dickinson LSR II flow cytometer and FACSDiva software (Version 8.0, Becton Dickinson, San Jose,

CA). An aliquot of bone morrow cells was lysed with cell culture lysis reagent and supernatant was collected after removing cell debris by centrifugation (14000 rpm for 10 min). 20ul of supernatant were taken and plated in white polystyrene, flat opaque bottom Corning® 96-well plate (Sigma-Aldrich, St Louis, MO, USA). Luciferase assay reagents were prepared according to the manufacturer's instructions. 100ul reagent was added to each sample. Luminescence was determined as relative light units (RLU) using the SpectraMax M5 microplate reader and the results were normalized by protein content determined by BCA assay.

4.2.7 Cy5-L61 uptake in $CD45^+$ hematopoietic cells and $CD11b^+$ cells (macrophages/monocytes) in BM in control mice.

6 male six-week old NOD/SCIDγc ^{null} (NSG) mice were injected with saline (100ul as control) and Cy5-L61 (0.011% L61 equivalent) mixed with 0.089% F127 in saline (100ul), which compose 0.1% SP1017. The BM of control mice were extracted by ice-cold HBSS 24h post-injection. All cells were collected and centrifuged down at 1500rpm for 10min. The supernatant was removed and cells were incubated with 2ml of ACK lysis buffer in 37°C water bath for 2min to remove the red cells. Another 25ml of HBSS was added to stop the lysis reaction. Cells were stained with FITC-CD45 and PE-CD11b according to the manufacturer's instructions. The cells were analyzed using Becton Dickinson LSR II flow cytometer and FACSDiva software (Version 8.0, Becton Dickinson, San Jose, CA).

4.2.8 Statistical analysis

For the antitumor study, the Kruska-Wallis test, a nonparametric test was used for overall comparison of the group means for paraprotein and BLI under different types of treatments as the data did not follow a normal distribution. To evaluate specific differences between BTZ and BTZ+SP1017 groups, Tukey's nonparametric multiple-

comparison method was used. Two-tailed *P* values less than 0.05 were considered significant in both tests.

4.3 Results and discussion

The human MM/SCID mice model was successfully established by injecting Luc^+/GFP^+ RPMI 8226 MM cells (2×10^6/100ul PBS/Mouse) into mice via tail vein. The tumor formation was validated by increased BLI signal observed in femur and other parts of skeleton (some mice also had increased BLI signal in soft tissue), increased expression of human lambda paraprotein, huge body weight loss and the progressing hind limb paralysis in the late stage. Tumor engraftment was observed 4 weeks post-inoculation by BLI, with concomitant elevation of serum human lambda levels. The presence of tumor cells in the BM microenvironment was confirmed by whole-body and skeleton BLI as well as the presence of GFP^+ tumor cells in the extracted BM analyzed by flow cytometry. From the BLI of skeleton, the tumor signal was observed in femur. Among the BM extracted from the femur about 2.6% of cells are GFP^+ tumor cells, indicating the tumor cells homing to the BM **(Fig.4.1)**. In addition, MM foci and osteolytic lesions were observed to be present in multiple sites of the axial skeleton and confirmed by histopathology and X-ray imaging, respectively (Data not shown). Thus, MM cells were proven to effectively home to skeleton and develop MM lesions in skeletal sites in this model. For the evaluation of treatment efficiency, 40 NSG mice were injected with Luc^+/GFP^+ RPMI 8226 MM cells (2*10^6/100ul PBS/Mouse) via tail vein. In 4 weeks post tumor implantation, tumor-bearing NSG mice were divided into 4 groups randomly (10 mice per group), treated with 1) 0.9% saline; 2) 0.1% SP1017 (100ul); 3) 0.5mg/kg BTZ; 4) 0.5mg/kg BTZ+0.1% SP1017 (100ul) for 4 weeks, twice weekly (on day 1, 4, 8, 11, 15, 18, 22, 25), which resemble the clinical BTZ regimen for MM. Treatment efficiency

A: Control mice without tumor

Left femur **Right femur**

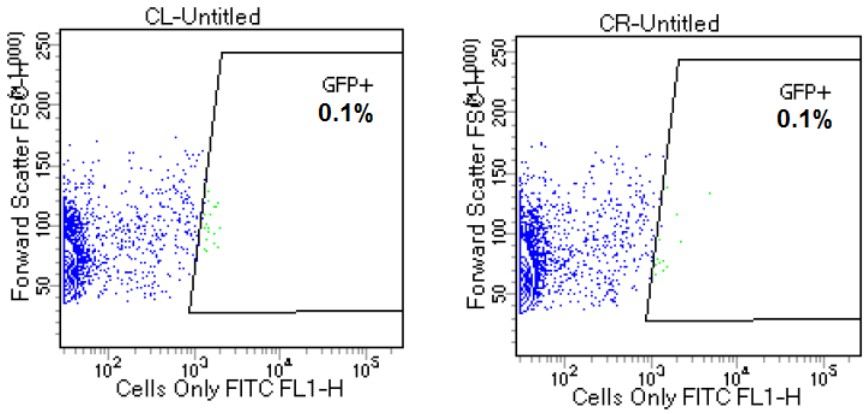

B: Tumor-bearing mice

Left femur **Right femur**

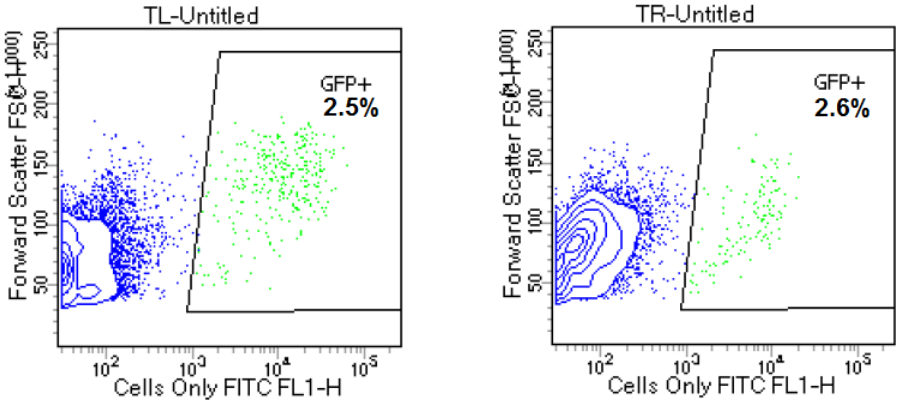

Fig.4.1 Luc^{+}/GFP^{+} RPMI 8226 MM cells in the femur of (A) one control mouse and (B) one tumor-bearing NSG mouse.

was elevated by measuring serum paraprotein levels twice a week and by weekly BLI imaging. After 4 weeks of treatments (day 24), the serum paraprotein level in the untreated controls was significantly elevated (85-fold increase) while both BTZ and BTZ+SP1017 combination treatments greatly suppressed the elevation of paraprotein over the whole treatment regimen and delayed the disease progression **(Fig.4.2A)**. Notably, serum level of paraprotein was significantly lower in the group of mice treated with BTZ+SP1017 combination compared to that of the BTZ alone after only 2 injections **(insert enlarged, Fig.4.2A)** and the significant differences between treatments continued to be observed even after the treatments were completed. These results were validated by BLI data, which also showed significantly higher inhibition of disease progression in mice treated with the combination therapy compared to BTZ alone **(Fig.4.2B)**. **Fig.4.3** showed the BLI images of four treatment groups on Day 28 (the third day after final injection), which visually indicates the better treatment efficiency of the combination therapy. The two parameters, the level of serum paraprotein and BLI signal, are well-correlated in indicating the tumor progression and the anti-tumor efficiency. The serum level of paraprotein can be a more quantitative indicator of disease progression while the BIL data can be a visualized reporter, which demonstrated bone morrow tropism of the RPMI 8226 MM cells. In addition, the combination therapy did not show systemic toxicity (no significant body weight change between groups, **Fig.4.4**) or hematological toxicity (no significant differences were observed between the treatment and control groups as determined by cell blood counting, **Table.4.1**) at the dosage (0.5 mg/kg BTZ and 0.1% SP1017 (100ul)) we used.

In previous work, Pluronic® block copolymer P85 was found to be accumulated in various tissues in the following order: liver>spleen>kidney>lung>brain [21]. However, no previous studies indicated whether the Pluronic® block copolymer can accumulate in the

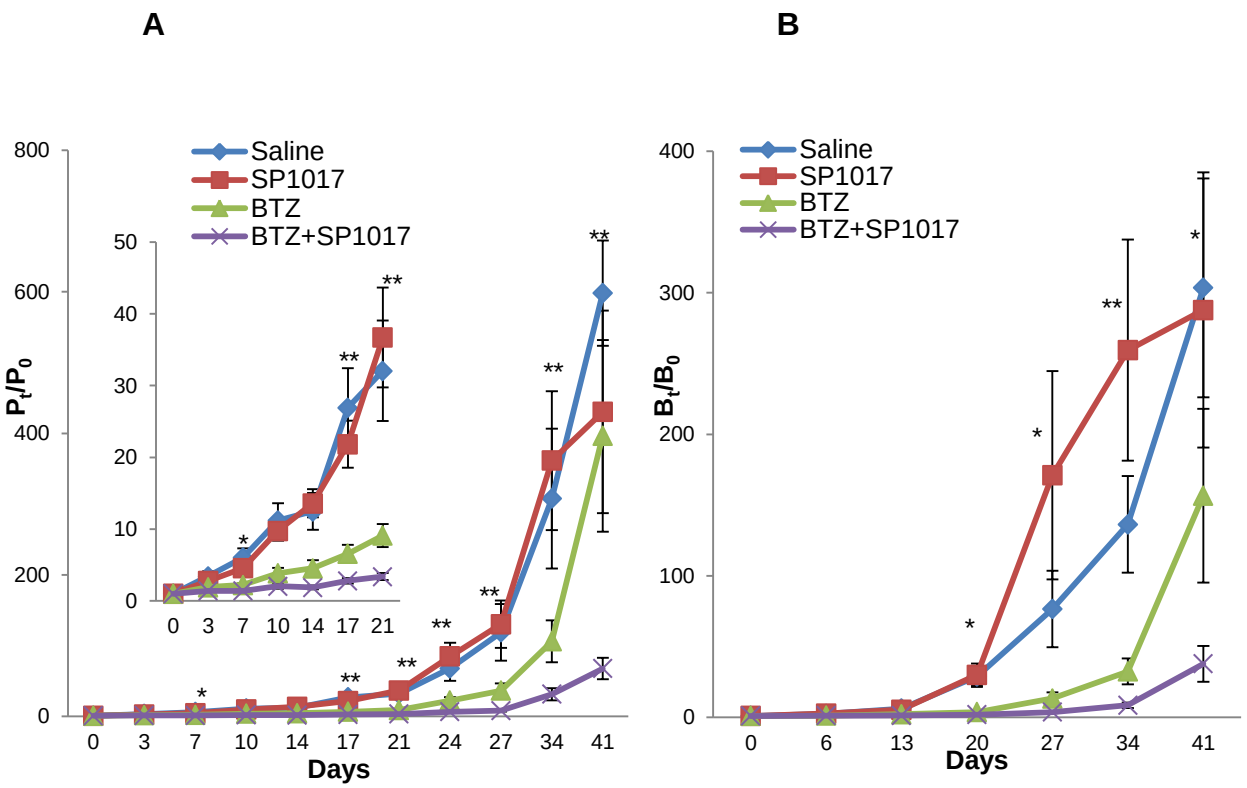

Fig.4.2 In vivo antitumor efficacy of BTZ+SP1017 combination therapy in Luc^+/GFP^+ RPMI 8226 human MM xenograft-bearing NSG mice. (A) Relative paraprotein levels (P_t/P_0) and (B) changes in tumor volume as indicated by relative radiance units (R_t/R_0) measured by means of BLI over time following IV administration of 1) 0.9% saline; 2) 0.1% SP1017 (100ul); 3) 0.5mg/kg BTZ; 4) 0.5mg/kg BTZ+0.1% SP1017 (100ul) on Day 1, 4, 8, 11, 15, 18, 22 and 25. Paraprotein level and radiance are normalized to respective values at the day before treatments were initiated (P_0 and R_0, respectively). Insert in panel **A** shows close-up of results up to 21 days following treatment initiation. Data presented as mean ± SEM.N=10 (*P<0.05, **P<0.01). Statistical significance between BTZ+SP1017 and BTZ groups was determined using Tukey's nonparametric multiple-comparison method.

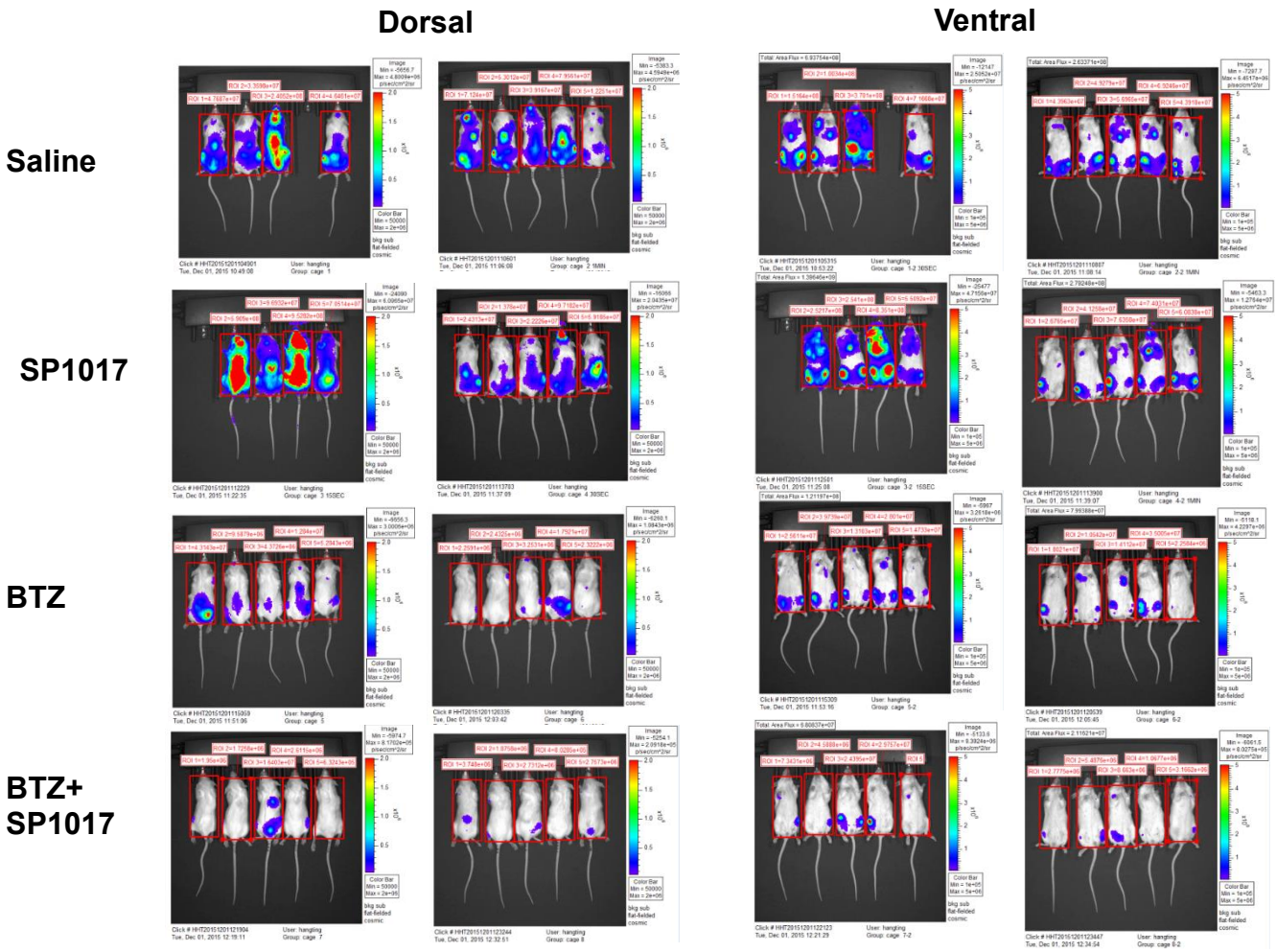

Fig.4.3. BLI images on the third day after all the 8 injections (Day 28) of four groups of NSG mice treated with of 1) 0.9% saline; 2) 0.1% SP1017 (100ul); 3) 0.5mg/kg BTZ; 4) 0.5mg/kg BTZ+0.1% SP1017 (100ul).

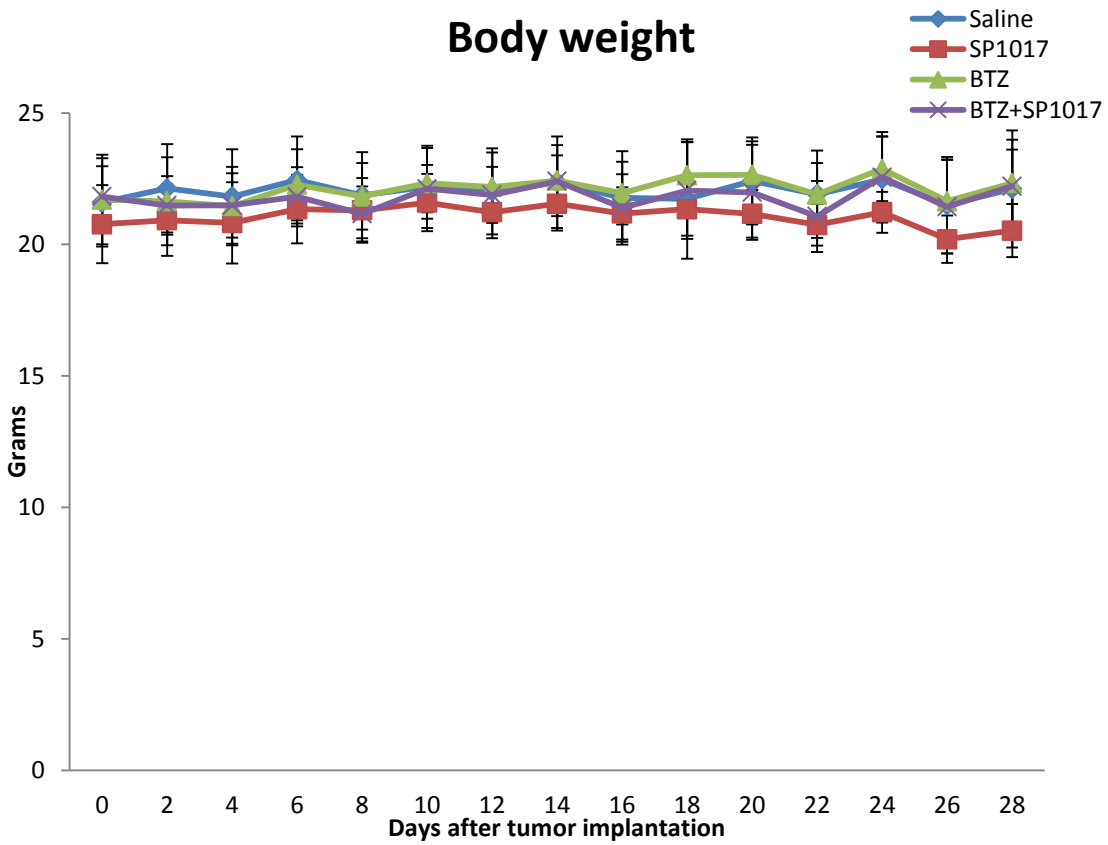

Fig.4.4. Body weight of tumor-bearing NSG mice which are received treatments of 1) 0.9% saline; 2) 0.1% SP1017 (100ul); 3) 0.5mg/kg BTZ; 4) 0.5mg/kg BTZ+0.1% SP1017 (100ul) on Day 1, 4, 8, 11, 15, 18, 22 and 25.

Table.4.1. Blood cell counting after 4 injections and 8 injections of 1) 0.9% saline; 2) 0.1% SP1017 (100ul); 3) 0.5mg/kg BTZ; 4) 0.5mg/kg BTZ+0.1% SP1017 (100ul).

	After 4 injections				After 8 injections			
	Control	SP1017	BTZ	BTZ+SP	Control	SP1017	BTZ	BTZ+SP
WBC(10^3/ul)	6.0±0.9	10.1±0.9**	13.4±3.9*	9.5±1.9*	8.1±2.7	7.2±1.4	12.4±4.5	7.2±2.3
RBC (10^6/ul)	9.3±0.1	8.2±1.3	9.0±0.4	8.5±0.6	9.2±0.2	8.8±0.6	8.0±1.2	8.5±0.3*
PLT (10^3/ul)	38.0±5.7	102.7±24.9*	110.7±89.6	83.3±26.8	38.7±18.9	65.0±5.7	93.7±43.4	43.8±25.2
HGB(g/dL)	15.5±0.5	14.8±0.4	15.2±0.3	14.9±0.1	14.4±0.4	14.6±1.3	14.0±0.5	14.2±0.3
HCT (%)	43.3±0.7	38.5±5.4	42.8±1.9	40.5±2.2	41.7±0.4	40.3±2.6	37.9±5.5	40.3±1.2
MCV (fL)	46.7±0.9	47.7±0.9	47.0±0.0	47.7±0.9	45.3±0.9	45.7±1.2	47.3±0.5*	47.5±0.5*
MCHC (g/dL)	35.8±0.7	39.5±7.2	35.7±1.4	37.0±2.3	34.7±0.8	36.2±3.3	37.7±4.5	35.4±1.7
RDWc (%)	19.5±0.2	19.3±0.4	20.5±0.3*	20.7±0.6	19.0±0.0	18.7±0.2	20.6±0.4*	21.1±0.5*

The data represent mean ±SD (n=3)

*Significantly different compared to control group, $p<0.05$

** Significantly different compared to control group, $p<0.01$

A

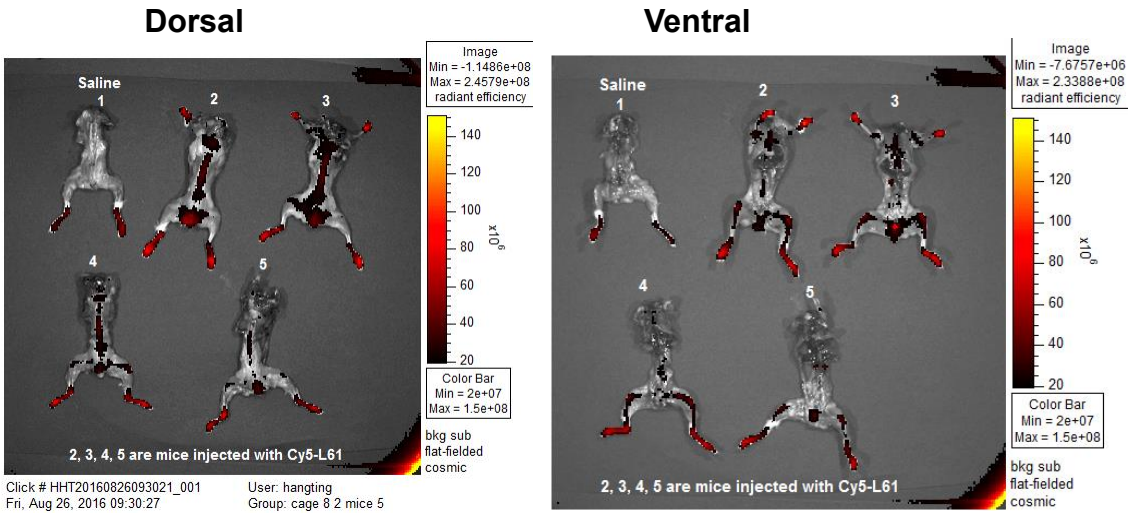

B

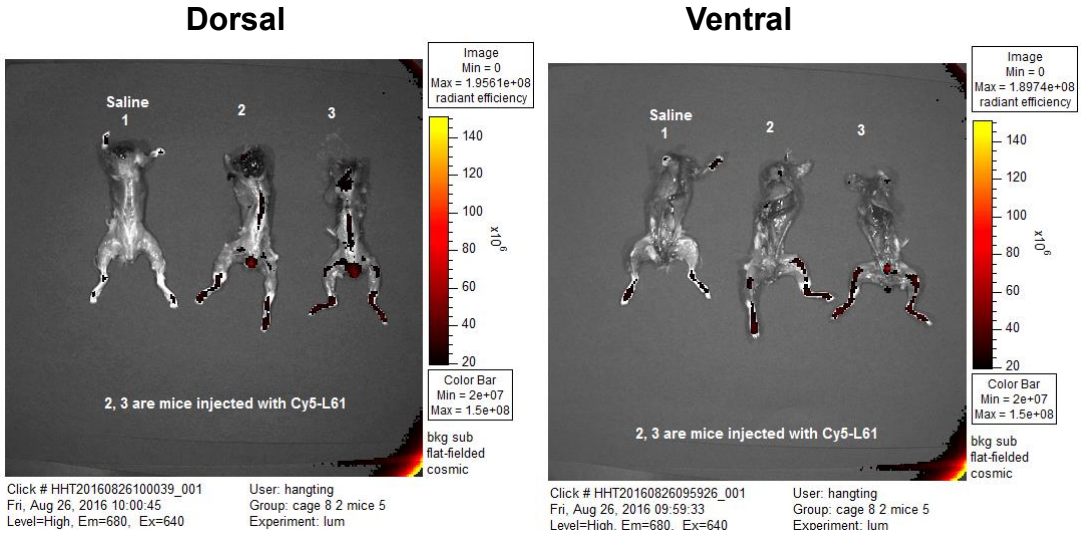

Fig. 4.5 The fluorescence (Cy5) images of mice skeleton of both (A) tumor-bearing mice and (B) control mice without tumor after 24h of injection of 0.011% Cy5-L61detected by IVIS with Ex=640nm and Em=680nm.

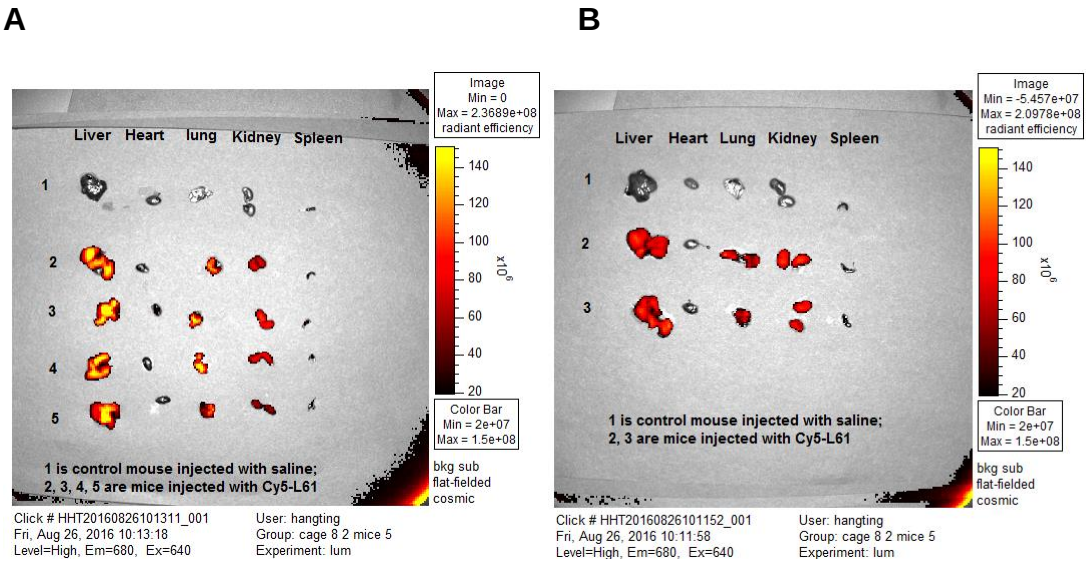

Fig. 4.6 The fluorescence (Cy5) images of mice organs (liver, heart, lung, kidney, spleen) of both (A) tumor-bearing mice and (B) control mice without tumor after 24h of injection of Cy5-L61 (0.011% L61 equivalent) detected by IVIS with Ex=640nm and Em=680nm.

A

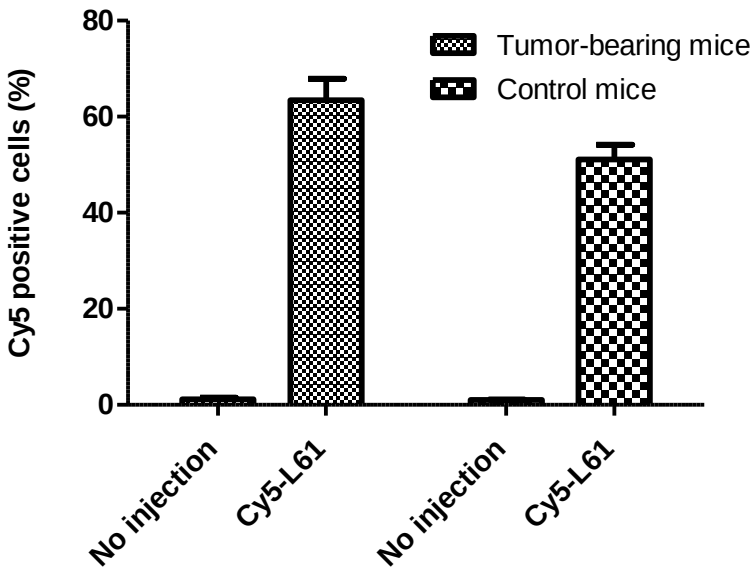

B

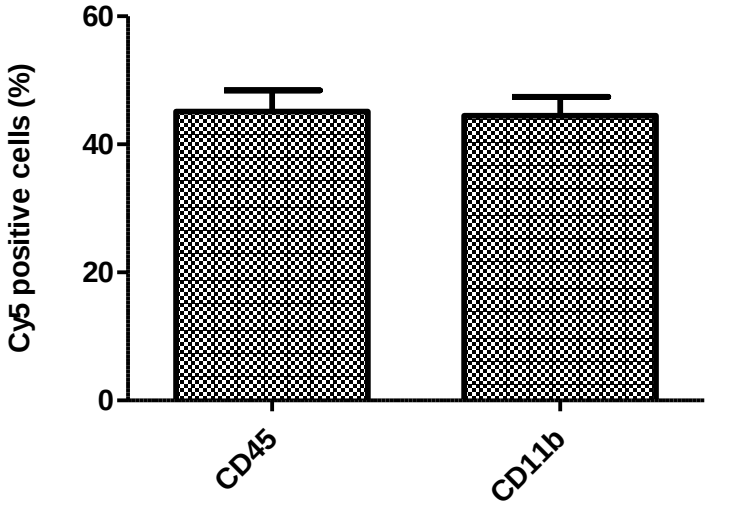

Fig. 4.7 (A) $Cy5^+$ cells in BM extracted from both tumor-bearing mice and control mice with or without injection of Cy5-L61 (0.011% L61 equivalent). N=3 (B) $Cy5^+$ cells in $CD45^+$ hematopoietic cells and $CD11b^+$ cells (macrophages/monocytes) in BM extracted from control mice with injection of Cy5-L61 (0.011% L61 equivalent). N=5

BM. Interestingly, the fluorescent signal of Cy5 was observed in the femur and spine in both tumor-bearing mice and control mice 24h post-injection of Cy5-L61 **(Fig. 4.5)**. We also found the accumulation of Cy5-L61 in the organs, such as liver, kidney and lung in both tumor-bearing mice and control mice **(Fig 4.6)**. The BM from femur was extracted and the $Cy5^+$ cells were analyzed by flow cytometry. We found about 63% of $Cy5^+$ cells in tumor-bearing mice and 51% of $Cy5^+$ cells in control mice **(Fig. 4.7A)**. These data indicate that Pluronic® L61 could accumulate in BM, thus playing an important role in sensitizing MM cells in the BM to proteasome inhibitors. Moreover, 45.1% of $CD45^+$ and 44.5% $CD11b^+$ cells in BM were associated with Cy5-L61 (**Fig. 4.7B**), indicating the uptake of the Pluronic® L61 by hematopoietic cells.

Dose-limiting peripheral neuropathy is the major toxicity issue with bortezomib, which leads to dose reductions or discontinuation and may impact both long-term quality of life and the ability to get subsequent therapies[22]. One way to reduce the systemic toxicity could be using nanocarrier to encapsulate the hydrophobic drug BTZ or drug combinations. Despite of the carrier function of Pluronic® micelles, the major limitations of Pluronic® block copolymers include the low micellization and solubilization capacity to hydrophobic drugs, as well as poor micellar stability upon dilution in the blood-steam due to relatively high CMC values. In addition, whether and how much the Pluronic® unimers can be truly transported to the tumor sites are big concerns. Thus, establishing a micellar formation of BTZ or CFZ based on amphiphilic block copolymers which have better micellar stability and can incorporate Pluronic® unimers to tumor sites as well as releasing the Pluronic® unimers into cytosol for exerting chemosensitization effect could be our future direction.

4.4 Conclusions

We demonstrated that combination of BTZ and SP1017 exerted enhanced antitumor efficacy compared to BTZ, delaying the disease progression without causing systemic toxicity or hematological toxicity. Moreover, we observed the accumulation of the Cy5-L61 in the BM which was proved by both fluorescence imaging and flow cytometry, indicating the Cy5-L61 could target and accumulate in the skeleton, thus playing an important role in sensitizing MM cells in the BM to proteasome inhibitors.

4.5 References

[1] Libouban H. The use of animal models in multiple myeloma. Morphologie. 2015 Jun;99(325):63-72.

[2] Azar HA. Experimental plasmacytomas in relation to human multiple myeloma. Ann 1974 May-Jun;4(3):157-163.

[3] Asosingh K, Radl J, Van Riet I, Van Camp B, Vanderkerken K. The 5TMM series: a useful in vivo mouse model of human multiple myeloma.
Hematol J. 2000;1(5):351-356.

[4] Vanderkerken K, Asosingh K, Croucher P, Van Camp B.. Multiple myeloma biology: lessons from the 5TMM models. Immunol Rev. 2003 Aug;194:196-206.

[5] Lwin ST, Edwards CM, Silbermann R. Preclinical animal models of multiple myeloma. Bonekey Rep. 2016 Feb 3;5:772.

[6] Manier S, Sacco A, Leleu X, Ghobrial IM, Roccaro AM. Bone marrow microenvironment in multiple myeloma progression. J Biomed Biotechnol. 2012;2012:157496.

[7] Alsina M[1], Boyce B, Devlin RD, Anderson JL, Craig F, Mundy GR, Roodman GD. Development of an in vivo model of human multiple myeloma bone disease. Blood. 1996 Feb15;87(4):1495-1501.

[8] Runnels JM[1], Carlson AL, Pitsillides C, Thompson B, Wu J, Spencer JA, Kohler JM, Azab A, Moreau AS, Rodig SJ, Kung AL, Anderson KC, Ghobrial IM, Lin CP. Optical techniques for tracking multiple myeloma engraftment, growth, and response to therapy. J Biomed Opt. 2011 Jan-Feb;16(1):011006.

[9] Mitsiades CS, Mitsiades NS, Bronson RT, Chauhan D, Munshi N, Treon SP, Maxwell CA, Pilarski L, Hideshima T, Hoffman RM, Anderson KC. Fluorescence imaging

of multiple myeloma cells in a clinically relevant SCID/NOD in vivo model: biologic and clinical implications. Cancer Res. 2003 Oct 15;63(20):6689-6696.

[10] Paton-Hough J, Chantry AD, Lawson MA. A review of current murine models of multiple myeloma used to access the efficacy of therapeutic agents on tumour growth and bone disease. Bone. 2015 Aug;77:57-68.

[11] Hideshima T, Anderson KC. Molecular mechanisms of novel therapeutic approaches for multiple myeloma. Nat Rev Cancer. 2002 Dec;2(12):927-937.

[12] Miyakawa Y, Ohnishi Y, Tomisawa M, Monnai M, Kohmura K, Ueyama Y, Ito M, Ikeda Y, Kizaki M, Nakamura M. Establishment of a new model of human multiple myeloma using NOD/SCID/gammac(null) (NOG) mice. Biochem Biophys Res Commun. 2004 Jan 9;313(2):258-262.

[13] Ito M, Hiramatsu H, Kobayashi K, Suzue K, Kawahata M, Hioki K, Ueyama Y, Koyanagi Y, Sugamura K, Tsuji K, Heike T, Nakahata T. NOD/SCID/gamma (c) (null) mouse: an excellent recipient mouse model for engraftment of human cells. Blood. 2002 Nov 1;100(9):3175-3182.

[14] McDermott SP, Eppert K, Lechman ER, Doedens M, Dick JE. Comparison of human cord blood engraftment between immunocompromised mouse strains. Blood. 2010 Jul 15;116(2):193-200.

[15] Lawson MA, Paton-Hough JM, Evans HR, Walker RE, Harris W, Ratnabalan D, Snowden JA, Chantry AD. NOD/SCID-GAMMA mice are an ideal strain to assess the efficacy of therapeutic agents used in the treatment of myeloma bone disease. PLoS One. 2015 Mar 13;10(3):e0119546.

[16] Dewan MZ, Watanabe M, Terashima K, Aoki M, Sata T, Honda M, Ito M, Yamaoka S, Watanabe T, Horie R, Yamamoto N. Prompt tumor formation and maintenance of

constitutive NF-kappaB activity of multiple myeloma cells in NOD/SCID/gammacnull mice. Cancer Sci. 2004 Jul;95(7):564-8.

[17] Schueler J, Wider D, Klingner K, Siegers GM, May AM, Wäsch R, Fiebig HH. Engelhardt M. Intratibial injection of human multiple myeloma cells in NOD/SCID IL-2Rγ (null) mice mimics human myeloma and serves as a valuable tool for the development of anticancer strategies. PLoS One. 2013 Nov 6;8(11):e79939.

[18] Fryer RA, Graham TJ, Smith EM, Walker-Samuel S, Morgan GJ, Robinson SP, Davies FE. Characterization of a novel mouse model of multiple myeloma and its use in preclinical therapeutic assessment. PLoS One. 2013;8(2):e57641.

[19] Swapnil S. Desale, et al. Targeted delivery of platinum-taxane combination therapy in ovarian cancer. J Control Release. 2015 Dec 28;220 (Pt B):651-659.

[20] Batrakova EV, Li S, Alakhov VY, Miller DW, Kabanov AV. Optimal Structure Requirements for Pluronic Block Copolymers in Modifying P-glycoprotein Drug Efflux Transporter Activity in Bovine Brain Microvessel Endothelial Cells J Pharmacol Exp Ther. 2003 Feb;304(2):845-854.

[21] Batrakova EV, Li S, Li Y, Alakhov VY, Elmquist WF, Kabanov AV. Distribution kinetics of a micelle-forming block copolymer Pluronic P85. J Control Release. 2004 Dec 10;100(3):389-397.

[22] Saad A. Khan et al. Experimental Approaches in the Treatment of Multiple Myeloma. Ther Adv Hematol. 2011 Aug; 2(4): 213–230.

CHAPTER V: SUMMARY

During the last decades, nanotechnology has provided new drug delivery systems for anti-cancer drugs which can improve its water solubility, minimize the side effects, increase the tumor-targeting distribution by passive or active targeting and overcome MDR drug resistance. Pluronic® block copolymers are found to be an efficient drug delivery system as well as chemosensitizers for MDR tumor cells. Here, in our study, we investigated the sensitization effect of SP1017 (the mixture of Pluronic® L61 and F127 with ratio 1:8 w/w) on both sensitive and resistant MM cell lines to proteasome inhibitors, explored the related molecular mechanisms and evaluated the treatment efficiency of the combination of SP1017 and proteasome inhibitor BTZ in human MM/SCID mice model.

Chapter II focuses on the sensitization effect of SP1017 on both sensitive and resistant MM cells to both the reversible BTZ and CFZ rather than normal hematological cell (PBMC) and non-hematological cells (MCF-7 human breast adenocarcinoma cells, HepG2 human liver carcinoma cells and Hela human cervix adenocarcinoma cells). 0.005% SP1017 (below the CMC of Pluronic® L61) potentiated 2-fold of both BTZ- and irreversible CFZ- induced cell cytotoxicity of three different sensitive MM cell lines due to cell apoptosis. SP1017 remained the comparable sensitization effect in BTZ-resistant RPMI 8226 cells while gained significant higher sensitization factor in CFZ-resistant RPMI 8226 cells due to the Pgp expression in CFZ-resistant MM cells rather than BTZ-resistant RPMI 8226 MM cells. SP1017 did not sensitize BTZ-induced apoptosis of normal hematological cell (PBMC), which indicates the potential of maintaining the anti-MM efficacy of the combination therapy while reducing hematological toxicities. Moreover, BTZ alone exhibiting less than encouraging results in non-hematologic tumor

cells compared with that to RPMI 8226 MM cells, indicating the specificity of the combination therapy in dealing with hematologic malignancies.

Chapter III focuses on the molecular mechanisms of the combination of SP1017+BTZ –induced MM cell apoptosis. Previous work indicated that Pluronics at relative low concentration can only sensitize MDR cancer cells rather than sensitive cells. Here in our study we firstly proved that at quite low concentration, SP1017 sensitized sensitive MM cells to proteasome inhibitors associated with : 1) increase of suppression of ChT-L proteolytic activity, concomitant with increased accumulation of ubiquitinated proteins and proteotoxic stress; 2) accumulation of Pluronic® L61 in ER and increase of ER stress response; 3) accumulation of Pluronic® L61 in Golgi apparatus, increase of Golgi fragmentation and reduction of secretion of paraprotein; 4) increase of GSH depletion, resulting in less ability to neutralize drug-induced oxidative stress; 5) increase of activation of both mitochondria-dependent (quick translocation of Pluronic® L61 into mitochondria, mitochondrial membrane potential loss, cytochrome c release and activation of caspase 9/3) and independent (activation of caspase 8/3) apoptotic pathways; 6) decrease of the expression of anti-apoptotic proteins. Moreover, the combination of SP1017 and BTZ effectively overcame both adhesion-mediated drug resistance and cytokines-mediated drug resistance (significant reduction of IL-6 secretion by BMSCs), indicating the great potential to use the combination for MM. The findings provide the strong rationale for the further investigation of the treatment efficiency of the combination therapy in human MM/SCID mice model and the future clinical evaluation in patients with relapsed and refractory myeloma. In addition, SP1017 in combination with BTZ and DEX leads to most pronounced anti-proliferative effect, indicating the potential of SP1017 used in corticosteroid sparing regimens to further

improve the therapeutic efficacy as well as limiting significant side effects that patient with multiple myeloma often experience.

Chapter IV focuses on the evaluation of the treatment efficacy of the combination of SP1017+BTZ in human MM/SCID mice model. The combination of BTZ and SP1017 exerted enhanced antitumor efficacy compared to BTZ, delaying the disease progression without causing systemic toxicity or hematological toxicity. Moreover, we observed the accumulation of the Cy5-L61 in the BM which was proved by both fluorescence imaging and flow cytometry, indicating the Cy5-L61 could target and accumulate in the skeleton, thus playing an important role in sensitizing MM cells in the BM to proteasome inhibitors.

Overall, the research supports the hypothesis SP1017 can sensitize multiple myeloma in vitro and in vivo by targeting multiple molecular mechanisms. Therefore, Pluronic® block copolymers are expected to be potential chemosensitizer used to sensitize MM cells via not only overcoming drug efflux pumps, but also involving multiple molecular mechanisms.

Our future study will focus on the evaluation of the sensitization effect of SP1017 on BTZ- and CFZ-resistant cells in vitro and in vivo and the exploration of the related molecular mechanisms. In addition, establishing a micellar formation of BTZ or CFZ based on amphiphilic block copolymers which have better micellar stability and can incorporate Pluronic® unimers to tumor sites as well as releasing the Pluronic® unimers into cytosol for exerting chemosensitization effect could be another future direction.